Radiation patterns of circular apertures with prescribed sidelobe levels

Radiation patterns of circular apertures
with prescribed sidelobe levels

by

S.C.J. Worm

August 1979

RADIATION PATTERNS OF CIRCULAR APERTURES WITH PRESCRIBED SIDELOBE LEVELS

by

S.C.J. Worm

TH-Report 79-E-97

ISBN 90-6144-097-1

E I N D H O V E N   U N I V E R S I T Y   O F   T E C H N O L O G Y

Department of Electrical Engineering

Eindhoven   The Netherlands

RADIATION PATTERNS OF CIRCULAR APERTURES WITH PRESCRIBED SIDELOBE LEVELS

by

S.C.J. Worm

TH-Report 79-E-97

ISBN 90-6144-097-1

Eindhoven

August 1979

Contents

Abstract

Some possibilities of controlling the sidelobes of circular apertures are investigated in this report. Special attention is paid to modifications of a method published by Ishimaru and Held. Source functions with different behaviour at the aperture edge are used to synthesize radiation patterns. The differences concern the value of the edge field and the value of the first edge-field derivative. Aperture distributions comprise series of Bessel functions, namely $\sum_n a_n J_o(u_n r)$ and $\sum_n a_n \{J_o(u_n r) - J_o(u_n)\}$ with u_n solution of $J_1(u) = 0$, and $\sum_n a_n J_o(u_n r)$ with u_n solution of $J_o(u) = 0$. The synthesis methods which are described, compared and modified allow a number of equal sidelobes, or a number of different sidelobe extrema over a certain region of space beyond the main beam to be prescribed. The computed patterns are compared with copolar specifications for satellite transmitting antennas and earth-station antennas. The patterns are computed to show the influence of the types of series expansions for the aperture distributions, and to show the possibilities of the synthesis methods.

Worm, S.C.J.

RADIATION PATTERNS OF CIRCULAR APERTURES WITH PRESCRIBED SIDELOBE LEVELS. TH-Report 79-E-97.
Eindhoven University of Technology, Department of Electrical Engineering, Eindhoven, The Netherlands. August 1979.

Address of the author:

Ir. S.C.J. Worm,
Group Electromagnetism and Circuit Theory,
Department of Electrical Engineering,
Eindhoven University of Technology,
P.O. Box 513,
5600 MB EINDHOVEN,
The Netherlands

Acknowledgement

The author wishes to express his thanks to dr. V. Vokurka and dr. M. Jeuken for suggesting the problem.

Introduction

Controlling the sidelobes of radiating apertures is acquiring ever greater importance in view of the growth of satellite communications. The reduction of sidelobe levels or sidelobe power reduces the interference between systems and allows more efficient use of the RF spectrum and the geostationary orbit.

The radiation patterns which can be realized theoretically depend on the type of source functions used in the expansion of the aperture illumination and the relative strength of the source functions.

There are synthesis methods which maximize the fraction of power radiated in a prescribed solid angle. As a result the fraction of power contained in the region outside this solid angle is minimized. Examples of these methods are given by Borgiotti [1] who uses hyperspheroidal functions and by Mironenko [8] who uses Legendre polynomials. Both types of source functions yield aperture fields with a finite value at the aperture edge.

Methods to synthesize a radiation pattern with a prescribed sidelobe level are given for instance by Taylor [10], Ishimaru and Held [5], and Kritskiy [7]. They are concerned merely with patterns having a number of equal sidelobes, so as to achieve minimum beam width for a given sidelobe level. The aperture illuminations consist of a series of Bessel functions of the first kind and the zeroth order. The aperture fields have a finite value at the aperture edge, except for one type of illumination used by Kritskiy, which has a zero value there.

A method developed by Kouznetsov [6] who uses power series in r, the normalized radial variable in the aperture, and reduces the level of the first sidelobe to a prescribed value is worth mentioning. This can be achieved with aperture fields having a finite or a zero edge value. For the same level of the first sidelobe the finite value edge fields result in a higher aperture efficiency and a lower decay rate of the remote sidelobes.

In this report, patterns are computed by a number of methods and a comparison is made with certain antenna gain specifications. In section 1 the Taylor distribution for a circular aperture [10] is investigated in connection with satellite antenna gain specifications [3]. In section 2 a synthesis method described by Ishimaru and Held [5] is briefly treated. Modified versions of this method are presented in section 3. The aperture fields consist of series of Bessel functions of the first kind and zeroth order. By judiciously choosing these functions one can generate aperture illuminations with a zero value and a nonzero first derivative of the edge field, or aperture illuminations with at the edge both the value and the first derivative of the field equal to zero. With the modified methods it is possible to prescribe individual sidelobe levels, allowing several different types of envelopes to be realized. The computed radiation patterns are compared with existing [2] and new specifications for the gain of earth-station antennas. The computations assume a nonblocked circular aperture throughout.

1. The Taylor distribution for a circular aperture

The formulas derived in [4], [9], and [10] are used to compare the radiation patterns of the Taylor distribution with the satellite transmitting antenna reference pattern which, for the copolar component, reads [3]

$$
\begin{array}{lll}
-12\left(\dfrac{\phi}{\phi_o}\right)^2 & \text{for} & 0 \leqslant \phi \leqslant 1.58\,\phi_o \\
-30 & \text{for} & 1.58\,\phi_o < \phi \leqslant 3.16\,\phi_o \\
-[17+25\,{}^{10}\log(\dfrac{\phi}{\phi_o})] & \text{for} & 3.16\,\phi_o < \phi
\end{array}
\qquad (1.1)
$$

after intersection with the minus on-axis gain, as the minus on-axis gain.

The angle measured from the main beam axis is ϕ and ϕ_o is the 3 dB beamwidth. The reference pattern is shown in fig. 1.

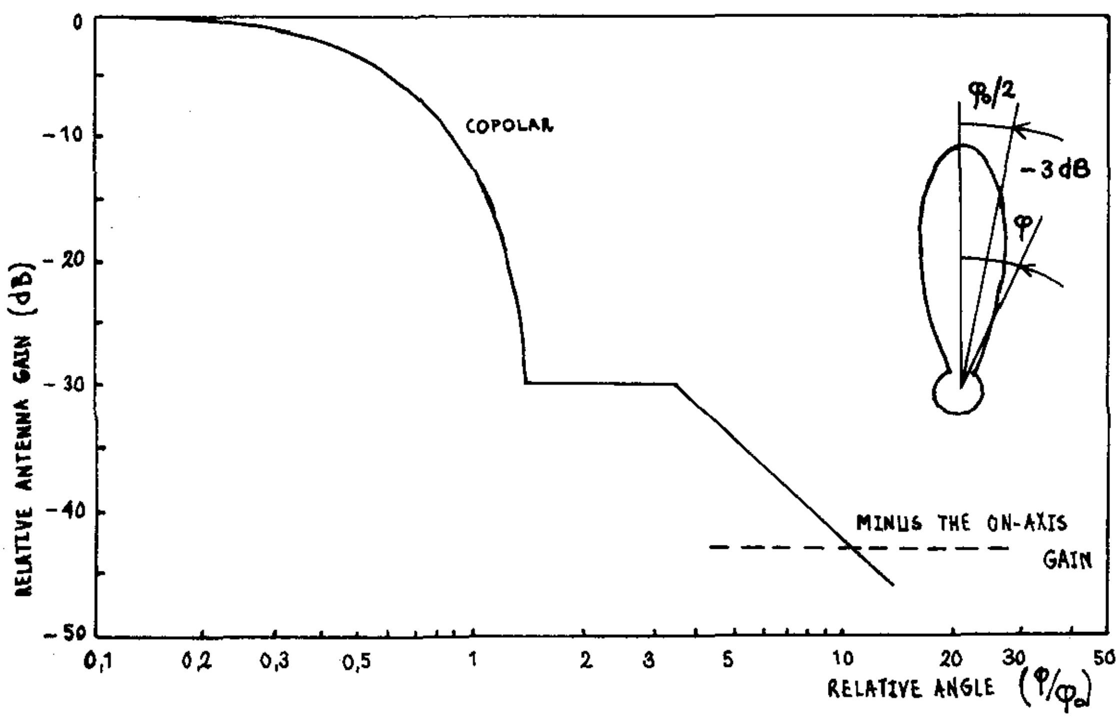

Fig. 1. Copolar component of satellite transmitting antenna reference pattern.

For easy reference the formulas for the aperture distributions, the far field [4], [10] and the efficiency [9] are summarized below.

The aperture distribution g(p) is

$$g(p) = \frac{2}{\pi^2} \sum_{m=o}^{\bar{n}-1} \frac{F(u_m,A,\bar{n})}{J_o^2(\pi u_m)} J_o(u_m p) \qquad (1.2)$$

where $F(u_o,A,\bar{n}) = 1$ if $m = 0$,

$$F(u_m,A,\bar{n}) = -J_o(\pi u_m) \frac{\prod_{n=1}^{\bar{n}-1} \left\{1 - \frac{u_m^2}{\sigma^2[A^2+(n-\frac{1}{2})^2]}\right\}}{\prod_{\substack{n=1 \\ n\neq m}}^{\bar{n}-1} \left\{1 - \frac{u_m^2}{u_n^2}\right\}} \quad \text{if} \quad m > 0,$$

$p = \pi\rho/a$ is a normalized radial variable if a is the aperture radius, A is related to the design sidelobe level η by $\eta = \cosh(\pi A)$, σ is the beam-broadening factor which equals $u_{\bar{n}}/\sqrt{A^2+(\bar{n}-\frac{1}{2})^2}$,

$\bar{n}$ is a parameter for $\bar{n} - 1$ equal sidelobes, πu_i is a zero of $J_1(\pi u) = 0$ so that the aperture field has a finite value at the aperture edge.

The point $\pi u_{\bar{n}}$ separates the region of equal sidelobes from that of decaying sidelobes. As $\bar{n}$ is increased more sidelobes are forced towards the level η and the beam width is decreased.

The radiation pattern $F(z,A,\bar{n})$ is

$$F(z,A,\bar{n}) = \frac{2J_1(\pi z)}{\pi z} \prod_{n=1}^{\bar{n}-1} \frac{\left\{1 - \frac{z^2}{\sigma^2[A^2+(n-\frac{1}{2})^2]}\right\}}{\left\{1 - \frac{z^2}{u_n^2}\right\}} \qquad (1.3)$$

where z is related to the wavelength λ, the aperture radius a, and the angle θ by $z = \frac{2a}{\lambda}\sin\theta$.

With aperture distributions the efficiency η_T is

$$\eta_T = \left[1 + \sum_{n=1}^{\bar{n}-1} \left\{\frac{F(u_n,A,\bar{n})}{J_o(\pi u_n)}\right\}^2\right]^{-1}. \qquad (1.4)$$

The efficiency is defined by the ratio of the maximum gain from the Taylor pattern to that from the uniformly illuminated aperture.

1.1. Some observations

a. The normalized radiation pattern of the ideal Taylor distribution for a circular aperture is [9]

$$F(z,A) = \frac{\cosh\{\pi(A^2-z^2)^{\frac{1}{2}}\}}{\eta} \quad \text{for the main beam,} \qquad (1.5)$$

and

$$F(z,A) = \frac{\cos\{\pi(z^2-A^2)^{\frac{1}{2}}\}}{\eta} \quad \text{for the sidelobes.} \qquad (1.6)$$

This optimum pattern is shown in fig. 2, it is optimum in its beam width sidelobe relationship.

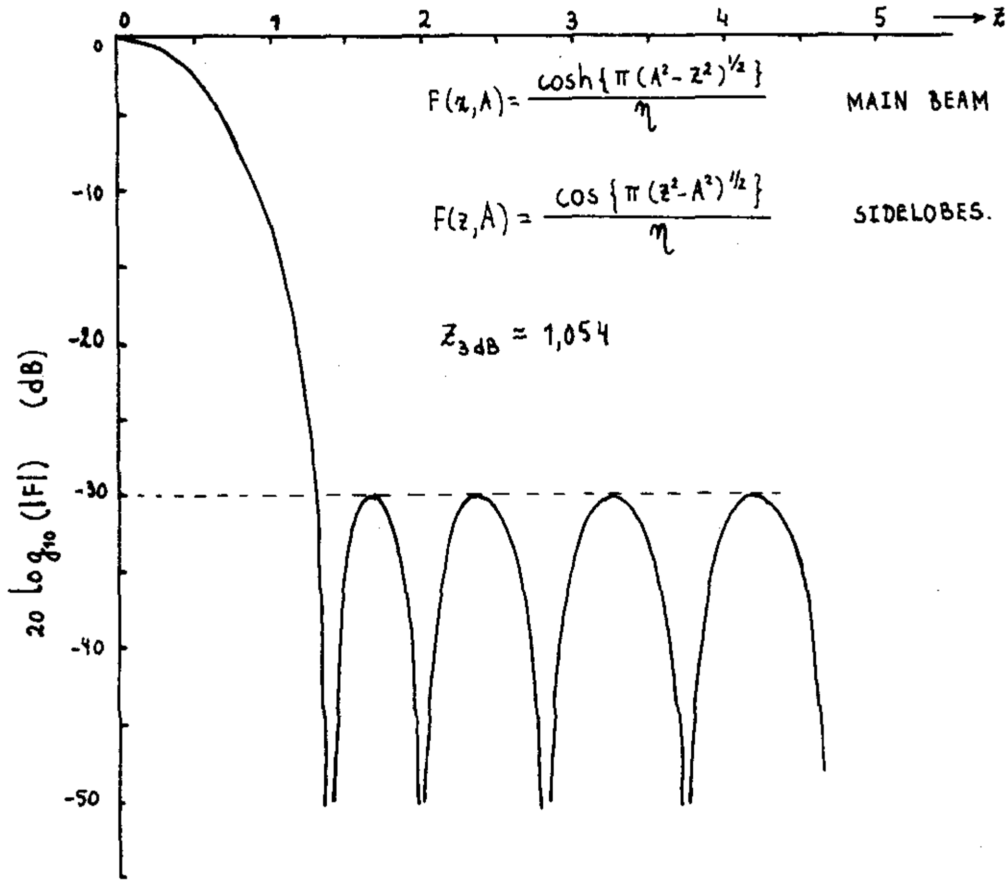

Fig. 2. An optimum pattern.

An approximation to the ideal pattern is realized by setting the first $\bar{n}-1$ sidelobes equal to each other while the remaining sidelobes decay as $(\sin\theta)^{-3/2}$. For higher values of $\bar{n}$ the approximation is closer and the beam-broadening factor tends to unity.

b. The zeros of the approximating pattern are $\sigma\sqrt{A^2+(n-\frac{1}{2})^2}$ with $n = 1,2,\ldots,\bar{n}-1, \bar{n}$ if $z \leqslant u_{\bar{n}}$. These are the zeros of $\cos\{\pi\sqrt{(\frac{z}{\sigma})^2-A^2}\}$. If $z \geqslant u_{\bar{n}}$ the zeros of the pattern are equal to the zeros of $J_1(\pi z)$. The beam-broadening factor σ coordinates the $\bar{n}$th zero of $\cos\{\pi\sqrt{(\frac{z}{\sigma})^2-A^2}\}$ and the $\bar{n}$th zero of $\frac{J_1(\pi z)}{\pi z}$, so that it can be computed from

$$\sigma = \frac{u_{\bar{n}}}{\sqrt{A^2+(\bar{n}-\frac{1}{2})^2}} \quad . \tag{1.7}$$

c. Taylor [11] uses a series of J_o-functions with a finite value at the aperture edge and adjusts the first zeros of the radiation pattern to the zeros of $\cos\{\pi\sqrt{(\frac{z}{\sigma})^2-A^2}\}$. Perhaps this kind of zeros can be employed if a series of J_o-functions is used with zero-edge values. In that case the radiation pattern is

$$F(z,A,\bar{n}) = \frac{J_o(\pi z)}{1-\frac{z^2}{u_o^2}} \prod_{n=1}^{\bar{n}-1} \left\{ \frac{1-\frac{z^2}{\sigma^2[A^2+(n-\frac{1}{2})^2]}}{1-\frac{z^2}{u_n^2}} \right\} \tag{1.8}$$

The aperture field is

$$g(p) = \sum_{m=0}^{\bar{n}-1} a_m J_o(u_m p) \ , \tag{1.9}$$

where πu_m is a zero of $J_o(\pi u) = 0$ and a_m is an excitation coefficient which equals

$$2\,\frac{F(z,A,\bar{n})\big|_{z=u_m}}{J_1^2(\pi u_m)} \quad . \tag{1.10}$$

Similar reasoning applies if the aperture field consists of the series

$$g(p) = \sum_{m=1}^{\bar{n}-1} a_m\{J_o(u_m p) - J_o(\pi u_m)\} \tag{1.11}$$

where πu_m is a zero of $J_1(\pi u) = 0$. In this case the zero $u_o = 0$ can be dropped. The radiation pattern is

$$F(z,A,\bar{n}) = \frac{2J_1(\pi z)}{\pi z(1-\frac{z^2}{u_1^2})} \prod_{n=2}^{\bar{n}-1} \left\{ \frac{1-\frac{z^2}{\sigma^2[A+(n-\frac{1}{2})^2]}}{1-\frac{z^2}{u_n^2}} \right\} \tag{1.12}$$

and the excitation coefficient a_m equals

$$2\,\frac{F(z,A,\bar{n})\big|_{z=u_m}}{J_o^2(\pi u_m)}\;. \tag{1.13}$$

The equations (1.8) and (1.12) have not been investigated further, because they don't allow individual sidelobes to be prescribed.

1.2. Results and conclusions

Equations (1.2), (1.3) and (1.4) have been programmed with $\bar{n}$ = 3,4,5 and 6, a design sidelobe level of -30 dB, and a design 3 dB beam width of 3 degrees.

In figures 6 - 9 the radiation patterns are shown together with the specifications (1.1). The computed sidelobe extrema, 3 dB beam width, aperture size and efficiency are also indicated. In figures 10 and 11 the accompanying aperture fields are shown.
The first $\bar{n}$-1 computed sidelobes are not exactly equal to each other. They decrease slightly with increasing distance from the main beam axis. The difference between the level of the first sidelobe and the design level is at least 0.4 dB.

One can notice that the decay rate of the far-out sidelobes is low. The efficiencies are high and range from 0.8377 to 0.8735.
With a prescribed sidelobe level of -30 dB and with $\bar{n}$ = 3,4,5 the computed copolar patterns fulfil the requirements imposed by eq. (1.1). If $\bar{n}$ = 6 the requirements are not fulfilled.

2. The method of Ishimaru and Held for the synthesis of radiation patterns from circular apertures

In order to be able to show the analogy between the method of Ishimaru and Held [5] and the further-developed methods and because we believe that the Ishimaru and Held paper has not been widely available we will deal with the relevant part of it briefly now.

Ishimaru and Held [5, part I] describe a method to synthesize a radiation pattern having a number of equal sidelobes. They want to realize a pattern approximating the optimum beam width sidelobe-level relationship. The optimum pattern has a minimum beam width for a given sidelobe level employing a given number of terms in the series expansion of the source field. After determining the level and the number N of the equal sidelobes, the first N zeros of the radiation pattern are computed.

The radiation pattern g(u) from a circular aperture with radius a is given by

$$g(u) = \int_0^1 f(r) J_0(ur) r\,dr \,, \tag{2.1}$$

where r is the normalized radial variable,
f(r) is the aperture distribution which is r-dependent only,
u equals $\frac{2\pi}{\lambda} a \sin\theta$ with θ the angle from broadside.

With N+1 terms in the aperture-field series expansion one can control N sidelobe levels. Assume that the field can be expanded in a series of Bessel functions,

$$\begin{aligned} f(r) &= \sum_{n=0}^{N} a_n J_0(u_n r) \qquad && \text{if} \quad 0 \leqslant r \leqslant 1 \\ &= 0 && \text{if} \quad r > 1 \,. \end{aligned} \tag{2.2}$$

The possible values of u_n are derived from the homogeneous boundary condition at r = 1

$$u_n J_0'(u_n) + h J_0(u_n) = 0 \tag{2.3}$$

where h is a constant.

An acceptable approximation of the optimum pattern can be obtained if the following requirements are fulfilled.

a. The zeros of the radiation pattern are real. Nonreal zeros tend to produce higher sidelobe levels and broader beam width.

b. The constant h is zero. Then the first zero of the radiation pattern is as near to the origin as possible.

c. The number N is finite. The lower limit follows from the desired level and the number of sidelobes higher than that level. The upper limit is mainly bounded by the supergain consideration.

With h=0 eq. (2.3) reduces to

$$J_o'(u_n) = -J_1(u_n) = 0 \tag{2.4}$$

so $u_o = 0$, $u_1 = 3.8317$, $u_2 = 7.0156$ etc. up to and including u_N. At $r = 1$ the value of the field is nonzero and that of the first derivative of the field is zero. A few source functions are shown in fig. 3.

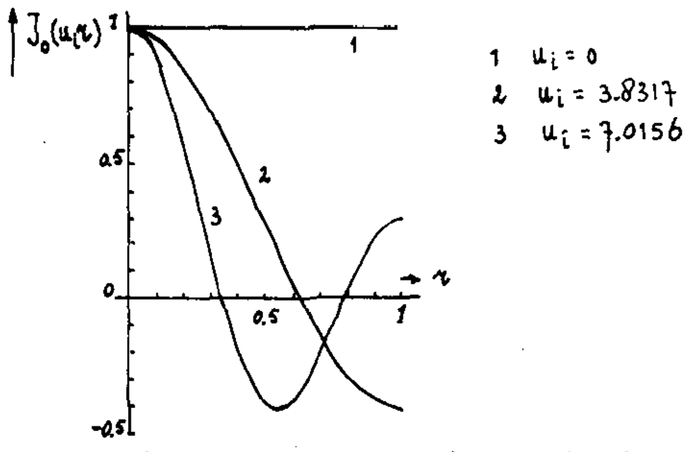

Fig. 3. Source functions $J_o(u_i r)$.

Substituting eq. (2.2) in the integral for the far field and employing eq. (2.4) yields

$$g(u) = \sum_{n=0}^{N} \left\{ -a_n u \frac{J_o(u_n)}{u_n^2 - u^2} J_1(u) \right\} \qquad \text{if} \quad u \neq u_n \tag{2.5}$$

$$= \tfrac{1}{2} a_n J_o^2(u_n) \qquad \text{if} \quad u = u_n \; . \tag{2.6}$$

After rewriting and normalizing eq. (2.5) the following form is obtained for the far field (see appendix A),

$$g(u) = \frac{2J_1(u)}{u} \prod_{n=1}^{N} \left\{ \frac{1-\dfrac{u^2}{(u_n+t_n)^2}}{1-\dfrac{u^2}{u_n^2}} \right\} \tag{2.7}$$

The first N zeros of the radiation pattern ($u<u_{N+1}$) are $u_n + t_n$ with $n = 1,2,\dots,N$. If $u \geqslant u_{N+1}$ the zeros of $g(u)$ are the zeros of $\dfrac{2J_1(u)}{u}$.

In the region $u_1 < u < u_{N+1}$ there are N sidelobes. Assume that the extrema occur in

$$u = M_n \quad \text{with} \quad n = 1,2,\dots,N. \tag{2.8}$$

The conditions for the optimum pattern are

$$|g(M_1)| = |g(M_2)| = \dots\dots\dots = |g(M_N)| = b \tag{2.9}$$

where b is the desired sidelobe level and g is given by eq. (2.7).

A relationship between the unknowns t_n, $n = 1,2,\dots,N$ and the desired sidelobe level is determined as follows.
If the variables t_n are small compared with u_n an expression for $g(M_n)$ can be deduced from eq. (2.7) which, together with eq. (2.9), yields N linear equations for N unknowns. Rewrite eq. (2.7) as

$$g(u) = \frac{2J_1(u)}{u} \prod_{n=1}^{N} \left\{ \frac{1+\dfrac{2u_n}{u_n^2-u^2}\,t_n + \dfrac{1}{u_n^2-u^2}\,t_n^2}{1+\dfrac{2}{u_n}\,t_n + \dfrac{1}{u_n^2}\,t_n^2} \right\}. \tag{2.10}$$

Assume that the terms with t_n^2 can be neglected and that the points M_n are located at about the middle of u_n and u_{n+1}. The remaining products in nominator and denominator can be approximated by series, so that

$$g(M_i) \approx \frac{2J_1(M_i)}{M_i} \cdot \frac{1+\sum\limits_{n=1}^{N} \dfrac{2u_n}{u_n^2-M_i^2}\,t_n}{1+\sum\limits_{n=1}^{N} \dfrac{2}{u_n}\,t_n} \tag{2.11}$$

with $i = 1,2,\dots,N$.

Assume that the points M_n are independent of t_n,

$$M_n = \frac{u_n+u_{n+1}}{2} . \tag{2.12}$$

Then eqs. (2.11) and (2.9) yield N linear equations for N unknowns t_n. If it is found that the variables t_n are not small enough to make eq. (2.11) valid and the optimum pattern is not approximated sufficiently closely, another set of variables t_n' can be computed. Assume that the first N zeros of the pattern closer to the optimum are $u_n+t_n+t_n'$. The pattern representation is

$$g_2(u) = \frac{2J_1(u)}{u} \prod_{n=1}^{N} \left\{ \frac{1-\dfrac{u^2}{(u_n+t_n+t_n')^2}}{1-\dfrac{u^2}{u_n^2}} \right\}$$

$$= \frac{2J_1(u)}{u} \prod_{n=1}^{N} \left\{ \frac{1-\dfrac{u^2}{(u_n+t_n+t_n')^2}}{1-\dfrac{u^2}{(u_n+t_n)^2}} \right\} \prod_{n=1}^{N} \left\{ \frac{1-\dfrac{u^2}{(u_n+t_n)^2}}{1-\dfrac{u^2}{u_n^2}} \right\}$$

$$= g_1(u) \prod_{n=1}^{N} \left\{ \frac{1-\dfrac{u^2}{(u_n+t_n+t_n')^2}}{1-\dfrac{u^2}{(u_n+t_n)^2}} \right\}, \tag{2.13}$$

if the first approximation to the optimum pattern is

$$g_1(u) = \frac{2J_1(u)}{u} \prod_{n=1}^{N} \left\{ \frac{1-\dfrac{u^2}{(u_n+t_n)^2}}{1-\dfrac{u^2}{u_n^2}} \right\}. \tag{2.14}$$

The eqs. (2.13) and (2.7) are similar. The procedure for computing t_n can also be used for t_n'. In eqs. (2.7) - (2.12) replace $\frac{2J_1(u)}{u}$ by $g_1(u)$, $u_n(+t_n)$ by $u_n+t_n(+t_n')$, t_n by t_n', $M_n = \frac{u_n+u_{n+1}}{2}$ by $M_n' = \frac{u_n+t_n+u_{n+1}+t_{n+1}}{2}$ and $\frac{2J_1(M_i)}{M_i}$ by $g_1(M_i')$.

The adjusted equation for $g(M_i)$ and the optimum condition (N equal sidelobes) yield N linear equations for N unknowns t_n'. As an example, a pattern is synthesized with three -25 dB sidelobes. The zeros of

$J_1(u)$ are assumed to be $u_0 = 0$, $u_1 = 3.83$, $u_2 = 7.016$ and $u_3 = 10.173$. The sidelobe extrema of $\frac{2J_1(u)}{u}$ are taken to be in $M_1 = 5.33$, $M_2 = 8.53$ and $M_3 = 11.70$. The -25 dB level means $b = 17.78^{-1}$. Solving for t_n, the first approximation is

$$g_1(u) = \frac{2J_1(u)}{u} \frac{[1-(\frac{u}{4.1625})^2][1-(\frac{u}{6.652})^2][1-(\frac{u}{9.620})^2]}{[1-(\frac{u}{3.83})^2][1-(\frac{u}{7.016})^2][1-(\frac{u}{10.173})^2]} . \qquad (2.15)$$

The first sidelobe of $g_1(u)$ is still higher than -25 dB so that it is necessary to compute t_n'. The improved pattern is

$$g_2(u) = \frac{2J_1(u)}{u} \frac{[1-(\frac{u}{4.2885})^2][1-(\frac{u}{6.561})^2][1-(\frac{u}{9.576})^2]}{[1-(\frac{u}{3.83})^2][1-(\frac{u}{7.016})^2][1-(\frac{u}{10.173})^2]} . \qquad (2.16)$$

The coefficients a_n are computed with

$$a_n = 2 \frac{g_2(u_n)}{J_o^2(u_n)} \qquad n = 1,2,\ldots,N. \qquad (2.17)$$

The aperture field which generates $g_2(u)$ is

$$f(r) = 2 + 0.935J_o(u_1 r) + 0.702J_o(u_2 r) - 1.10J_o(u_3 r). \qquad (2.18)$$

The coefficients we have computed differ from those given by Ishimaru and Held [5].

If the method of Taylor is used in synthesizing a radiation pattern with three -25 dB sidelobes one gets

$$g_T(u) = \frac{2J_1(u)}{u} \frac{[1-(\frac{u}{4.34})^2][1-(\frac{u}{6.57})^2][1-(\frac{u}{9.58})^2]}{[1-(\frac{u}{3.83})^2][1-(\frac{u}{7.016})^2][1-(\frac{u}{10.173})^2]} . \qquad (2.19)$$

The patterns $g_1(u)$, $g_2(u)$ and $g_T(u)$ are shown in figs. 12 and 13. The first zero of $g_2(u)$ is nearer to the origin than the first zero of $g_T(u)$ so that $g_2(u)$ has the minimum beam width. For $g_2(u)$ and $g_T(u)$ the deviations from the required levels are of the same magnitude.

The maximum gain G is given by

$$G = \frac{8\pi^2 a^2}{\lambda^2} \frac{\left|\int_o^1 f(r) r dr\right|^2}{\int_o^1 |f(r)|^2 r dr} . \qquad (2.20)$$

Substituting for f(r) yields

$$G = \frac{8\pi^2 a^2}{\lambda^2} \frac{g^2(0)}{\sum\limits_{n=0}^{N} \frac{1}{2} a_n J_o^2(u_n)} \; . \tag{2.21}$$

Using $2a = D$ and $a_n = \dfrac{2g(u_n)}{J_o^2(u_n)}$ results in

$$G = \left(\frac{\pi D}{\lambda}\right)^2 \frac{g^2(0)}{\sum\limits_{n=0}^{N} \dfrac{g^2(u_n)}{J_o^2(u_n)}} \; . \tag{2.22}$$

3. The modified methods with other source functions

3.1. Source functions with a zero edge field and a nonzero first derivative of the edge field

In this section we will employ the source functions which arise on the assumption $h = \infty$ in eq. (2.3). The aperture field $f(r)$ consists of a series of Bessel functions

$$f(r) = \sum_{n=0}^{N} a_n J_o(u_n r) \qquad 0 \leqslant r \leqslant 1 ,$$
$$= 0 \qquad r > 1 . \tag{3.1}$$

If $h = \infty$ the homogeneous boundary condition, eq. (2.3), reduces to

$$J_o(u_n) = 0 . \tag{3.2}$$

The possible values of u_n are now $u_0 = 2.4048$, $u_1 = 5.5201$ etc. up to and including u_N. A few source functions are shown in fig. 4.

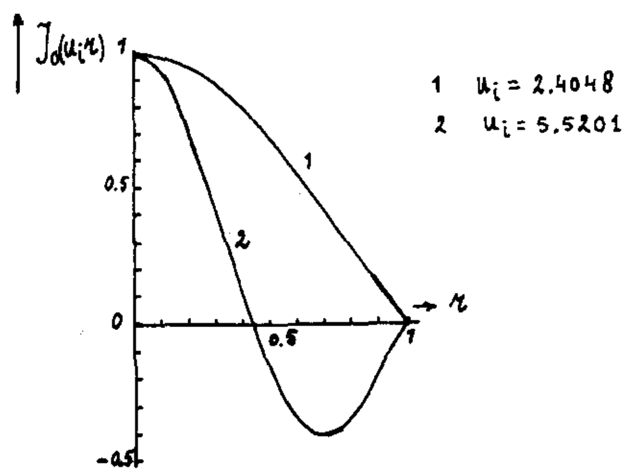

Fig. 4. Source functions $J_o(u_i r)$.

N sidelobe levels can be controlled with N+1 source functions. The far field is

$$g(u) = \int_o^1 f(r) J_o(ur) r dr \tag{2.1}$$

and with eq. (3.1) and eq. (3.2) $g(u)$ is computed as

$$g(u) = \sum_{n=0}^{N} \{a_n \frac{u_n}{u_n^2 - u^2} J_1(u_n) J_o(u)\} \qquad \text{if } u \neq u_n \tag{3.3}$$

$$g(u) = \tfrac{1}{2} a_n J_1^2(u_n) \qquad \text{if } u = u_n. \tag{3.4}$$

Rewriting and normalizing eq. (3.3) in the same way as eq. (2.5) gives

$$g(u) = J_o(u) \frac{\prod_{n=1}^{N} \left\{1 - \frac{u^2}{(u_n+t_n)^2}\right\}}{\prod_{n=0}^{N} \left\{1 - \frac{u^2}{u_n^2}\right\}}. \tag{3.5}$$

If $u \geqslant u_{N+1}$ the zeros of g(u) are the zeros of $J_o(u) = 0$. If $u < u_{N+1}$ the zeros of g(u) are u_n+t_n, $n = 1,2,\dots,N$. To show the analogy with the far field where h = 0, eq. (3.5) is written as

$$g(u) = \frac{J_o(u)}{1-\frac{u^2}{u_o^2}} \prod_{n=1}^{N} \left\{\frac{1-\frac{u^2}{(u_n+t_n)^2}}{1-\frac{u^2}{u_n^2}}\right\} \tag{3.6}$$

The factor $\frac{J_o(u)}{1-\frac{u^2}{u_o^2}}$ is proportional to the field of $J_o(u_o r)$ shown in fig. 14. The first sidelobe is -27.5 dB and the second is -36.4 dB down. The zeros, the efficiency and the 3 dB beam width are also indicated. The changes in the aperture field can be small in order to lower the first sidelobe to -30 dB, for instance.

Where h = 0 the expression for the far field is

$$g(u) = \frac{2J_1(u)}{u} \prod_{n=1}^{N} \left\{\frac{1-\frac{u^2}{(u_n+t_n)^2}}{1-\frac{u^2}{u_n^2}}\right\} \tag{2.7}$$

The factor $\frac{2J_1(u)}{u}$ is proportional to the field of the uniformly illuminated aperture. The first sidelobes are -17.6 dB and -23.8 dB down. Write eq. (3.6) as

$$g(u) = \frac{J_o(u)}{1-\frac{u^2}{u_o^2}} \prod_{n=1}^{N} \left\{\frac{1+\frac{2u_n}{u_n^2-u^2} t_n + \frac{1}{u_n^2-u^2} t_n^2}{1+\frac{2}{u_n} t_n + \frac{1}{u_n^2} t_n^2}\right\}. \tag{3.7}$$

In order to determine a relationship between the variables t_n and the prescribed sidelobe extrema we proceed in the same way as in section 2. Assume that the extrema occur at the points M_i at about the middle of u_i and u_{i+1}. Assume t_n is small compared to u_n so that terms with t_n^2 can be dropped. The products in nominator and denominator can be replaced by series and

$$g(M_i) \approx \frac{J_o(M_i)}{1 - \frac{M_i^2}{u_o^2}} \cdot \frac{1 + \sum_{n=1}^{N} \frac{2u_n}{u_n^2 - M_i^2} t_n}{1 + \sum_{n=1}^{N} \frac{2}{u_n} t_n} \tag{3.8}$$

with $i = 1,2,\ldots,N$.

We introduce the following conditions for the sidelobe levels

$$\begin{aligned} |g(M_1)| &= b_1 \\ &\vdots \\ |g(M_N)| &= b_N \end{aligned} \tag{3.9}$$

N equal sidelobes is a special case of eq. (3.9). The points M_n are taken to be independent of t_n

$$M_n = \frac{u_n + u_{n+1}}{2} . \tag{3.10}$$

Then the equations (3.8) and (3.9) provide N linear equations for N unknowns t_n. The first approximation $g_1(u)$ to the desired pattern is

$$g_1(u) = \frac{J_o(u)}{1 - \frac{u^2}{u_o^2}} \prod_{n=1}^{N} \left\{ \frac{1 - \frac{u^2}{(u_n + t_n)^2}}{1 - \frac{u^2}{u_n^2}} \right\} . \tag{3.11}$$

If this approximation deviates too much one can introduce the variables t_n' to describe the better pattern $g_2(u)$

$$g_2(u) = \frac{J_o(u)}{1 - \frac{u^2}{u_o^2}} \prod_{n=1}^{N} \left\{ \frac{1 - \frac{u^2}{(u_n + t_n + t_n')^2}}{1 - \frac{u^2}{u_n^2}} \right\}$$

$$= g_1(u) \prod_{n=1}^{N} \left\{ \frac{1 - \dfrac{u^2}{(u_n+t_n+t'_n)^2}}{1 - \dfrac{u^2}{u_n^2}} \right\} . \tag{3.12}$$

The computation of t'_n follows the same lines as the computation of t_n due to the similarity of eq. (3.12) and eq. (3.6).

In eqs. (3.6) - (3.11) replace $J_o(u)/(1-\frac{u^2}{u_o^2})$ by $g_1(u)$, $u_n(+t_n)$ by $u_n+t_n(+t'_n)$ t_n by t'_n, $M_n = \frac{u_n+u_{n+1}}{2}$ by $M'_n = \frac{u_n+t_n+u_{n+1}+t_{n+1}}{2}$ and $J_o(M_i)/(1-\frac{M_i^2}{u_o^2})$ by $g_1(M'_i)$

Again N linear equations are obtained for N variables and the t'_n are easily solved.

Instead of eq. (3.10) one can also use

$$M_n = \frac{u_n+d_n u_{n+1}}{2} \tag{3.13}$$

where $d_n \lesssim 1$. Then the points M_n can be chosen in better agreement with the real positions of the sidelobe extrema. The weight factors d_n can be estimated from the pattern of $J_o(u_o r)$.

The excitation coefficients a_n are computed with

$$a_n = 2\, \frac{g(u_n)}{J_1^2(u_n)} \qquad n = 0,1,2,\ldots,N. \tag{3.14}$$

The maximum gain G is derived from

$$G = \frac{8\pi^2 a^2}{\lambda^2} \, \frac{\left|\int_o^1 f(r)r dr\right|^2}{\int_o^1 |f(r)|^2 r dr} . \tag{2.20}$$

Substituting the source functions we are concerned with, yields

$$G = \frac{8\pi^2 a^2}{\lambda^2} \, \frac{g^2(0)}{\sum_{n=0}^{N} \frac{1}{2} a_n^2 J_1^2(u_n)} \tag{3.15}$$

and with $2a = D$ and eq. (3.14),

$$G = \left(\frac{\pi D}{\lambda}\right)^2 \frac{g^2(0)}{\sum\limits_{n=0}^{N} \frac{g^2(u_n)}{J_1^2(u_n)}} \quad . \tag{3.16}$$

The difference $\Delta g(dB)$ between the normalized power patterns of $J_o(u_o r)$ and $\sum\limits_{n=0}^{N} a_n J_o(u_n r)$ for large values of u is estimated as

$$\Delta g(dB) \approx 40 \sum_{n=1}^{N} {}^{10}\log\left(1+\frac{t_n}{u_n}\right) \quad . \tag{3.17}$$

With suitable values of the variables b_i in eq. (3.9) the pattern envelopes can be made to fulfil, for instance, the specifications for earth-station antennas [2]. The following requirements for G_i, the gain relative to isotropic, are represented in fig. 15:

$$\text{I} \quad G_i = 32 - 25 * \log(\theta^o) \quad \text{dB} \tag{3.18a}$$

$$\text{II} \quad G_i = 32 - 30 * \log(\theta^o) \quad \text{dB} \tag{3.18b}$$

$$\text{III} \quad G_i = 32 - 35 * \log(\theta^o) \quad \text{dB} \tag{3.18c}$$

$$\text{IV} \quad G_i = 25 - 25 * \log(\theta^o) \quad \text{dB} \tag{3.18d}$$

These formulas are assumed to apply to the region beyond the first sidelobe peak, that is at and beyond $\theta(\text{degr}) \approx 100 \frac{\lambda}{D}$, until -10 dB relative to isotropic is reached.

3.2. Results and conclusions

The method described in section 3.1. is used to compute a number of radiation patterns. In figs. 16-20 we represent computed patterns and aperture distributions if only the first sidelobe is prescribed at a certain level. Furthermore, some zeros, the efficiency, the gain reduction relative to the uniformly illuminated aperture, the 3 dB beam width and the excitation coefficients are indicated. If we compare these 5 patterns with each other and with the 'reference' pattern of fig. 14 (no sidelobes prescribed) we note that:

- The deviation between the prescribed and computed level increases if the difference between the required level and the level of the first sidelobe of the 'reference' pattern is increased. The deviations in the first approximation patterns are less than 0.9 dB.
- Increasing the first sidelobe, relative to the 'reference' pattern,

results in a shift of the first zero u_1+t_1 towards the origin, an increase of the efficiency and a decrease of the 3 dB beam width. The shift of the first zero results in opposite signs for the excitation coefficients a_o and a_1.

- Lowering the first sidelobe, relative to the 'reference' pattern, results in a shift of the first zero u_1+t_1 away from the origin, a decrease of the efficiency and an increase of the 3 dB beam width. The shift of the first zero now results in a_o and a_1 having the same sign.
- For greater values of the difference between the prescribed level and the level of the first sidelobe of the 'reference' pattern, the shift of the first zero as well as the ratio of the excitation coefficients $|\frac{a_1}{a_o}|$ are greater.
- The difference between the first and the second sidelobe level of a pattern decreases if the level of the first sidelobe is decreased.
- The estimated differences Δg, eq. (3.17), range from -4.05 dB to 2.11 dB. These values are computed for the -17.0 dB and the -35.1 dB sidelobe patterns. The differences between the computed and the 'reference' pattern range from -4.4 dB to 2.2 dB for the fifth sidelobe. Hence the value of Δg is almost reached at $u \approx 20$.
- The decay of the sidelobe extrema is greater than the decay of G_i, eq. (3.18a-d). These specifications are therefore fulfilled if the peak of the first sidelobe is below the curves I - IV of fig. 15 when the gain reduction is taken into account.
- If the first sidelobe is prescribed to have a higher (lower) value than the first lobe of the 'reference' pattern, the normalized aperture field for $0 < r < 1$ is higher (lower) than the aperture field generating the 'reference' pattern.

In figs. 21-25 we represent computed patterns and aperture distributions if two or more sidelobes are prescribed to have equal levels. In most cases it is necessary to compute a second approximation because the levels in the first approximation deviate more than 1 dB (otherwise an arbitrarily chosen value) from the required levels. The results of each approximation are indicated: the computed levels, the zeros, the excitation coefficients, the efficiency, the gain reduction relative to a uniformly illuminated aperture and the 3 dB beam width. If we compare the pattern with three -25 dB sidelobes of fig. 21 with those of figs. 12 and 13 we observe that the sidelobe levels not prescribed are lower and decay faster, and that the 3 dB beam width has increased (the first zero of the pattern is further away from the origin). These effects are due to the fact that we are now dealing with zero-edge aperture fields. If we compare the patterns of figs. 22-25, having two or more sidelobes prescribed to have the -30 dB level, with the Taylor patterns of figs. 6-9 we note that the required levels are now reached more accurately, that the 3 dB beam widths are greater and that the sidelobes not prescribed are lower and decay faster. The efficiencies are lower than in the case of the Taylor patterns. If we look at the accompanying aperture distributions we see that the Taylor distributions (figs. 10 and 11) are smoother, which is imputed to the different source functions and to the fact that the sidelobes of the Taylor patterns are actually decaying instead of being equal. If we compare the patterns in figs. 22-25 with each other we see that with an increasing number of equal sidelobes the zeros have shifted more and more towards the origin, the 3 dB beam width is decreased and efficiency is increased. With N-1 prescribed sidelobes the width of the lobes 1 up to and including N-1 increases. For instance in fig. 25 these widths are successively 2.22, 2.80, 3.34, 3.57 and 4.26. The width of sidelobes not prescribed is always equal to the distance between the zeros of $J_o(u)$, which is approximately 3.14.

The requirements set by eq. (3.18a-d) are not all fulfilled. The patterns of figs. 22-24 meet a-d, a-c and a-b, respectively, while the pattern of fig. 25 meets none of these requirements.

In figs. 26-33 we show computed patterns, aperture distributions and other relevant data when, starting at different levels for the first sidelobe, the decay rate of the first 3 or 4 extrema is prescribed. Once again, if there is a deviation of more than 1 dB between a required and a computed level a second approximation is made. Decay rates of 4,5,6,7 and 8 dB are required and the starting levels are -30, -33, -36 and -48 dB. However, not all the combinations of rates and levels are investigated. At the cost of the efficiency and with increasing 3 dB beam width the starting level can be decreased and the decay rate can be increased.

All the diagrams shown meet the requirements of eq. (3.18a-d).

The computed differences Δg according to eq. (3.17) for the patterns of fig. 26 and fig. 33 are, respectively, 0.2 dB and 7.8 dB. These final values are almost reached at the fifth sidelobe extrema ($u \approx 20$) because the actual differences (compare with fig. 14) are 0.3 dB and 9.4 dB.

The normalized aperture distributions for the described patterns are smooth functions which, for $0 < r < 1$, are lower than the distributions for the pattern with none of the sidelobes prescribed (fig. 14).

Finally, in figs. 34-36 some cases are illustrated in which the first sidelobe is required to be lower than the second. We observe that the required levels are reached within the 1 dB limit in the second approximation, except the -50 dB level in fig. 36.
The 3 dB beam widths are increased and the efficiencies are decreased compared with the pattern of fig. 14. The differences Δg according to eq. (3.17) and the actual differences to the pattern of fig. 14 at $u \approx 20$ are equal for these three patterns. They are respectively -0.3, 0.2 and 1.6 dB.

The patterns meet the specifications imposed by the equations (3.18a-d).

The normalized aperture distributions for these patterns are smooth functions having lower values for $0 < r < 1$ than the distribution $J_o(u_o r)$ shown in fig. 14.

In conclusion we can say that the method described in section 3.1. is flexible, accurate and capable of handling several types of sidelobe envelopes. The source functions having zero-edge values ensure a more rapid decay of the sidelobes not prescribed than do the distributions with non-zero edge values.

3.3. Source functions with both the field and the first derivative of the field equal to zero at r = 1

The aperture field is taken to be a series of the form

$$f(r) = \sum_{n=1}^{N} a_n\{J_o(u_n r)-J_o(u_n)\} \qquad 0 \leqslant r \leqslant 1 \,,$$
$$= 0 \qquad r > 1 \,, \tag{3.19}$$

where the values of u_n are determined by

$$J_1(u_n r) = 0 \quad \text{at} \quad r = 1. \tag{3.20}$$

The normalized source functions with $u_1 = 3.8317$ and $u_2 = 7.0156$ are shown in fig. 5.

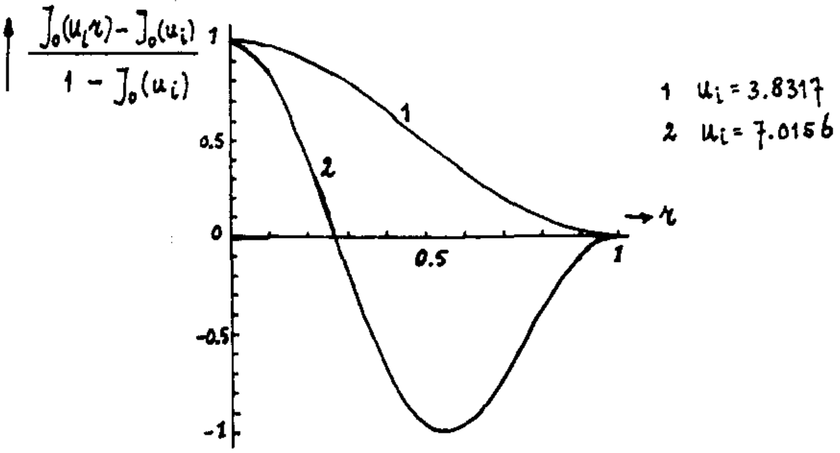

Fig. 5. Source functions.

With N source functions, N-1 sidelobe levels can be controlled.

Now the radiation pattern of a circular aperture is

$$g(u) = \sum_{n=1}^{N} \left\{\frac{-a_n u_n^2}{(u_n^2-u^2)u}\right\} J_o(u_n)J_1(u) \qquad \text{if} \quad u \neq u_n \,, \tag{3.21}$$

$$= \tfrac{1}{2}a_n J_o^2(u_n) \qquad \text{if} \quad u = u_n \,. \tag{3.22}$$

Eq. (3.21) can be written in a form similar to eq. (2.7) and eq. (3.6), namely

$$g(u) = \frac{2J_1(u)}{u(1-\frac{u^2}{u_1^2})} \prod_{n=2}^{N} \left\{ \frac{1-\frac{u^2}{(u_n+t_n)^2}}{1-\frac{u^2}{u_n^2}} \right\} \tag{3.23}$$

The factor $2J_1(u)/u(1-\frac{u^2}{u_1^2})$ is proportional to the field of the aperture distribution $J_o(u_1 r) - J_o(u_1)$, see fig. 37. The first sidelobe is -35.1 dB down.

Assume that the variables t_n are small compared to u_n and the sidelobe extrema occur in the points M_i at about the middle of u_i and u_{i+1}. Suppose further that the points M_i are independent of the variables t_n. It will be evident from the foregoing treatment in sections 2 and 3.1. that N-1 linear equations for N-1 unknowns t_n are deduced from the approximation

$$g(M_i) \approx \frac{2J_1(M_i)}{M_i(1-\frac{M_i^2}{u_1^2})} \cdot \frac{1+\sum_{n=2}^{N} \frac{2u_n}{u_n^2-M_i^2} t_n}{1+\sum_{N=2}^{N} \frac{2}{u_n} t_n} \tag{3.24}$$

with $i = 1,2,\ldots,N-1$ and the condition

$$\begin{array}{l} |g(M_1)|=b_1 \\ \vdots \\ |g(M_{N-1})|=b_{N-1} \end{array} \tag{3.25}$$

The variables b_1-b_{N-1} are the prescribed sidelobe levels. The first approximation $g_1(u)$ to the desired pattern is

$$g_1(u) = \frac{2J_1(u)}{u(1-\frac{u^2}{u_1^2})} \prod_{n=2}^{N} \left\{ \frac{1-\frac{u^2}{(u_n+t_n)^2}}{1-\frac{u^2}{u_n^2}} \right\} \quad . \tag{3.26}$$

If the sidelobe levels of $g_1(u)$ differ too much from the desired levels, the variables t_n' are introduced to make the computation of the better approximation $g_2(u)$ possible,

$$g_2(u) = g_1(u) \prod_{n=2}^{N} \left\{ \frac{1-\dfrac{u^2}{(u_n+t_n+t'_n)^2}}{1-\dfrac{u^2}{(u_n+t_n)^2}} \right\} . \tag{3.27}$$

Eq. (3.27) and eq. (3.23) are similar so that the scheme used to relate linearly the sidelobe levels and the variables t_n can be employed to do the same for the levels and the variables t'_n.

After the desired pattern has been obtained the excitation coefficients a_n are computed from

$$a_n = \frac{2g(u)\big|_{u=u_n}}{J_o^2(u_n)} \qquad \text{with } n = 1,2,\ldots,N. \tag{3.28}$$

The maximum gain G for the aperture with radius a is

$$G = \frac{8\pi^2 a^2}{\lambda^2} \frac{\left|\int_o^1 f(r)rdr\right|^2}{\int_o^1 |f(r)|^2 rdr} . \tag{2.20}$$

With the applied source functions, 2a = D and eq. (3.28) G becomes

$$G = \left(\frac{\pi D}{\lambda}\right)^2 \frac{g^2(0)}{\left\{\sum_{n=1}^{N} \dfrac{g(u_n)}{J_o(u_n)}\right\}^2 + \sum_{n=1}^{N} \dfrac{g^2(u_n)}{J_o^2(u_n)}} . \tag{3.29}$$

An estimate for the difference Δg(dB) between the extrema of the normalized power patterns of $\{J_o(u_1r)-J_o(u_1)\}$ and $\sum_{n=1}^{N} a_n\{J_o(u_nr)-J_o(u_n)\}$ is for great values of u

$$\Delta g(\text{dB}) \approx 40 \sum_{n=2}^{N} {}^{10}\log\left(1+\frac{t_n}{u_n}\right) . \tag{3.30}$$

3.4. Results and conclusions

The method of section 3.3. is used in the numerical computation of several radiation patterns.

In figs. 38 and 39 we show the patterns having the first sidelobe prescribed at -30 dB and -33 dB, respectively. These levels are higher than the -35.1 dB level of the pattern of $J_o(u_1r) - J_o(u_1)$, fig. 37, which for the moment, is the 'reference' pattern. The first zero of each of the patterns shifts towards the origin, the 3 dB beam width decreases and the efficiency increases relative to the 'reference' pattern. Because of the shift towards the origin, the excitation coefficients a_1 and a_2 have opposite signs.

The differences Δg according to eq. (3.30) are for the patterns of fig. 38 and fig. 39, -1.6 dB and -0.6 dB, respectively, while the actual differences for the fifth sidelobes are respectively -1.8 dB and -0.7 dB.

The patterns meet the requirements imposed by the equation (3.18a-d).

The normalized aperture fields for $0 < r < 1$ are somewhat higher than the aperture field for the 'reference' pattern.

For equal sidelobes we have given some examples in figs. 40-44. In some of these cases even a second approximation does not allow us to obtain differences between required and computed levels less than 1 dB. The diagrams shown have two or more equally prescribed sidelobes. The efficiencies are higher and the 3 dB beam widths are lower than in the case of the 'reference' pattern. With two -30 dB or -40 dB lobes the required levels are adequately approximated and the aperture fields remain rather smooth. With three or more -30 dB sidelobes the required levels are not reached in two approximations and the aperture fields are not very smooth. Apparently the changes in the levels relative to the 'reference' pattern are too great, and although the method is capable of handling more than two approximations, no more than two have been carried out.

In figs. 45-48 we show some computed patterns, aperture distributions and relevant data, starting at different levels for the first sidelobe. The decay rate of the first three extrema is prescribed. Now the deviations between required and computed levels are less than 1 dB with one or two approximations. The efficiencies and 3 dB beam widths differ little from the 'reference' values (fig. 37) 0.5 and 4.8 due to the chosen sidelobe levels.

The patterns meet the requirements of eq. (3.18a-d).

The differences Δg according to eq. (3.30), computed for instance for the patterns of figs. 47 and 48, are respectively 2.3 dB and 1.2 dB. The actual differences at the fifth sidelobe extrema are 2.4 dB and 1.2 dB.

The normalized aperture fields of figs. 45-48 are smooth and have changed little compared to the aperture distribution of fig. 37.

In fact many more cases could be handled but the results and observations would be similar to those of section 3.2. The differences are found in the magnitude of some characteristics. If patterns with the same prescribed levels are synthesized with the source functions of section 3.1. and section 3.3., then with the last-named we find the following:

- the zeros of the radiation pattern are further away from the origin, so that the 3 dB beam width is greater;
- the efficiency is lower;
- the sidelobes not prescribed are lower and decay faster.

This is clearly demonstrated in the patterns of figs. 45 and 31 for sidelobes prescribed at -36, -41 and -46 dB and in the patterns of figs. 47 and 33 for sidelobes prescribed at -48, -52 and -56 dB.

In conclusion, we can say also that the method described in section 3.3., using source functions with both the field and the first derivative of the aperture field equal to zero at $r = 1$ enables us to prescribe several types of sidelobe envelopes. These source functions ensure an even more rapid decay of the unprescribed sidelobes than do the source functions with only the field values equal to zero at $r=1$.

References

[1] Borgiotti, G.
DESIGN OF CIRCULAR APERTURES FOR HIGH BEAM EFFICIENCY AND LOW SIDELOBES. Alta Frequenza, Vol. 40 (1971), No. 8, p. 652-657.

[2] C.C.I.R. Recommendation 465-1. REFERENCE EAERTH STATION RADIATION PATTERN FOR USE IN COORDINATION AND INTERFERENCE ASSESSMENT IN THE FREQUENCY RANGE FROM 2 TO ABOUT 10 GHz. In: C.C.I.R. XIIIth Plenary Assembly, Geneva, 1974. P. 155-156. Geneva: International Telecommunication Union, 1975.

[3] FINAL ACTS OF THE WORLD ADMINISTRATIVE RADIO CONFERENCE FOR THE PLANNING OF THE BROADCASTING-SATELLITE SERVICE IN FREQUENCY BANDS 11.7-12.2 GHz (IN REGIONS 2 AND 3) AND 11.7-12.5 GHz (IN REGION 1). Geneva: International Telecommunication Union, 1977. P. 102.

[4] Hansen, R.C.
TABLES OF TAYLOR DISTRIBUTIONS FOR CIRCULAR APERTURE ANTENNAS. IRE Trans. Antennas and Propagation, Vol. AP-8 (1960), No. 1, p. 23-26.

[5] Ishimaru, A. and G. Held
ANALYSIS AND SYNTHESIS OF RADIATION PATTERNS FROM CIRCULAR APERTURE. Canadian Journal of Physics, Vol. 38 (1960), No. 1, p. 78-99.

[6] Kouznetsov, V.D.
SIDELOBE REDUCTION IN CIRCULAR APERTURE ANTENNAS. In: Int. Conf. on Antennas and Propagation; London, 28-30 Nov. 1978. IEE Conf. Publication, No. 169. London: Institution of Electrical Engineers, 1978. P. 422-427.

[7] Kritskiy, S.V. and M.T. Novosartov
DERIVATION OF THE OPTIMUM FIELD DISTRIBUTIONS FOR ANTENNAS WITH A CIRCULAR APERTURE. Radio Engineering and Electronic Physics, Vol. 19 (1974), No. 5, p. 23-30.

[8] Mironenko, I.G.
SYNTHESIS OF A FINITE-APERTURE ANTENNA MAXIMIZING THE FRACTION OF POWER RADIATED IN A PRESCRIBED SOLID ANGLE. Telecommunications and Radio Engineering, Vol. 21-22 (1967), No. 4, p. 99-104.

[9] Rudduck, R.C., D.C.F. Wu and R.F. Hyneman
DIRECTIVE GAIN OF CIRCULAR TAYLOR PATTERNS. Radio Science, Vol. 6 (1971), No. 12, p. 1117-1121.

[10] Taylor, T.T.
DESIGN OF CIRCULAR APERTURES FOR NARROW BEAMWIDTH AND LOW SIDELOBES. IRE Trans. Antennas and Propagation, Vol. AP-8 (1960), No. 1, p. 17-22.

Appendix A

Derivation of eq. (2.7).

Start with eq. (2.5) for the far field g(u). Use $J_o(u_o)=J_o(0) = 1$, then g(u) becomes

$$g(u) = J_1(u) \sum_{n=0}^{N} \frac{-a_n u J_o(u_n)}{u_n^2-u^2} =$$

$$= \frac{J_1(u)}{u}\left[a_o - \frac{a_1 u^2 J_o(u_1)}{u_1^2-u^2} - \ldots\ldots\ldots - \frac{a_N u^2 J_o(u_N)}{u_N^2-u^2}\right]$$

$$= \frac{J_1(u)}{u}\left[a_o - \frac{a_1 \frac{1}{u_1^2} J_o(u_1)}{1-\frac{u^2}{u_1^2}} - \ldots\ldots\ldots - \frac{a_N \frac{1}{u_N^2} J_o(u_N)}{1-\frac{u^2}{u_N^2}}\right]$$

$$= \frac{J_1(u)}{u}\left[\frac{a_o(1-\frac{u^2}{u_1^2})\ldots(1-\frac{u^2}{u_N^2}) - \ldots - a_N\frac{1}{u_N^2}J_o(u_N)(1-\frac{u^2}{u_1^2})\ldots(1-\frac{u^2}{u_{N-1}^2})}{(1-\frac{u^2}{u_1^2})\ldots(1-\frac{u^2}{u_N^2})}\right]$$

The nominator of the form between brackets is a polynomial in u^2 of order N, the zeros of which can be expressed by $(u_n+t_n)^2$ with $n=1,2,\ldots,N$, so that g(u) can be written as

$$g(u) = \frac{2J_1(u)}{u} \prod_{n=1}^{N} \left\{\frac{1-\frac{u^2}{(u_n+t_n)^2}}{1-\frac{u^2}{u_n^2}}\right\} \qquad (2.7)$$

if at the same time g(0) is normalized to 1.

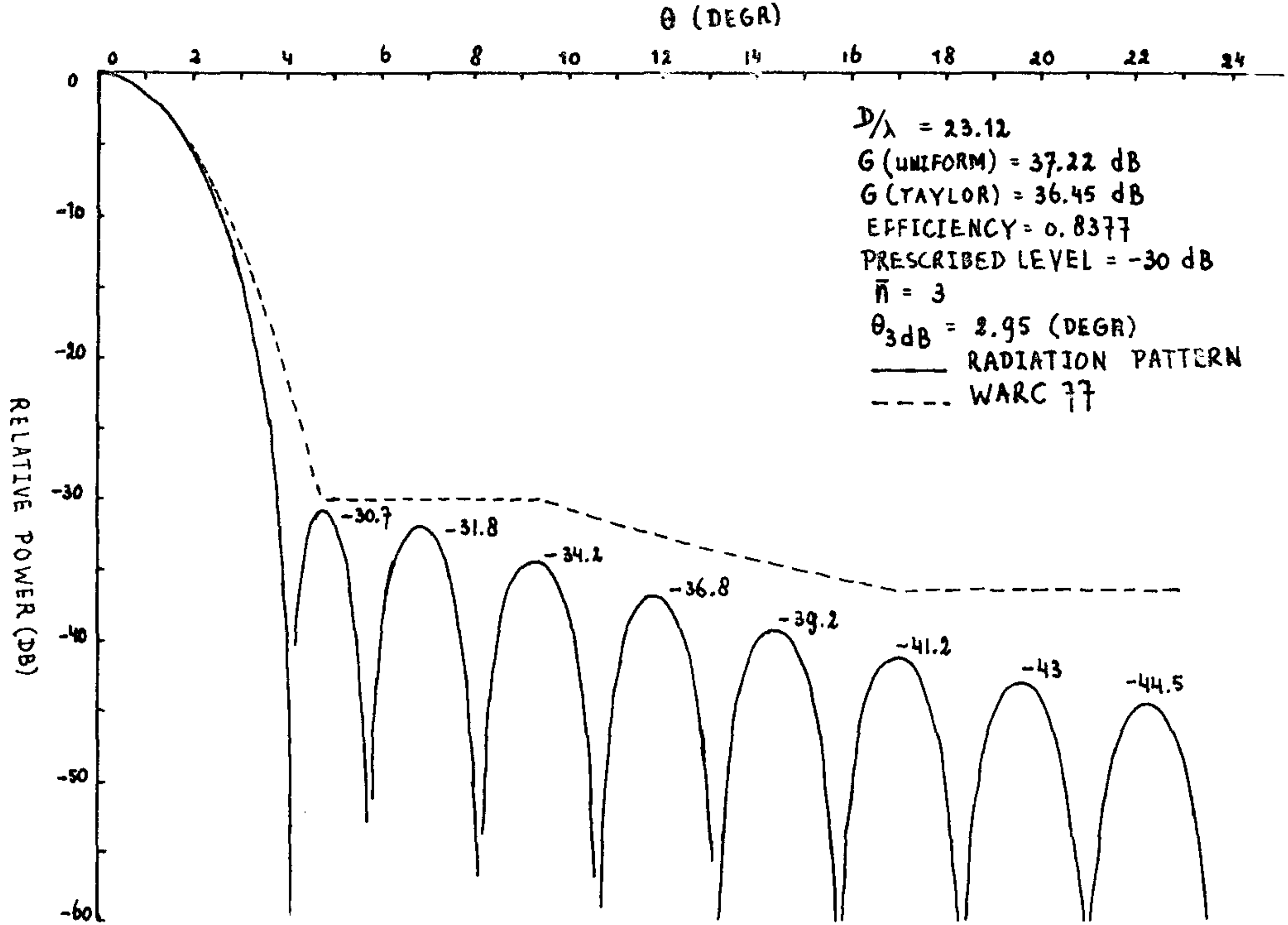

FIG. 6 : TAYLOR CIRCULAR APERTURE PATTERN FOR -30 dB SIDELOBES WITH $\bar{n} = 3$.

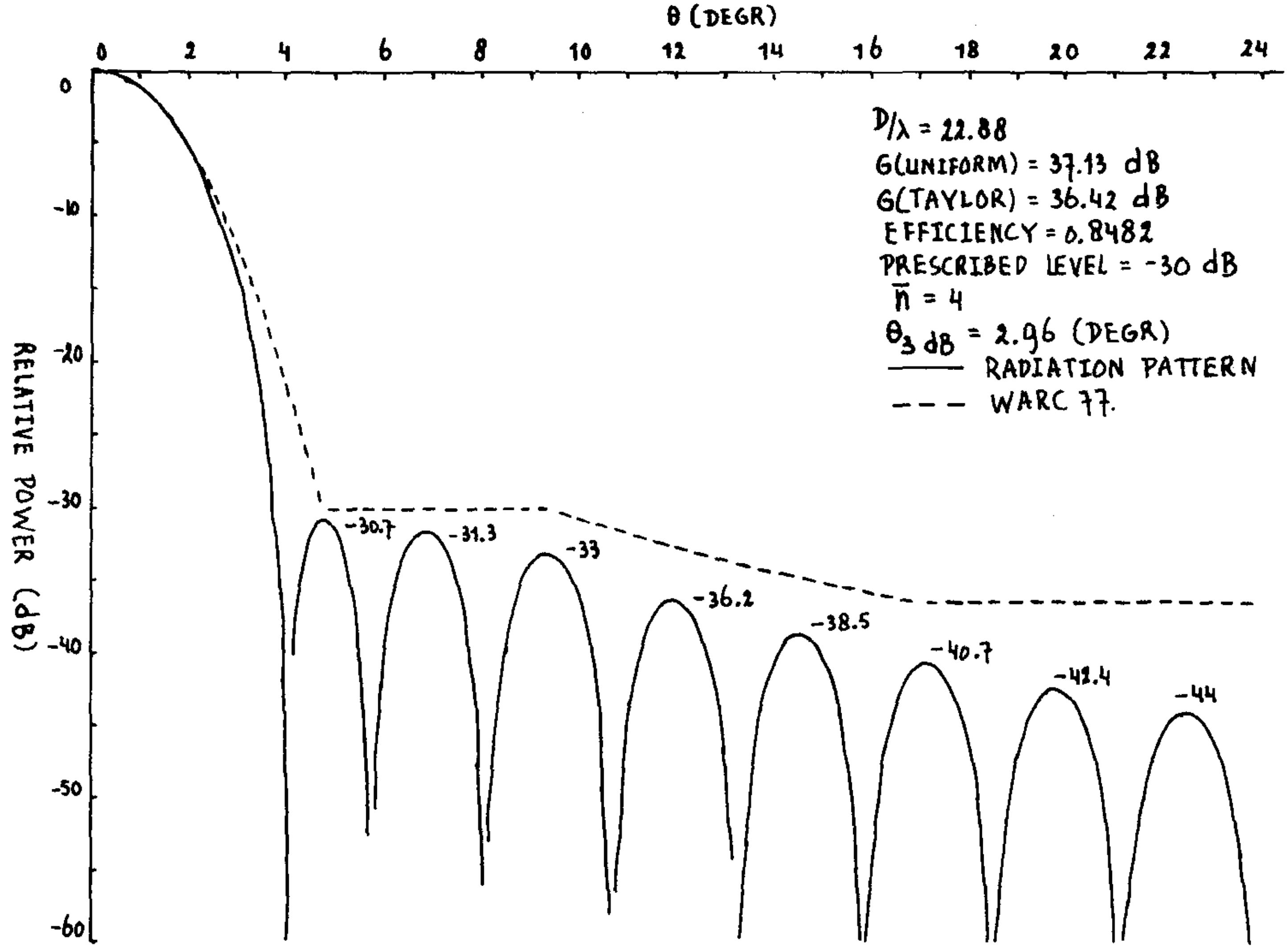

FIG. 7 : TAYLOR CIRCULAR APERTURE PATTERN FOR -30 dB SIDELOBES WITH $\bar{n} = 4$.

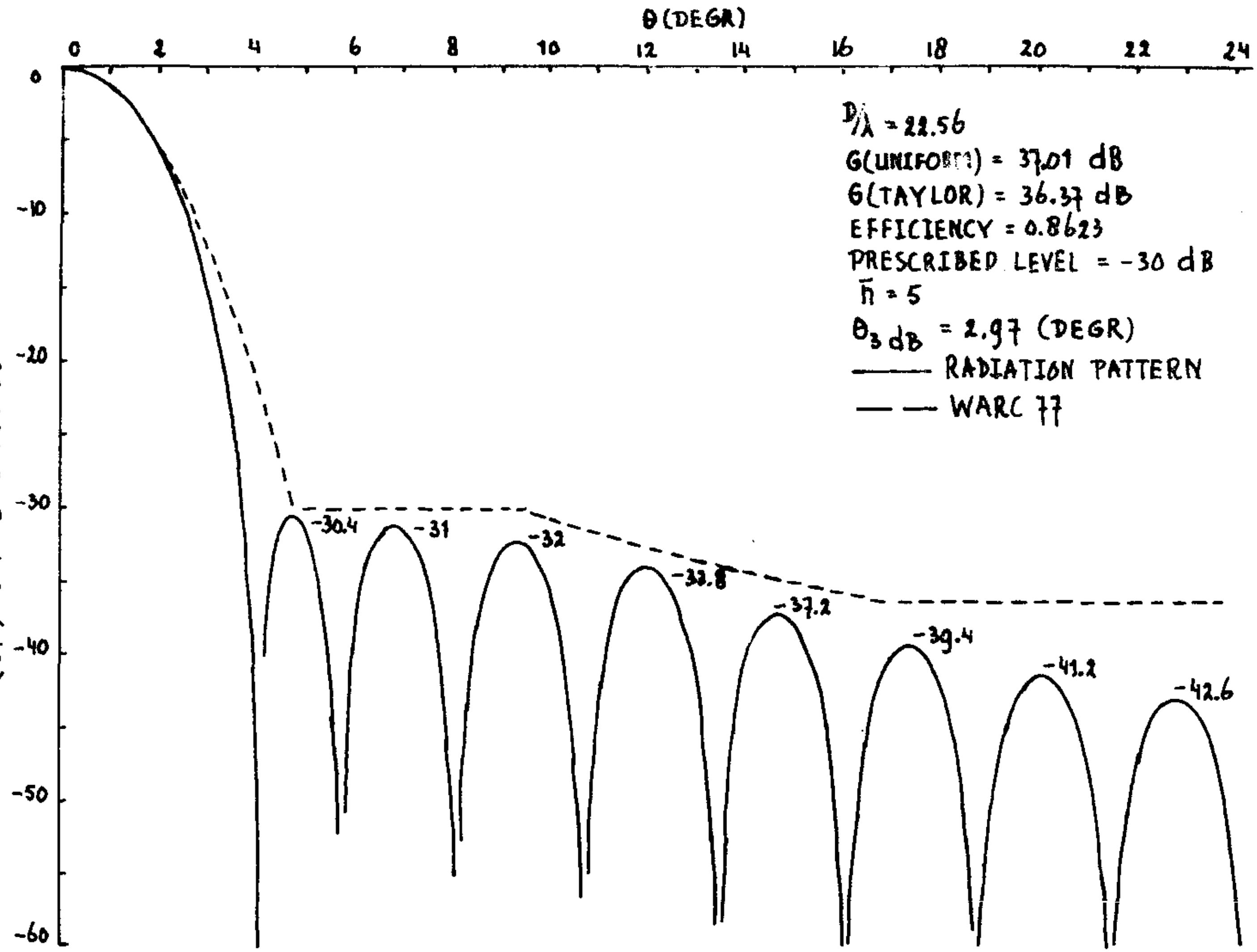

FIG. 8 : TAYLOR CIRCULAR APERTURE PATTERN FOR -30 dB SIDELOBES WITH $\bar{n} = 5$.

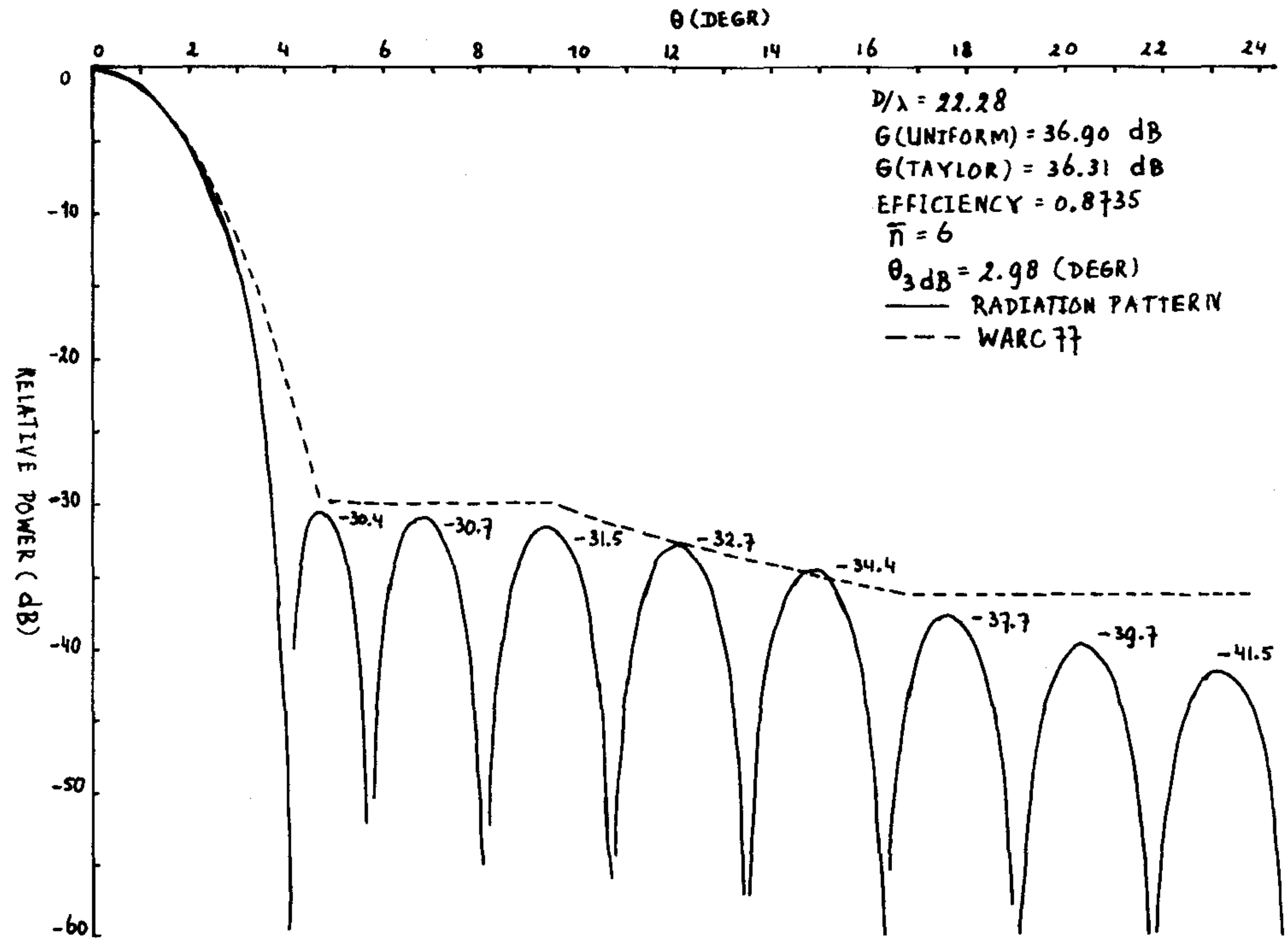

FIG. 9 : TAYLOR CIRCULAR APERTURE PATTERN FOR -30 dB SIDELOBES WITH $\bar{n}$ = 6.

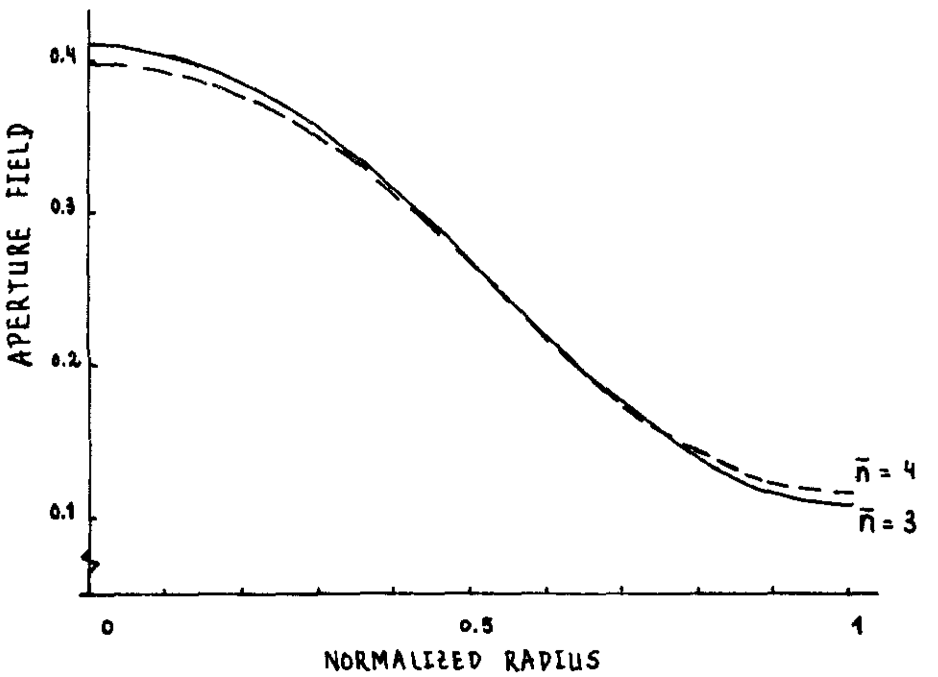

FIG. 10 : CIRCULAR APERTURE DISTRIBUTIONS FOR TAYLOR PATTERNS WITH $\bar{n}$-1 SIDELOBE EXTREMA OF -30 dB.

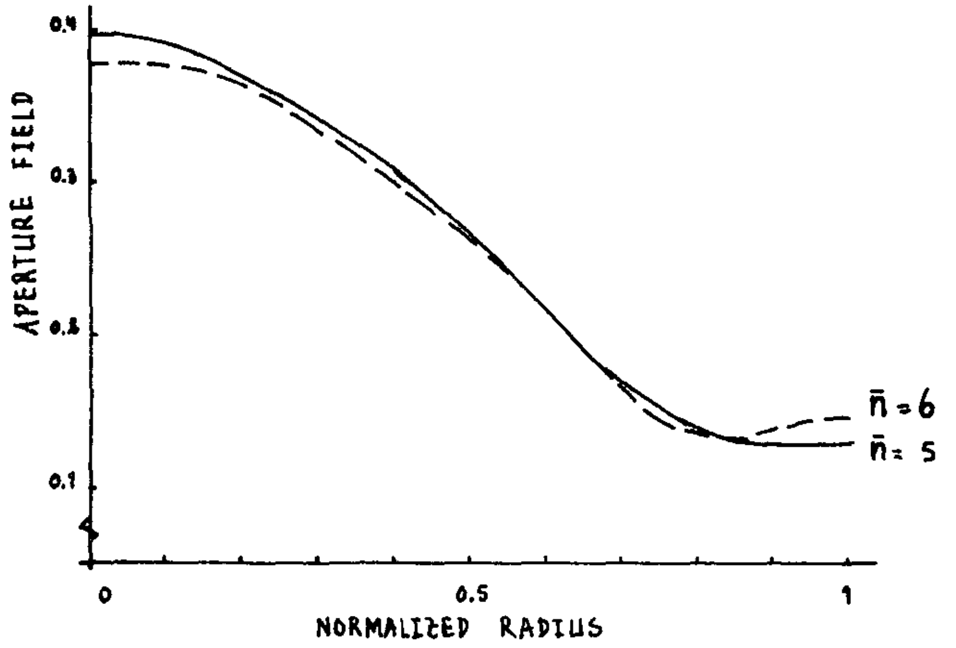

FIG. 11 : CIRCULAR APERTURE DISTRIBUTIONS FOR TAYLOR PATTERNS WITH $\bar{n}$-1 SIDELOBE EXTREMA OF -30 dB.

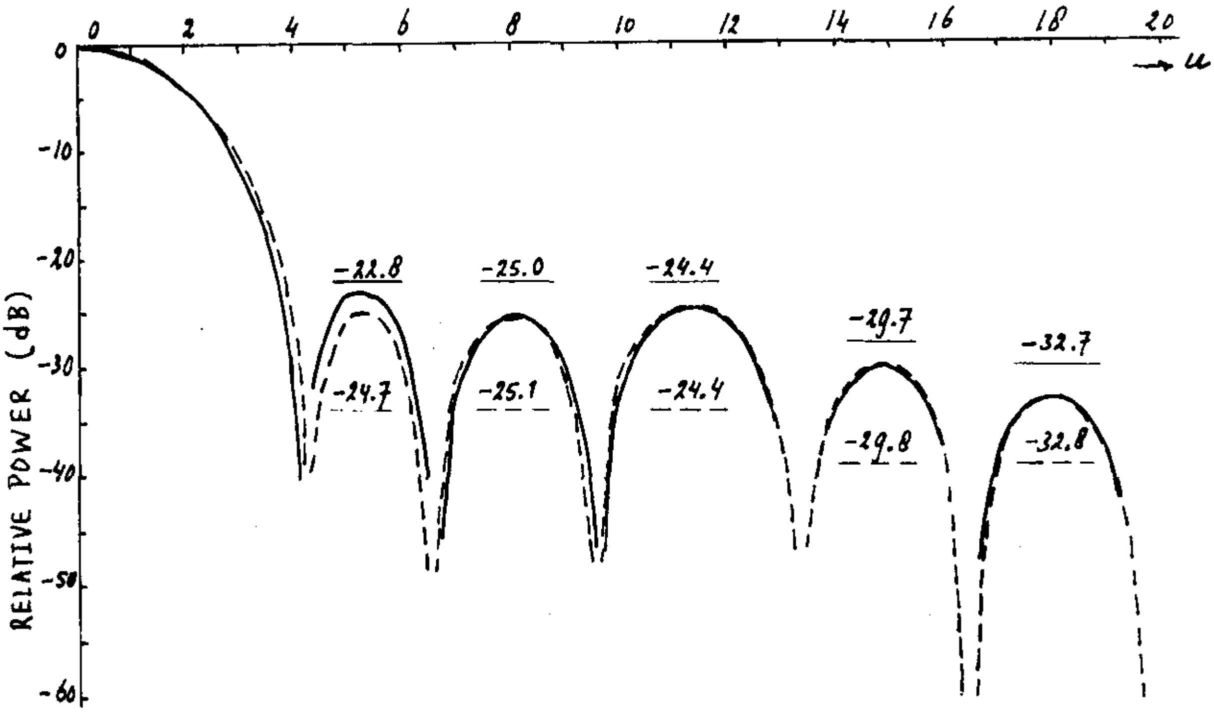

FIG. 12 : RADIATION PATTERNS WITH THREE -25 dB SIDELOBES ACCORDING TO EQ.(2-15) ——— AND EQ.(2-16) - - - .

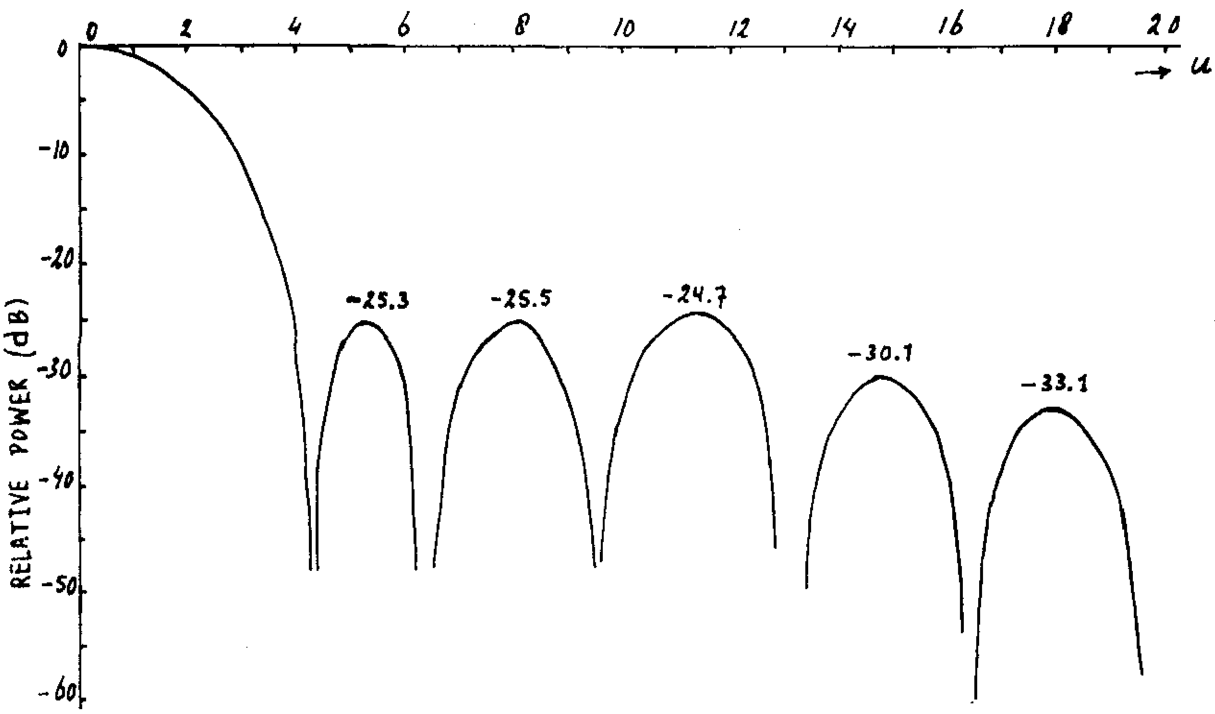

FIG. 13 : RADIATION PATTERN WITH THREE -25 dB SIDELOBES ACCORDING TO EQ. (2-19).

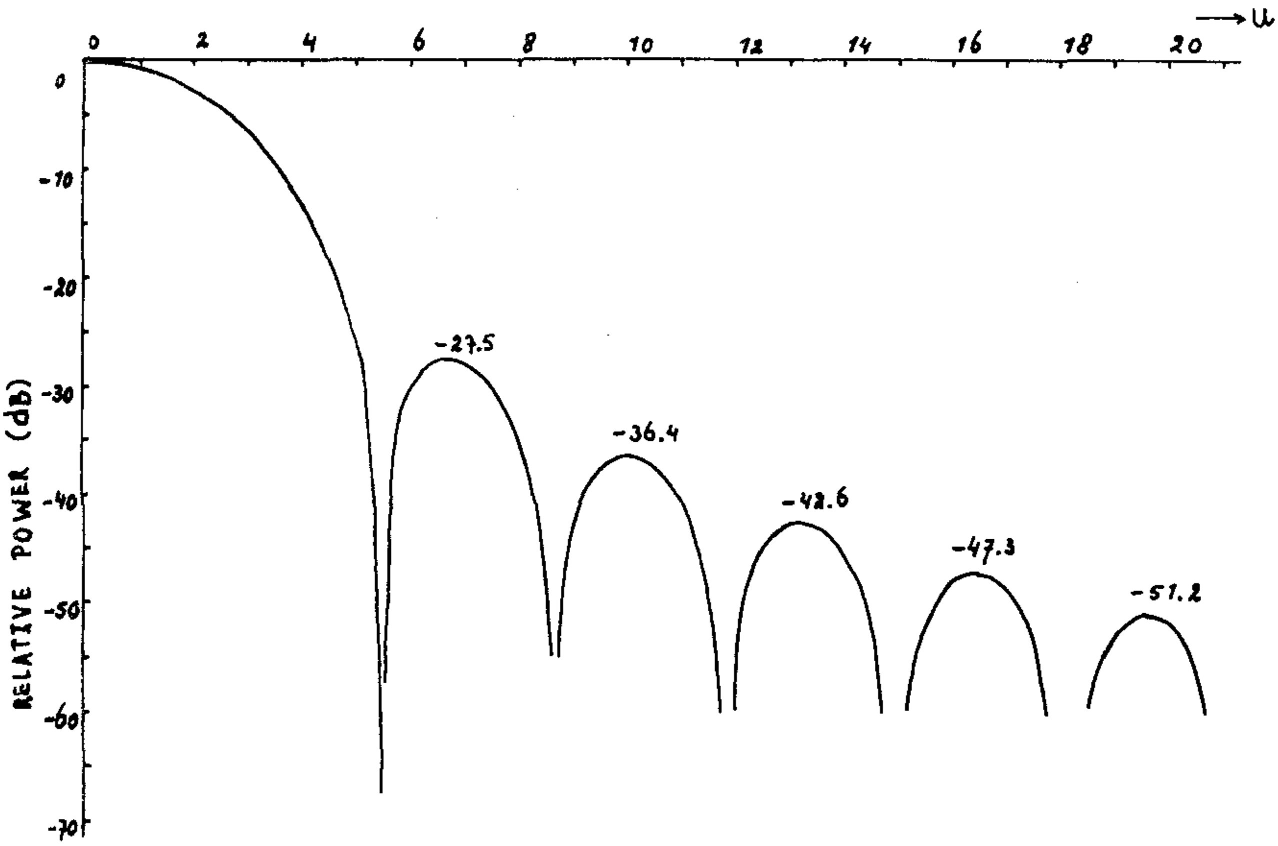

ZEROS : $u_1 = 5.5201$

$u_2 = 8.6537$

$u_3 = 11.7915$

$u_4 = 14.9309$

$u_5 = 18.0711$

$u_6 = 21.2116$

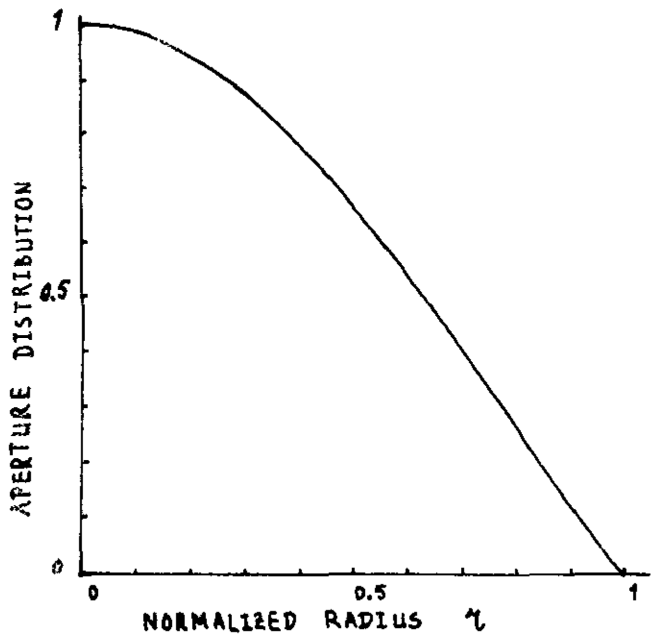

EFFICIENCY : 0.6917

GAINREDUCTION : 1.6 dB

$u_{3dB} = 4.15$

FIG. 14 : APERTURE DISTRIBUTION $J_0(2.4048\,r)$ AND RADIATION PATTERN $20 \log_{10} \left| \dfrac{J_0(u)}{1 - \left(\dfrac{u}{2.4048}\right)^2} \right|$

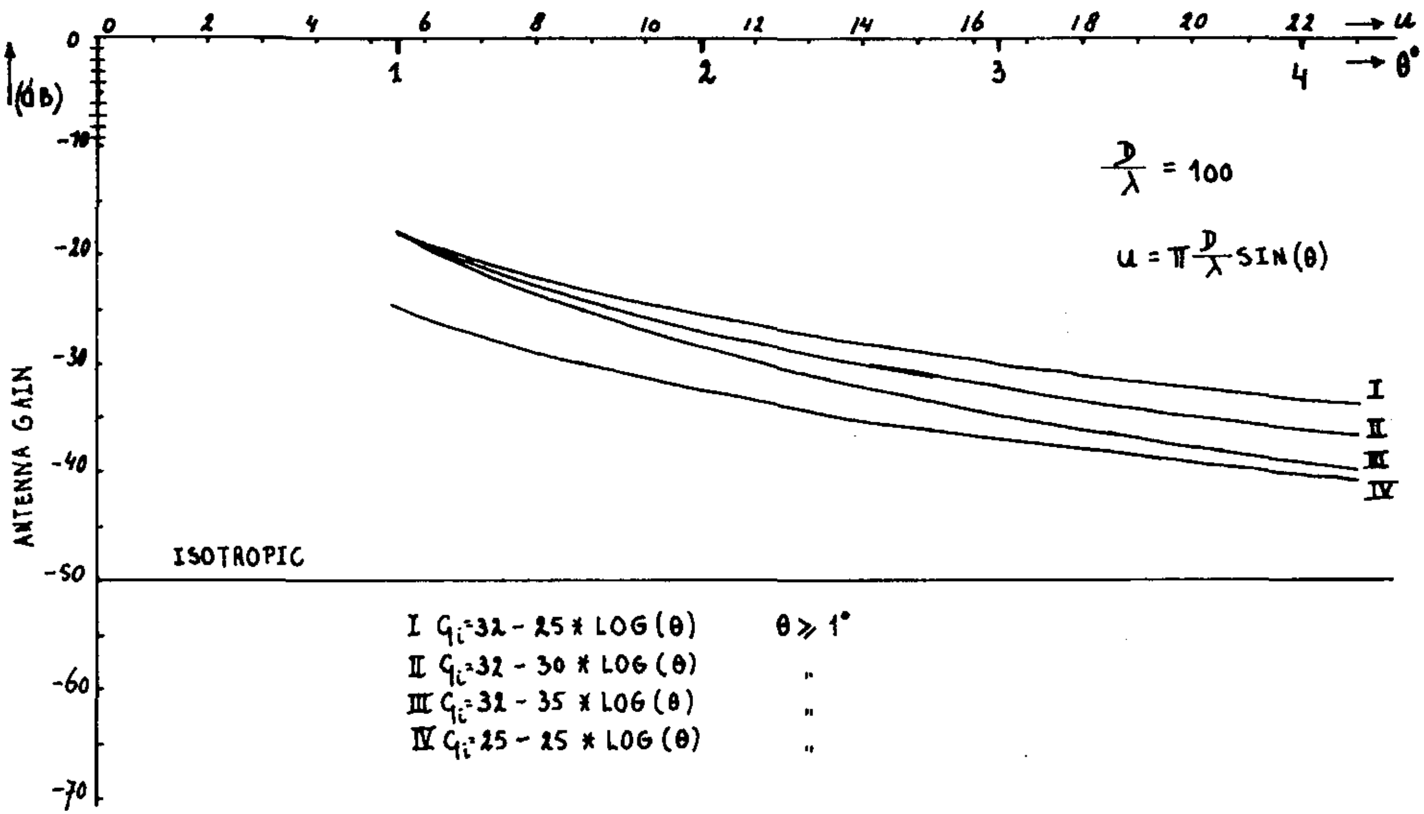

FIG. 15 : EARTH STATION ANTENNA RADIATION PATTERN ENVELOPES

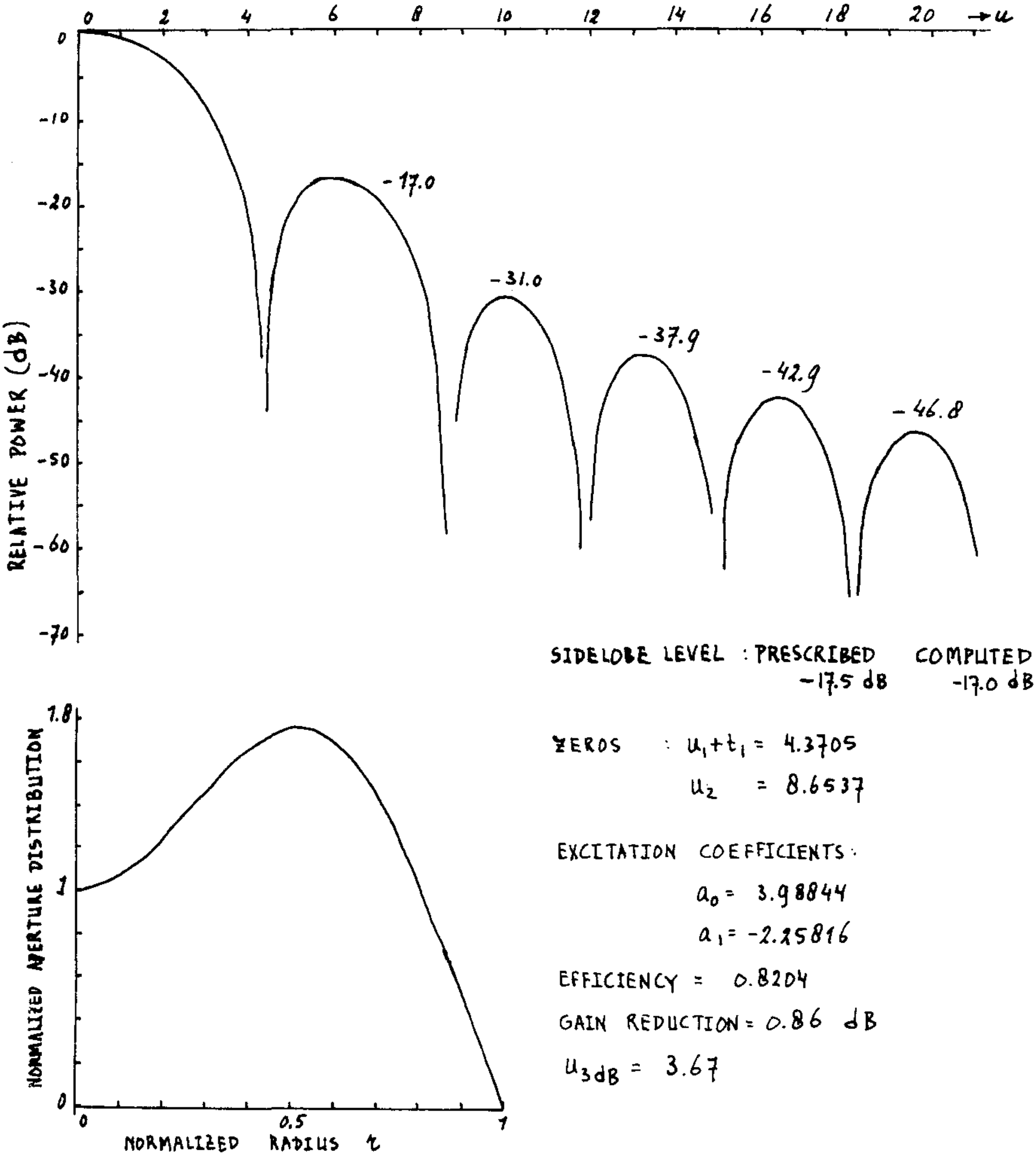

FIG. 16 : APERTURE DISTRIBUTION $\sum_{n=0}^{1} a_n J_0(u_n r)$ AND RADIATION PATTERN

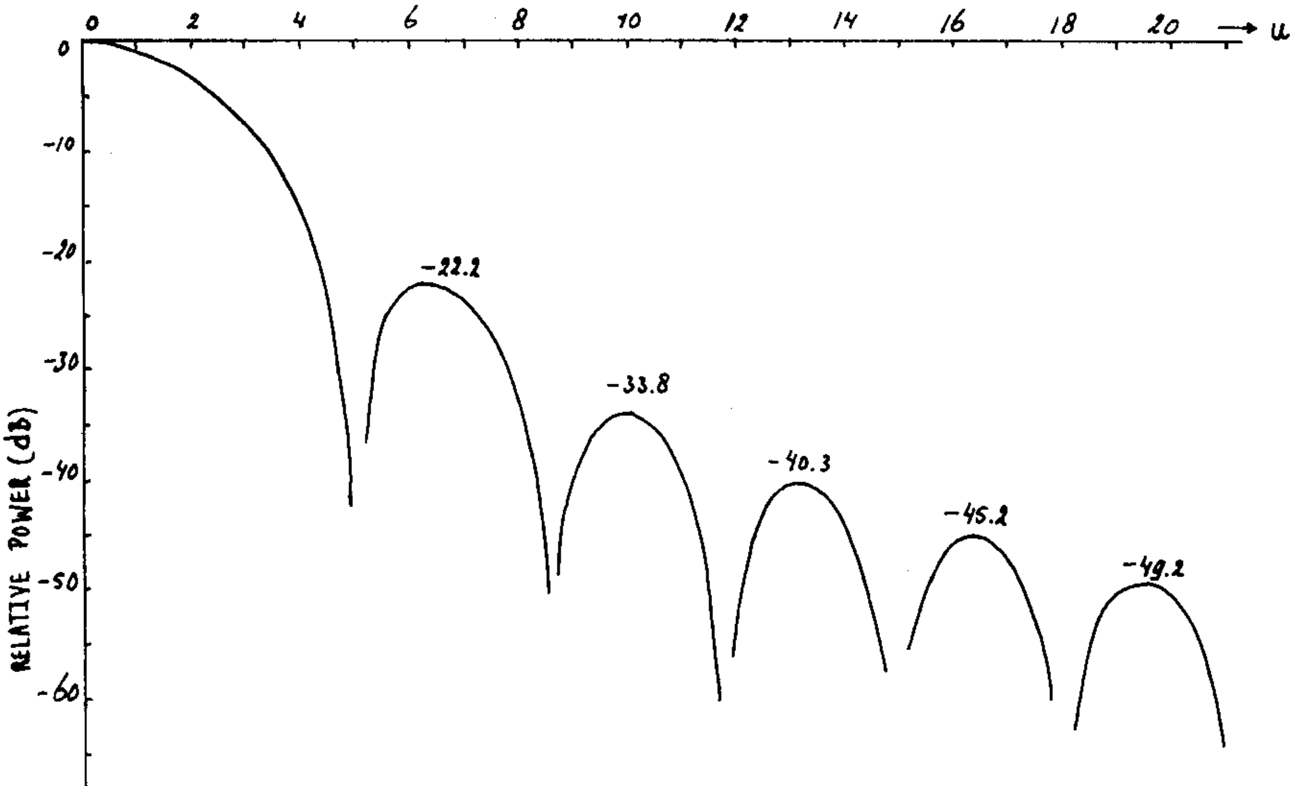

SIDELOBE LEVEL	PRESCRIBED	COMPUTED
	-22.5 dB	-22.2 dB

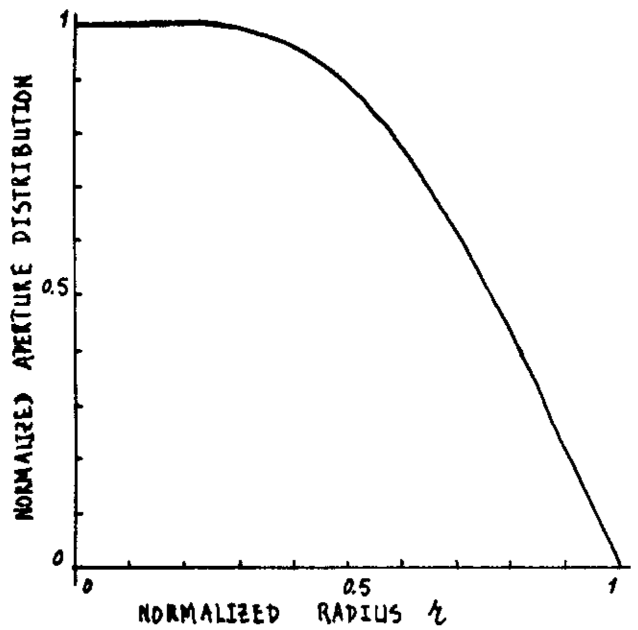

ZEROS $u_1 + t_1 = 4.9553$
$u_2 = 8.6537$

EXCITATION COEFFICIENTS
$a_0 = 4.37308$
$a_1 = -0.91311$

EFFICIENCY = 0.7623

GAIN REDUCTION = 1.18 dB

$u_{3dB} = 3.94$

FIG. 17: APERTURE DISTRIBUTION $\sum_{n=0}^{1} a_n J_0(u_n r)$ AND RADIATION PATTERN.

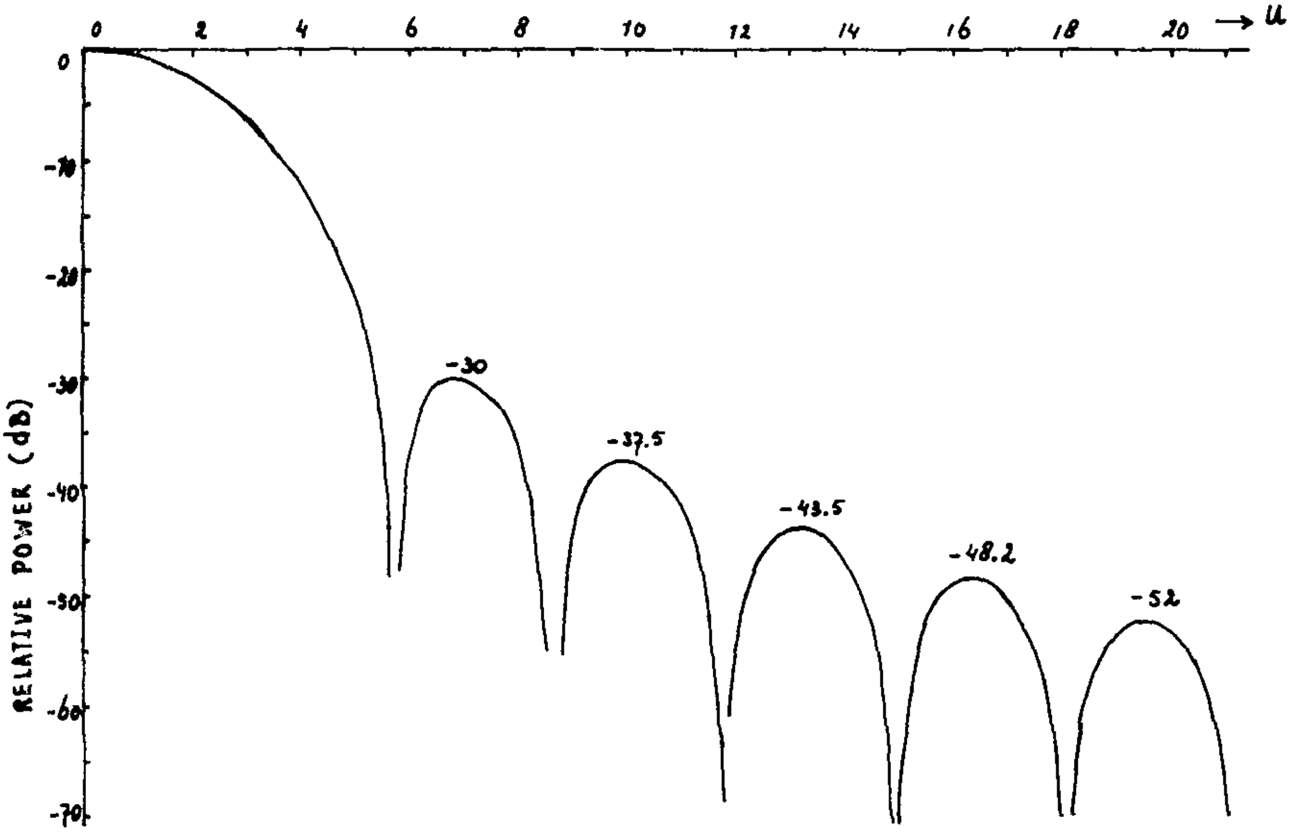

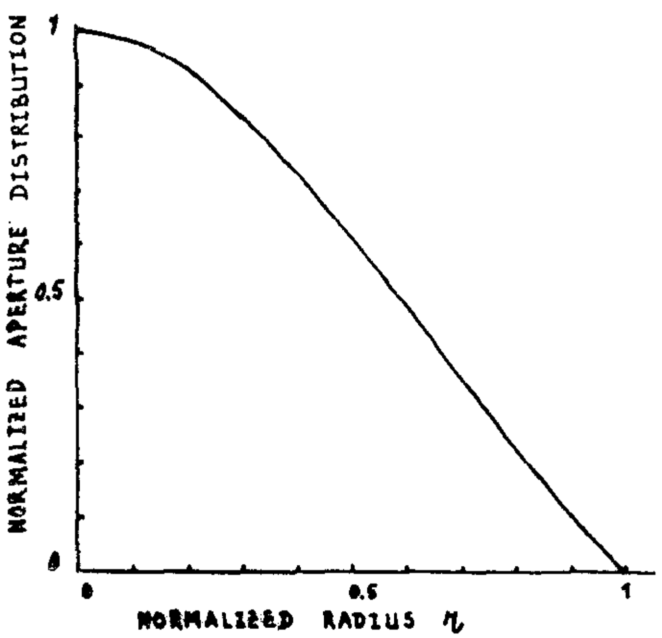

SIDELOBE LEVEL : PRESCRIBED -30 dB | COMPUTED -30 dB

ZEROS : $u_1 + t_1 = 5.7666$
$u_2 = 8.6537$

EXCITATION COEFFICIENTS:
$a_0 = 4.72546$
$a_1 = 0.31911$

EFFICIENCY : 0.6640

GAIN REDUCTION : 1.78 dB

$u_{3dB} = 4.23$

FIG. 18 : APERTURE DISTRIBUTION $\sum_{n=0}^{1} a_n J_0(u_n r)$ AND RADIATION PATTERN.

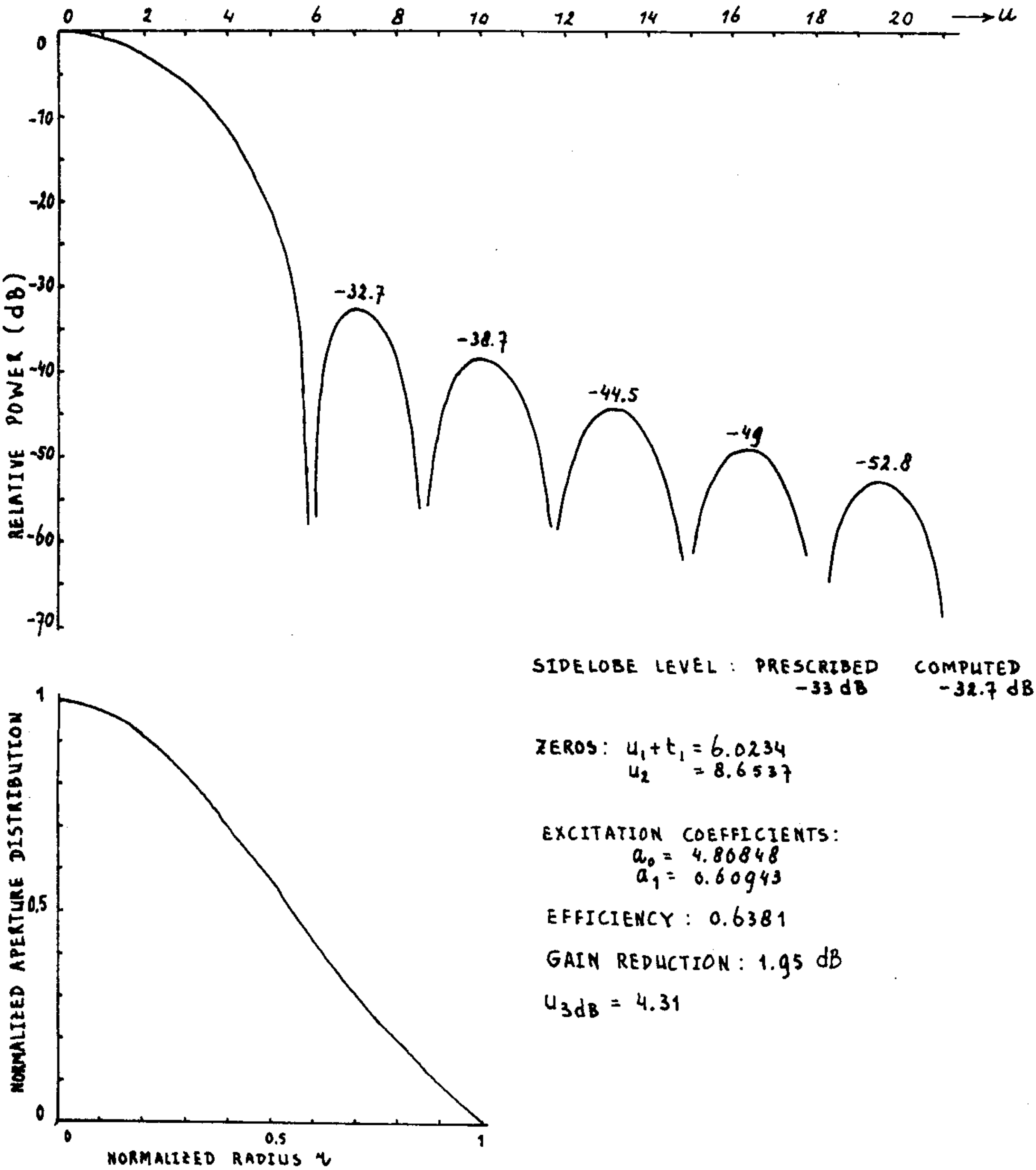

FIG. 19 : APERTURE DISTRIBUTION $\sum_{m=0}^{1} a_m J_0(u_m r)$ AND RADIATION PATTERN.

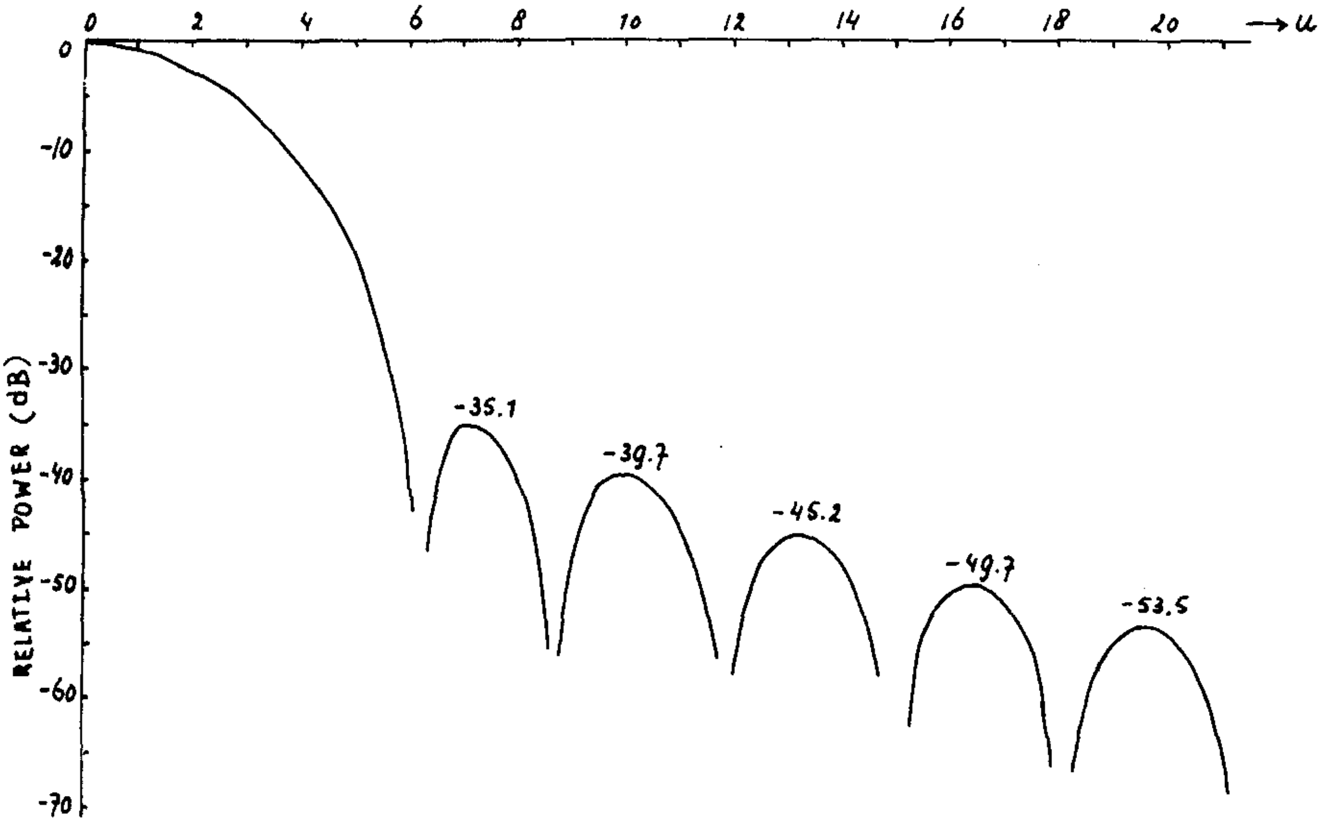

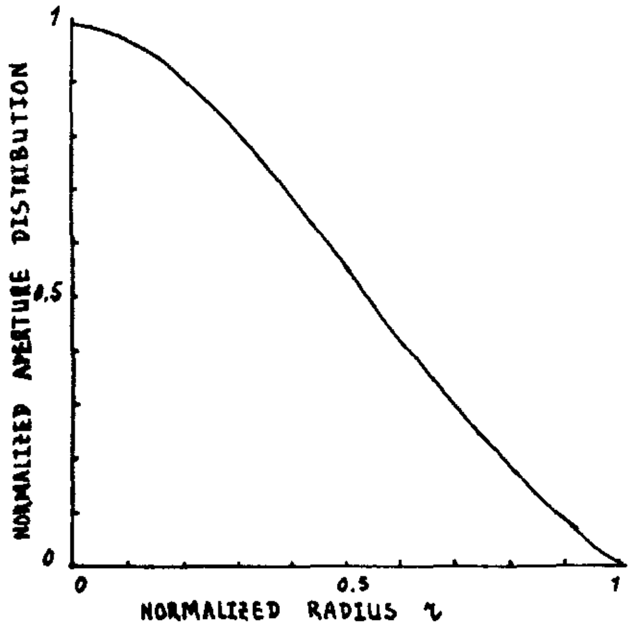

SIDELOBE LEVEL :	PRESCRIBED	COMPUTED
	-36 dB	-35.1 dB

ZEROS : $u_1+t_1 = 6.2335$
$u_2 = 8.6537$

EXCITATION COEFFICIENTS :
$a_0 = 4.86889$
$a_1 = 0.82069$

EFFICIENCY : 0.6191

GAIN REDUCTION : 2.08 dB

$u_{3\,dB} = 4.37$

FIG. 20 : APERTURE DISTRIBUTION $\sum_{m=0}^{1} a_m J_0(u_m r)$ AND RADIATION PATTERN.

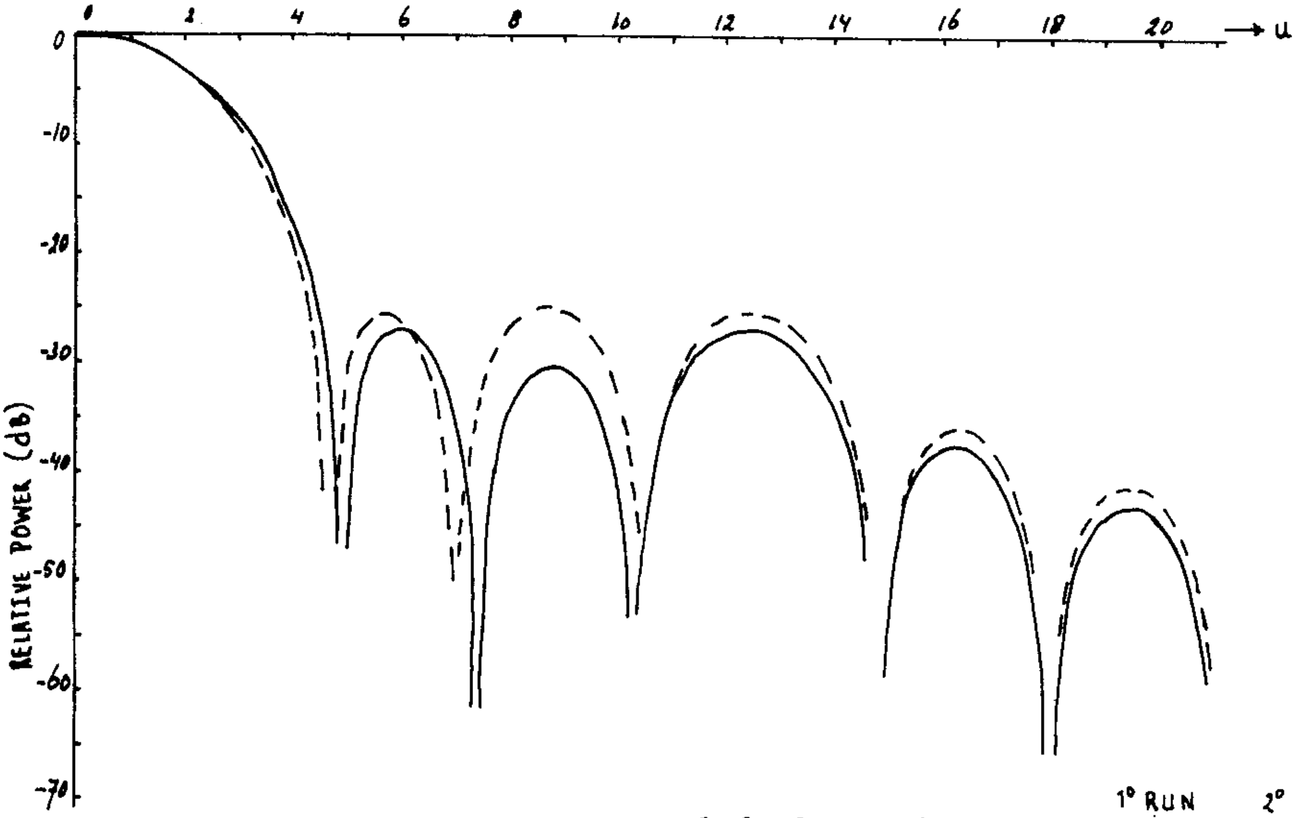

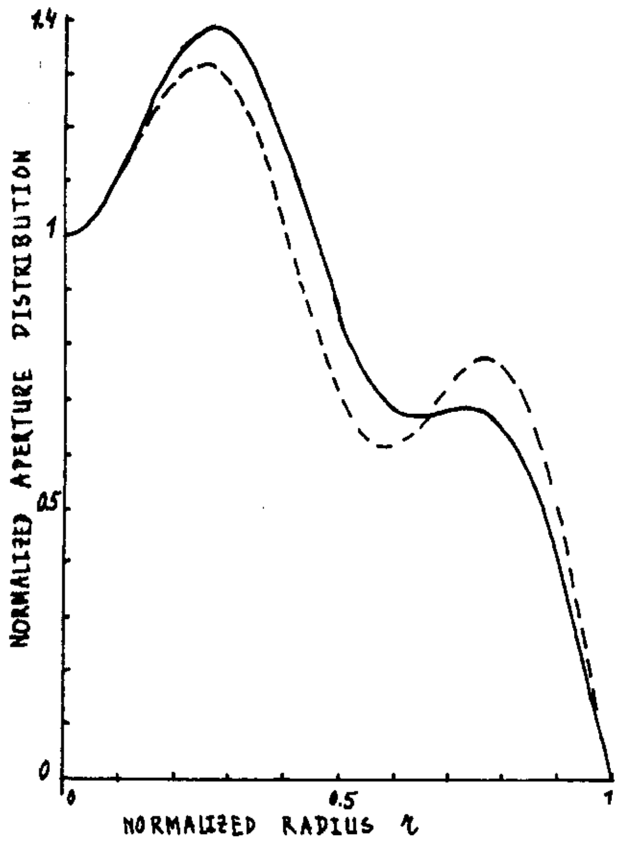

		1° RUN	2° RUN
SIDELOBE LEVEL	PRESCRIBED	COMPUTED	
	-25 dB	-26.7 dB	-25.5 dB
	-25	-30.3	-24.8
	-25	-26.8	-25.1
	—	-37.6	-35.7
	—	-42.7	-40.9
ZEROS	u_1+t_1	4.9486	4.6798
	u_2+t_2	7.4880	7.0534
	u_3+t_3	10.3241	10.5005
	u_4	14.9309	14.9309
EXCITATION COEFFICIENTS			
	a_0	4.19067	3.98630
	a_1	-0.65141	-0.89795
	a_2	0.81407	1.55490
	a_3	-1.51913	-1.80574
EFFICIENCY		0.8078	0.8460
GAIN REDUCTION		0.93 dB	0.73 dB
u_{3dB}		3.97	3.65

FIG. 21 : APERTURE DISTRIBUTION $\sum_{n=0}^{3} a_n J_0(u_n r)$ AND RADIATION PATTERN

——— FIRST APPROXIMATION   – – – SECOND APPROXIMATION

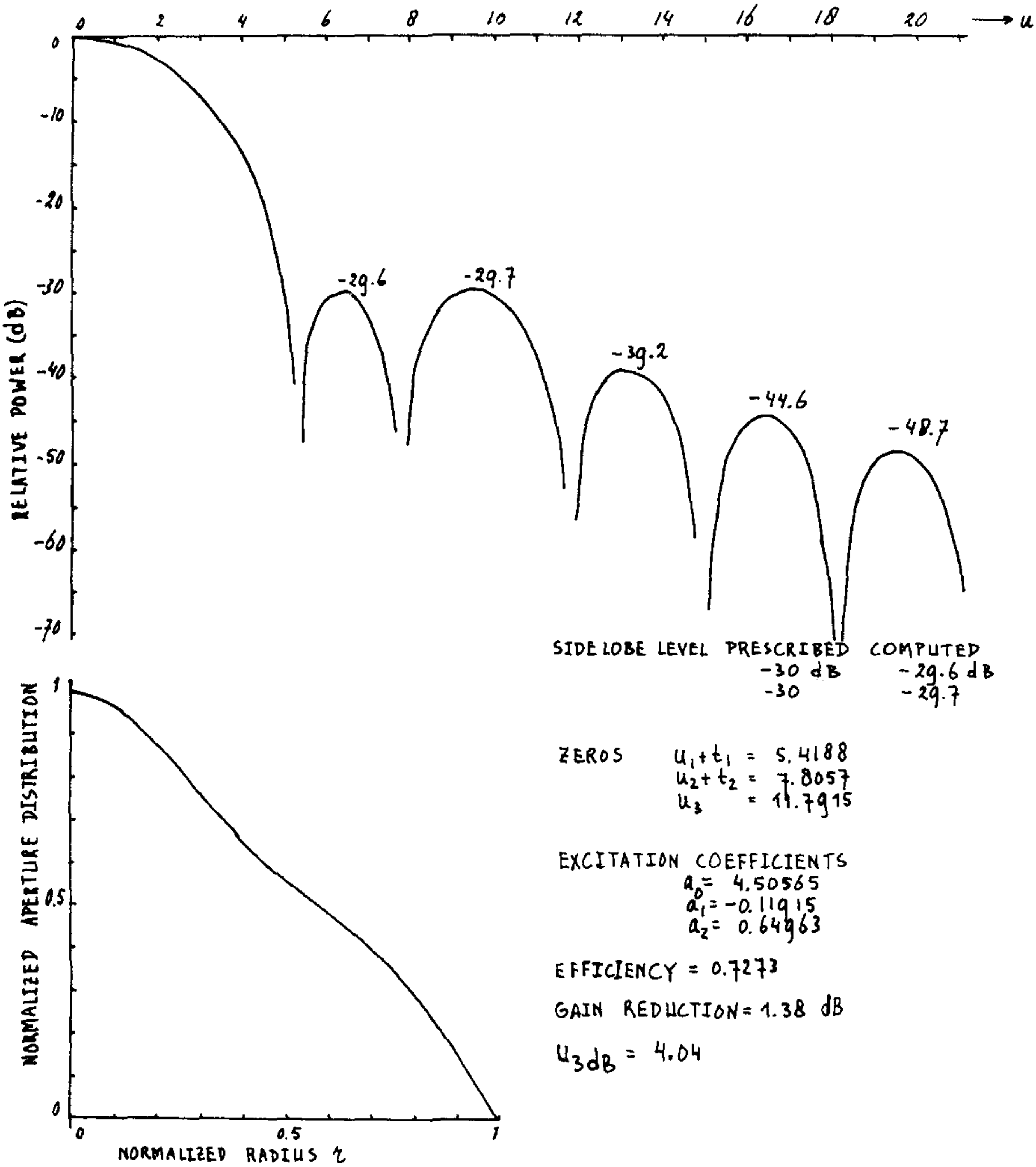

FIG. 22 : APERTURE DISTRIBUTION $\sum_{n=0}^{2} a_n J_0(u_n r)$ AND RADIATION PATTERN.

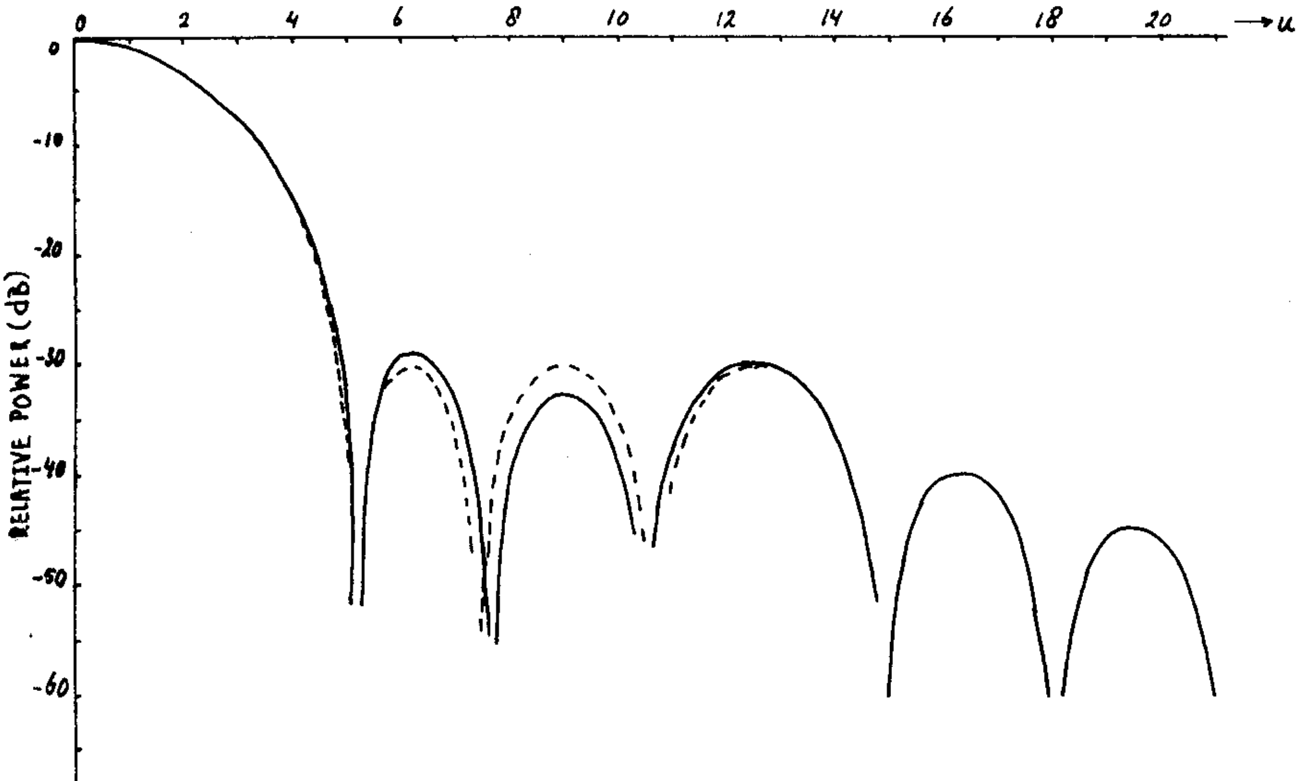

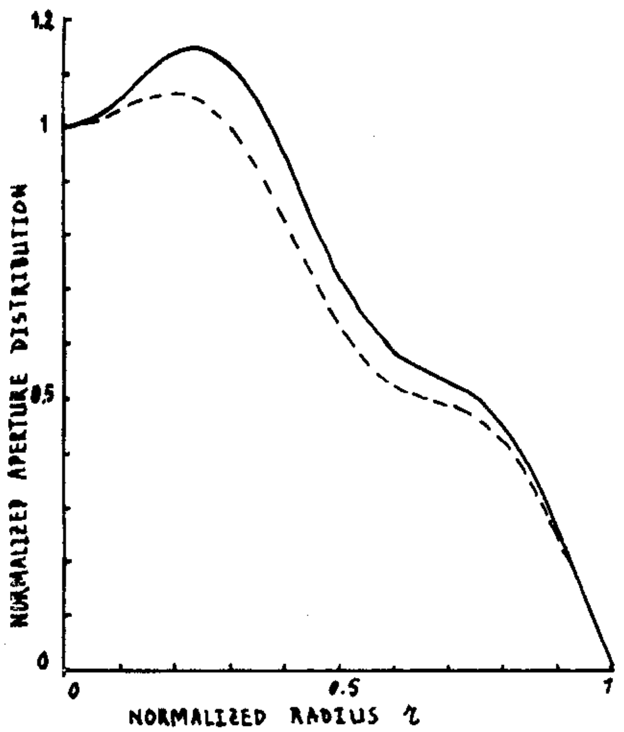

		1° RUN	2° RUN
SIDELOBE LEVELS	PRESCRIBED	COMPUTED	
	-30 dB	-28.7 dB	-30.0 dB
	-30	-32.5	-29.8
	-30	-29.7	-30.0
	—	-39.7	-39.6
	—	-44.7	-44.5
ZEROS	u_1+t_1	5.2157	5.2405
	u_2+t_2	7.6970	7.4444
	u_3+t_3	10.5059	10.6945
	u_4	14.9309	14.9309
EXCITATION COEFFICIENTS	a_0	4.35513	4.34203
	a_1	-0.34468	-0.29499
	a_2	-0.58960	0.83014
	a_3	-1.03641	-0.95273
EFFICIENCY		0.7685	0.7712
GAIN REDUCTION		1.14 dB	1.13 dB
$u_{3\,dB}$		3.91	3.90

FIG. 23 : APERTURE DISTRIBUTION $\sum_{m=0}^{3} a_m J_0(u_m r)$ AND RADIATION PATTERN.

—— FIRST APPROXIMATION — — — SECOND APPROXIMATION.

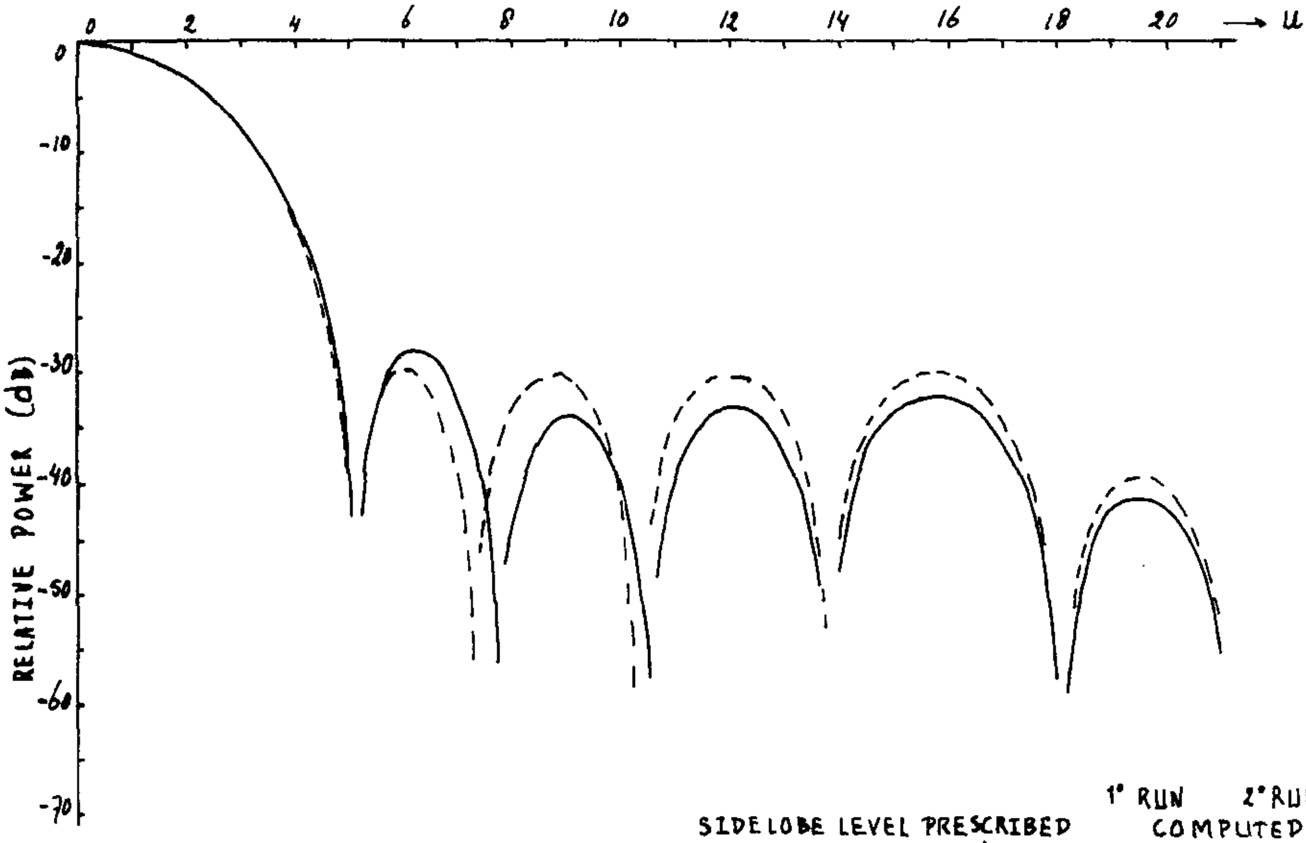

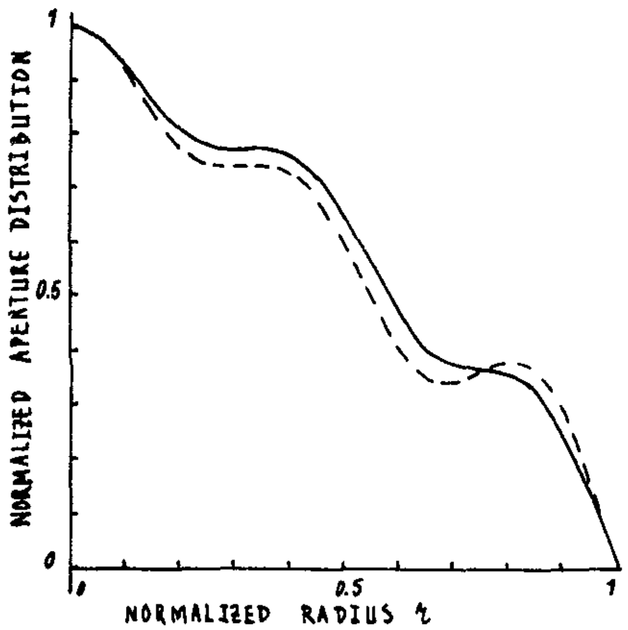

		1° RUN	2° RUN
		COMPUTED	
SIDELOBE LEVEL PRESCRIBED	-30 dB	-28.2 dB	-29.8 dB
	-30	-34.0	-30.3
	-30	-33.4	-30.0
	-30	-32.1	-30.0
	—	-41.4	-39.4
ZEROS	u_1+t_1	5.1567	5.0976
	u_2+t_2	7.7664	7.2656
	u_3+t_3	10.4361	10.2747
	u_4+t_4	13.7542	13.7694
	u_5	18.0711	18.0711
EXCITATION COEFFICIENTS	a_0	4.31261	4.21270
	a_1	-0.41266	-0.41221
	a_2	0.49391	0.82680
	a_3	-0.77459	-1.15065
	a_4	0.94897	1.21858
EFFICIENCY		0.7816	0.8024
GAIN REDUCTION		1.07 dB	0.96 dB
$u_{3\,dB}$		3.88	3.81

FIG. 24 : APERTURE DISTRIBUTION $\sum_{m=0}^{4} a_m J_0(u_m r)$ AND RADIATION PATTERN.

——— FIRST APPROXIMATION – – – SECOND APPROXIMATION

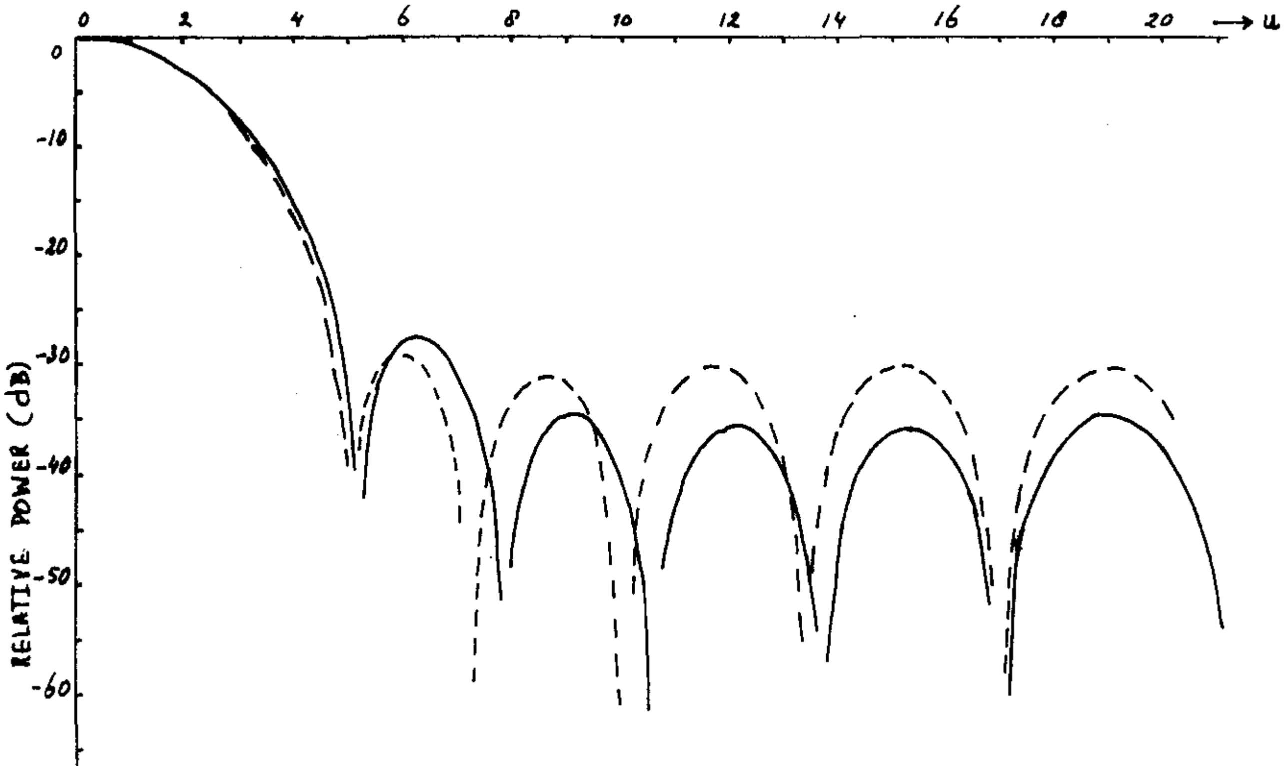

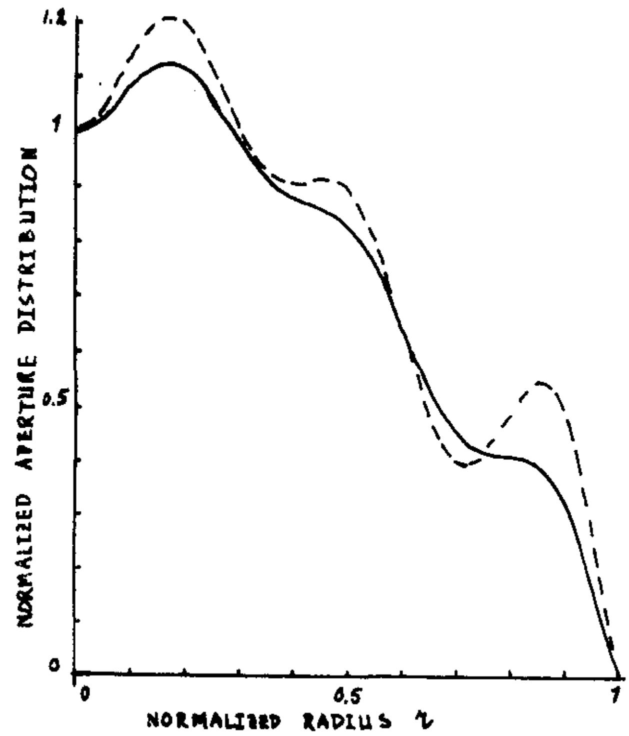

		1° RUN	2° RUN
SIDELOBE LEVELS	PRESCRIBED	COMPUTED	
	-30 dB	-27.9 dB	-29.4 dB
	-30	-34.9	-31.3
	-30	-35.9	-30.4
	-30	-36.2	-30.4
	-30	-34.9	-30.5
ZEROS	u_1+t_1	5.1535	5.0034
	u_2+t_2	7.8623	7.2241
	u_3+t_3	10.5447	10.0293
	u_4+t_4	13.6616	13.3786
	u_5+t_5	16.9653	16.9485
	u_6	21.2116	21.2116
EXCITATION COEFFICIENTS			
	a_0	4.31480	4.13167
	a_1	-0.42342	-0.48784
	a_2	0.43069	0.73669
	a_3	-0.58229	-1.11115
	a_4	0.68250	1.39260
	a_5	-0.80065	-1.35998
EFFICIENCY		0.7827	0.8196
GAIN REDUCTION		1.06 dB	0.86 dB
u_{3dB}		3.88	3.75

FIG. 25: APERTURE DISTRIBUTION $\sum_{m=0}^{5} a_m J_0(u_m r)$ AND RADIATION PATTERN.

—— FIRST APPROXIMATION — — — SECOND APPROXIMATION

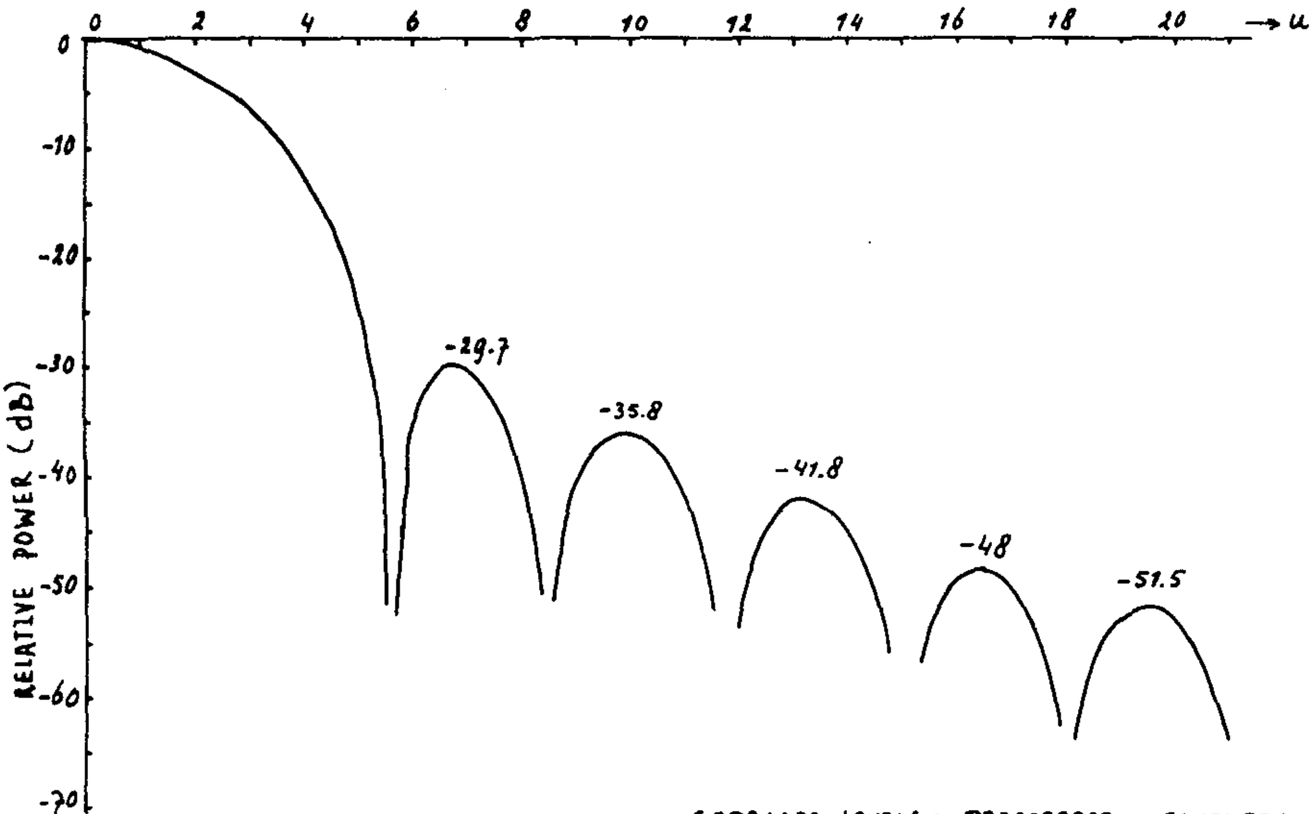

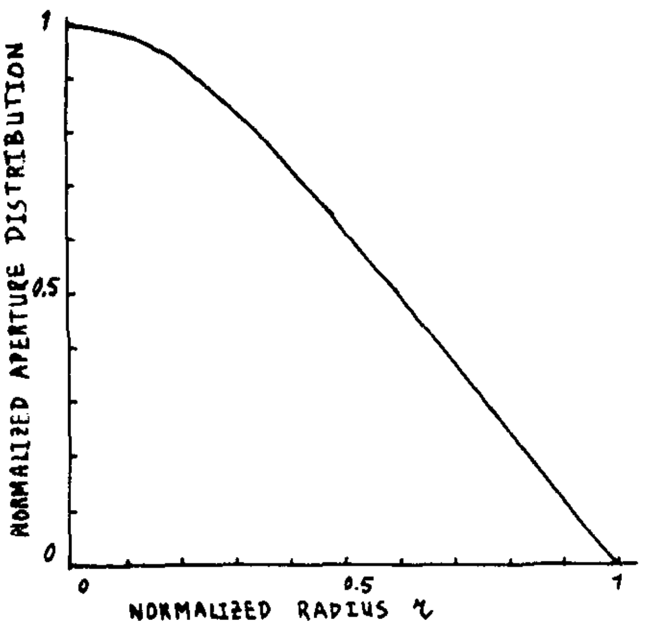

SIDELOBE LEVELS:

PRESCRIBED	COMPUTED
-30 dB	-29.7 dB
-36	-35.8
-42	-41.8
-48	-48

ZEROS: $u_1+t_1 = 5.6826$
$u_2+t_2 = 8.4748$
$u_3+t_3 = 11.7456$
$u_4+t_4 = 15.0310$
$u_5 = 18.0711$

EXCITATION COEFFICIENTS:
$a_0 = 4.67911$
$a_1 = 0.20918$
$a_2 = 0.10232$
$a_3 = -0.01754$
$a_4 = -0.02612$

EFFICIENCY: 0.6778

GAIN REDUCTION 1.69 dB

$u_{3dB} = 4.19$

FIG. 26: APERTURE DISTRIBUTION $\sum_{m=0}^{4} a_m J_0(u_m r)$ AND RADIATION PATTERN

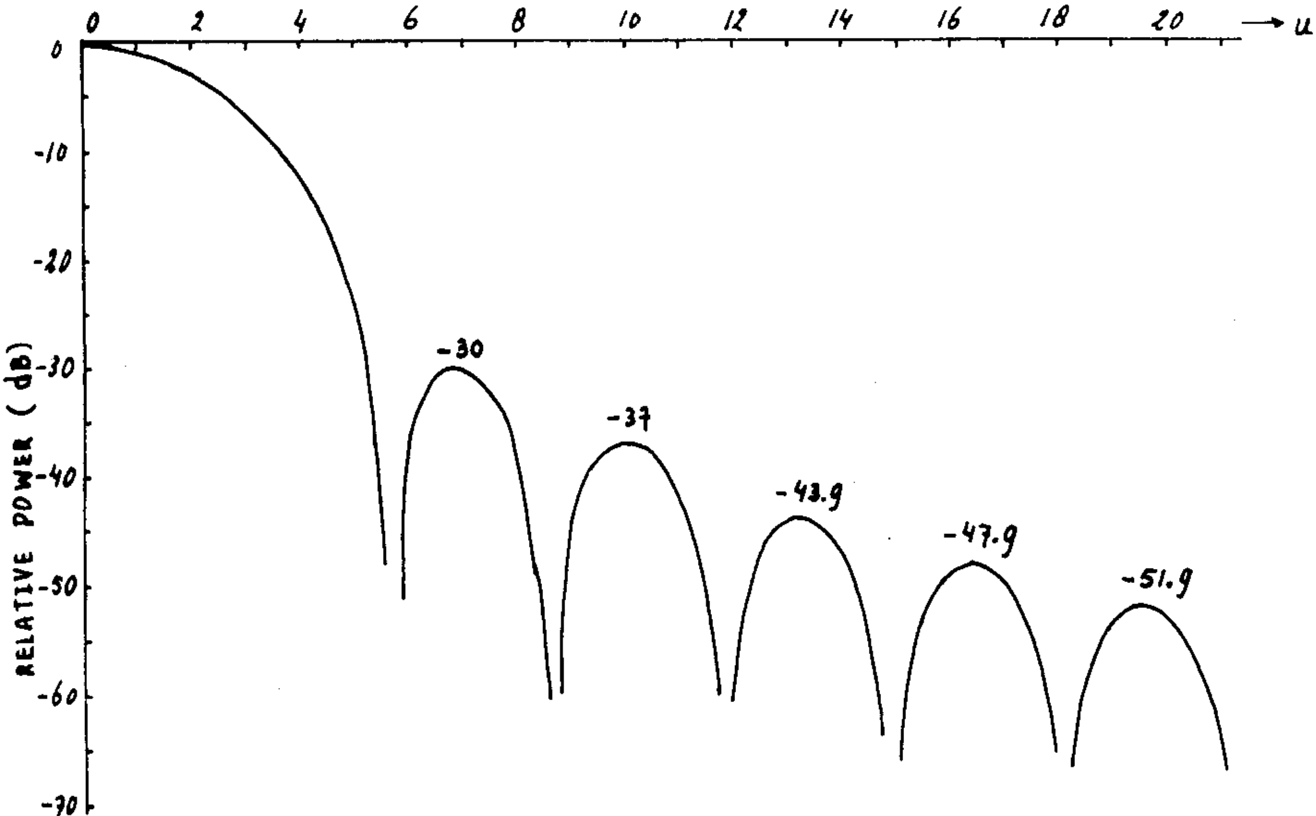

SIDELOBE LEVELS :

PRESCRIBED	COMPUTED
-30 dB	-30 dB
-37	-37
-44	-43.9
-48	-47.9

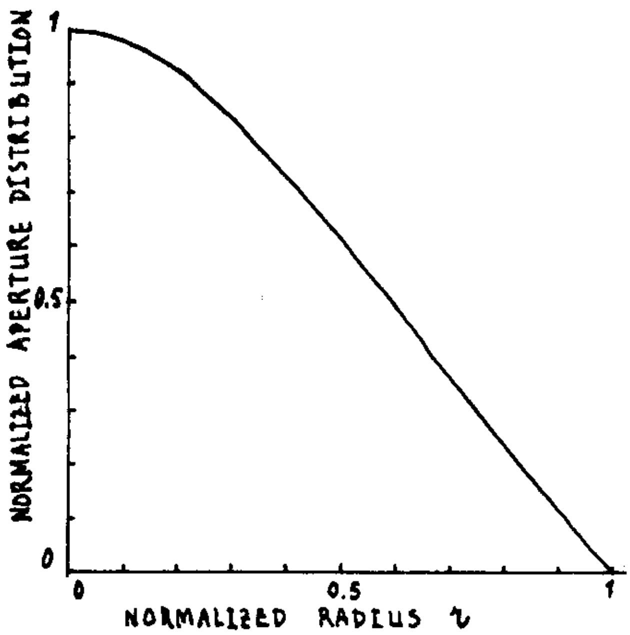

ZEROS: $u_1 + t_1 = 5.7536$
$u_2 + t_2 = 8.6083$
$u_3 + t_3 = 11.8463$
$u_4 + t_4 = 14.8919$
$u_5 = 18.0711$

EXCITATION COEFFICIENTS :
$a_0 = 4.71800$
$a_1 = 0.30169$
$a_2 = 0.02422$
$a_3 = 0.01878$
$a_4 = 0.00893$

EFFICIENCY : 0.6662

GAIN REDUCTION : 1.76 dB

$u_{3dB} = 4.22$

FIG. 27 : APERTURE DISTRIBUTION $\sum_{m=0}^{4} a_m J_0(u_m r)$ AND RADIATION PATTERN

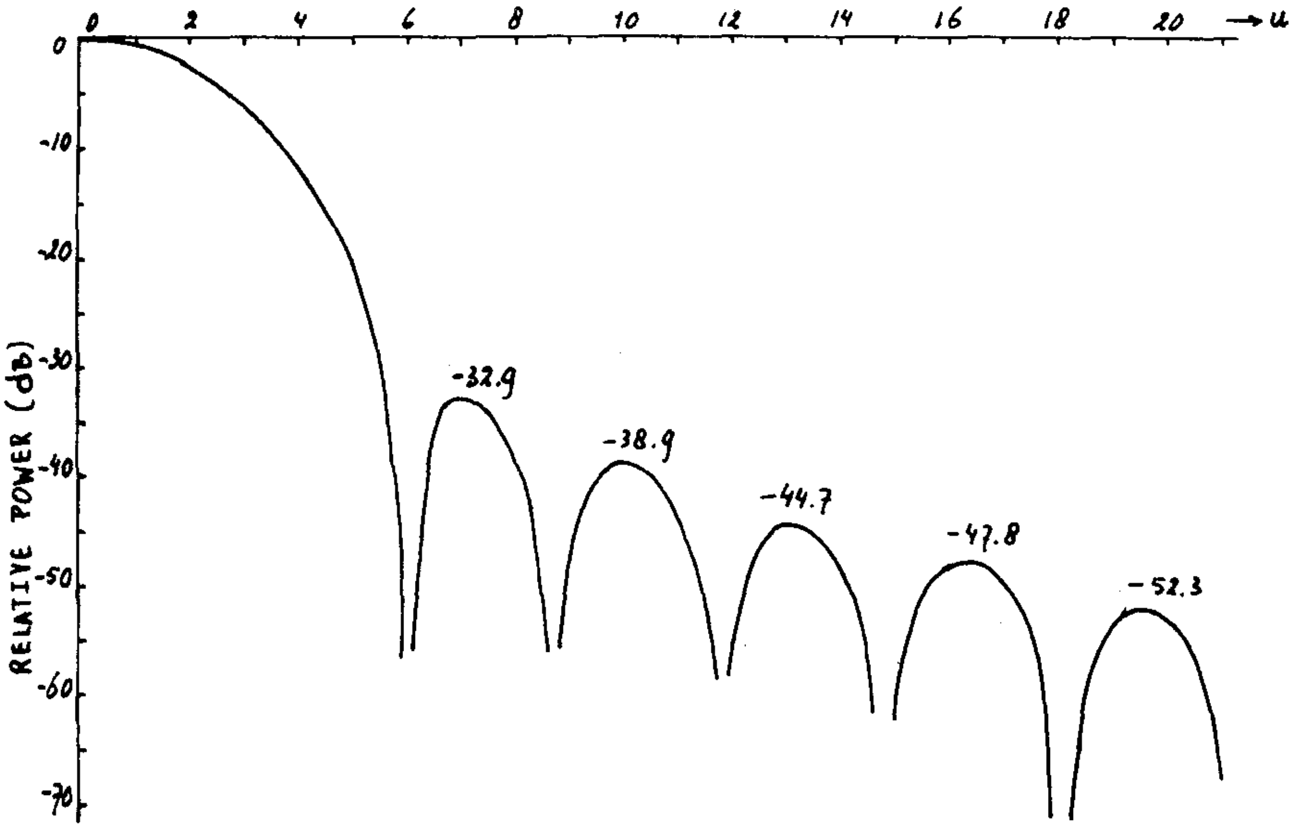

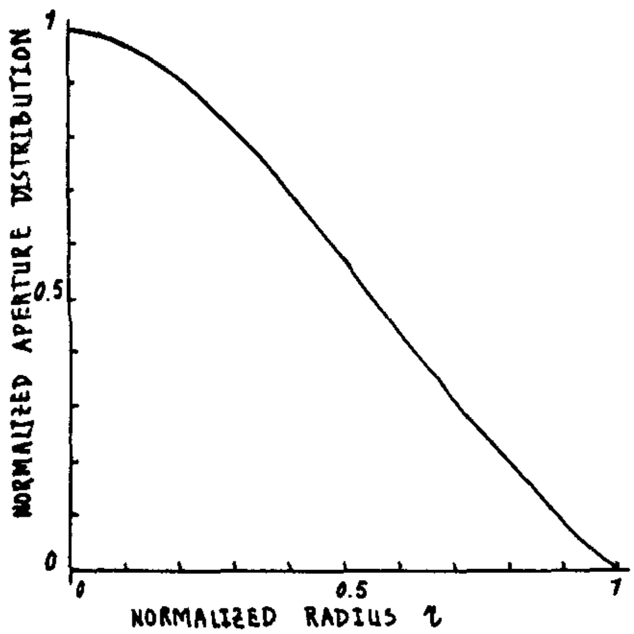

SIDELOBE LEVELS:

PRESCRIBED	COMPUTED
-33 dB	-32.9
-39	-38.9
-45	-34.7
-48	-47.8

ZEROS: $u_1+t_1 = 6.0301$
$u_2+t_2 = 8.6390$
$u_3+t_3 = 11.7481$
$u_4+t_4 = 14.7787$
$u_5 = 18.0711$

EXCITATION COEFFICIENTS:
$a_0 = 4.80493$
$a_1 = 0.61175$
$a_2 = 0.00616$
$a_3 = -0.01232$
$a_4 = 0.03301$

EFFICIENCY : 0.6390

GAIN REDUCTION : 1.95 dB

$u_{3dB} = 4.30$

FIG. 28: APERTURE DISTRIBUTION $\sum_{n=0}^{4} a_n J_0(u_n r)$ AND RADIATION PATTERN

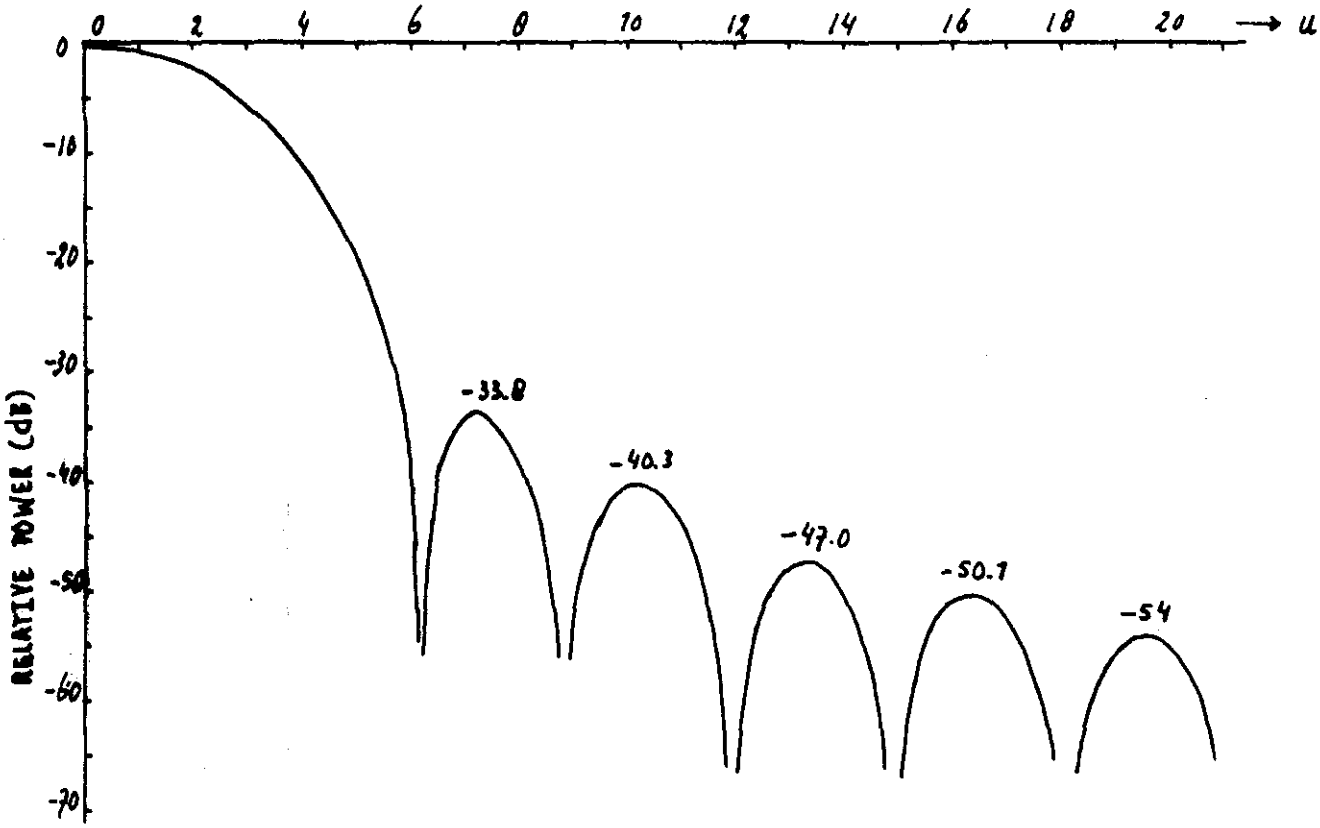

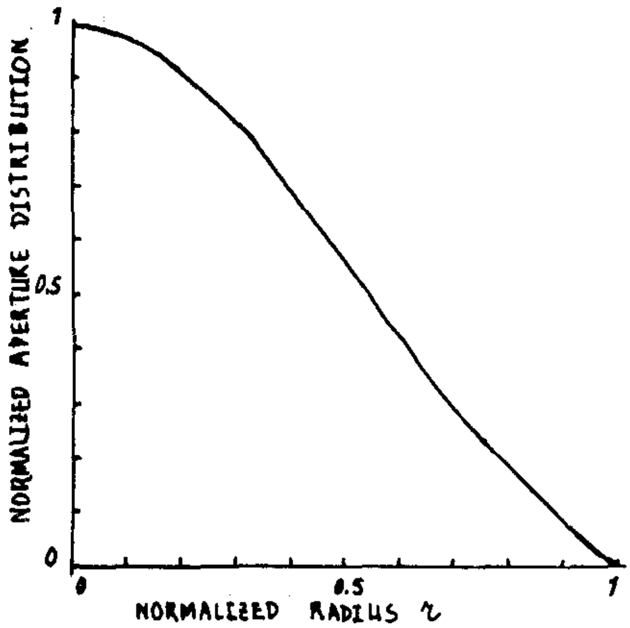

SIDELOBE LEVELS:

PRESCRIBED	COMPUTED
-33 dB	-33.8 dB
-40	-40.3
-47	-47.0
-50	-50.7

ZEROS: $u_1+t_1 = 6.1915$
$u_2+t_2 = 8.8222$
$u_3+t_3 = 11.9835$
$u_4+t_4 = 14.8721$
$u_5 = 18.0711$

EXCITATION COEFFICIENTS:
$a_0 = 4.87683$
$a_1 = 0.80488$
$a_2 = -0.06791$
$a_3 = 0.03646$
$a_4 = 0.01015$

EFFICIENCY: 0.6174

GAIN REDUCTION: 2.09 dB

$u_{3dB} = 4.38$

FIG. 29: APERTURE DISTRIBUTION $\sum_{n=0}^{4} a_n J_0(u_n r)$ AND RADIATION PATTERN.

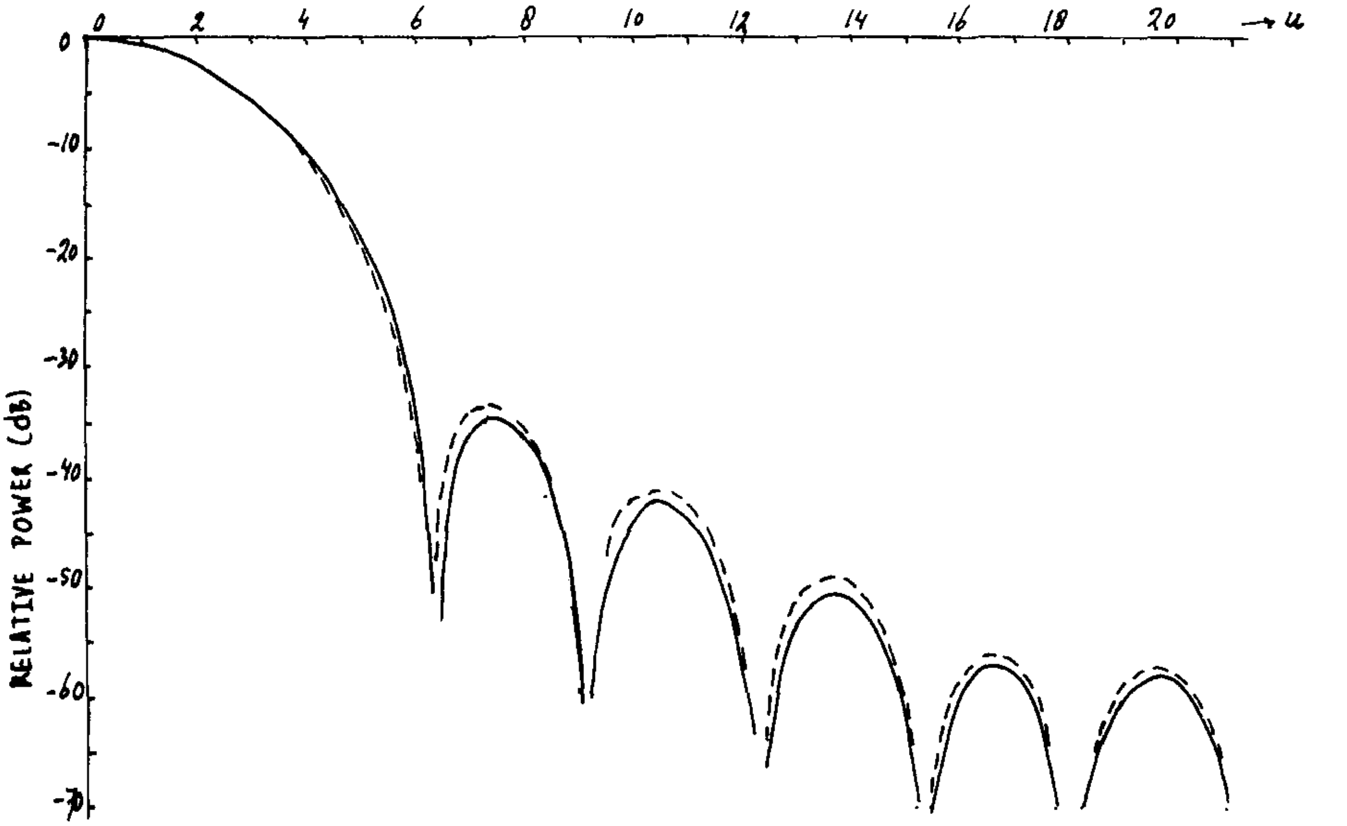

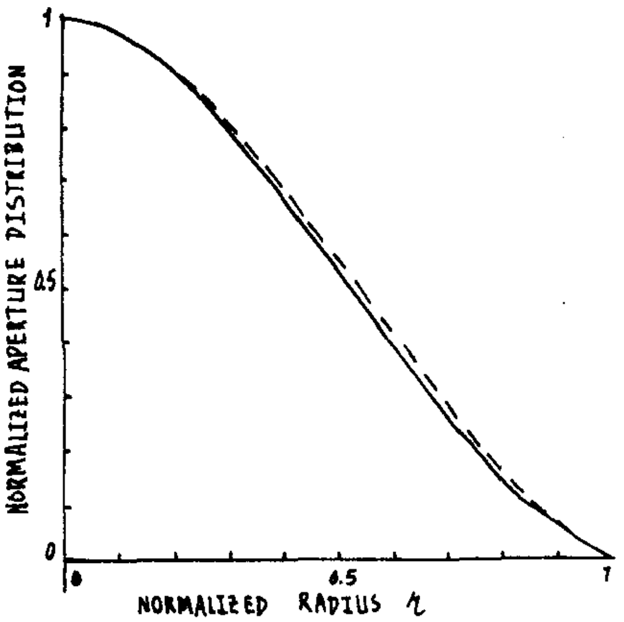

		1° RUN	2° RUN
SIDELOBE LEVELS	PRESCRIBED	COMPUTED	
	-33 dB	-34.6 dB	-33.1
	-41	-42.2	-41.0
	-49	-50.5	-48.8
	-57	-57.0	-56.1
	—	-58.1	-57.2
ZEROS	u_1+t_1	6.4381	6.258
	u_2+t_2	9.1819	9.094
	u_3+t_3	12.3913	12.305
	u_4+t_4	15.3769	15.39
	u_5	18.0711	18.07
EXCITATION COEFFICIENTS			
	a_0	4.99612	4.939
	a_1	1.12274	0.92
	a_2	0.18865	-0.17
	a_3	0.11407	0.112
	a_4	0.04753	-0.05
EFFICIENCY		0.5823	0.5
GAIN REDUCTION		2.35 dB	2.22
u_{3dB}		4.50	4.4

FIG. 30 : APERTURE DISTRIBUTION $\sum_{n=0}^{4} a_n J_0(u_n r)$ AND RADIATION PATTERN

—— FIRST APPROXIMATION — — — SECOND APPROXIMATION

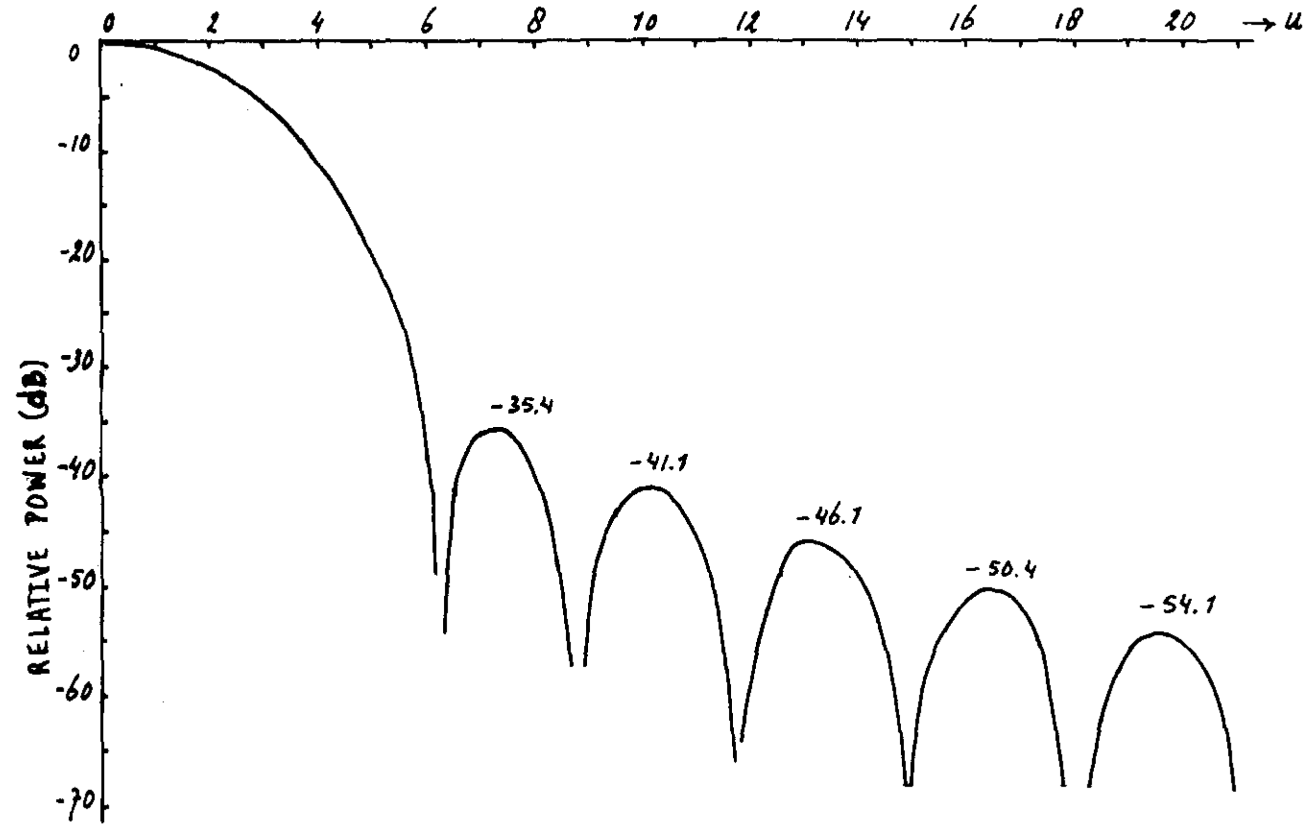

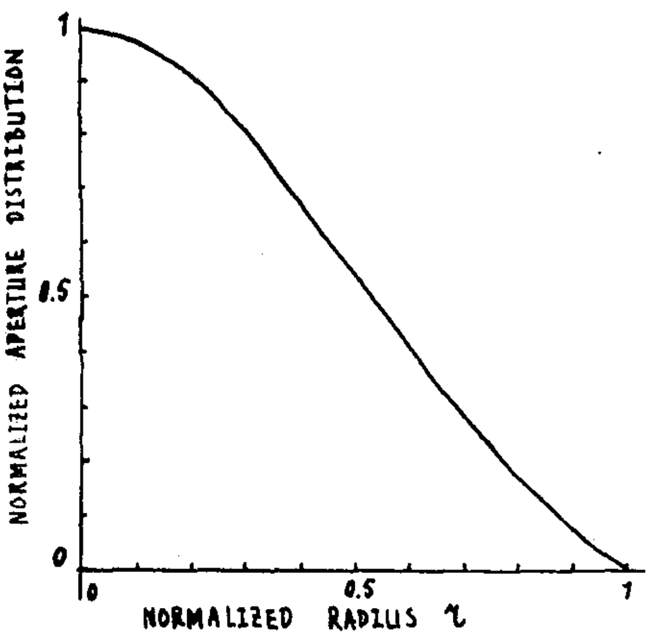

SIDELOBE LEVELS:	PRESCRIBED	COMPUTED
	-36 dB	-35.4
	-41	-41.1
	-46	-46.1

ZEROS: $u_1+t_1 = 6.3181$
$u_2+t_2 = 8.7963$
$u_3+t_3 = 11.8050$
$u_4 = 14.9309$

EXCITATION COEFFICIENTS:
$a_0 = 4.90518$
$a_1 = 0.92027$
$a_2 = -0.05193$
$a_3 = 0.00344$

EFFICIENCY: 0.6082

GAIN REDUCTION: 2.16 dB

$u_{3dB} = 4.40$

FIG. 31: APERTURE DISTRIBUTION $\sum_{m=0}^{3} a_m J_0(u_m r)$ AND RADIATION PATTERN.

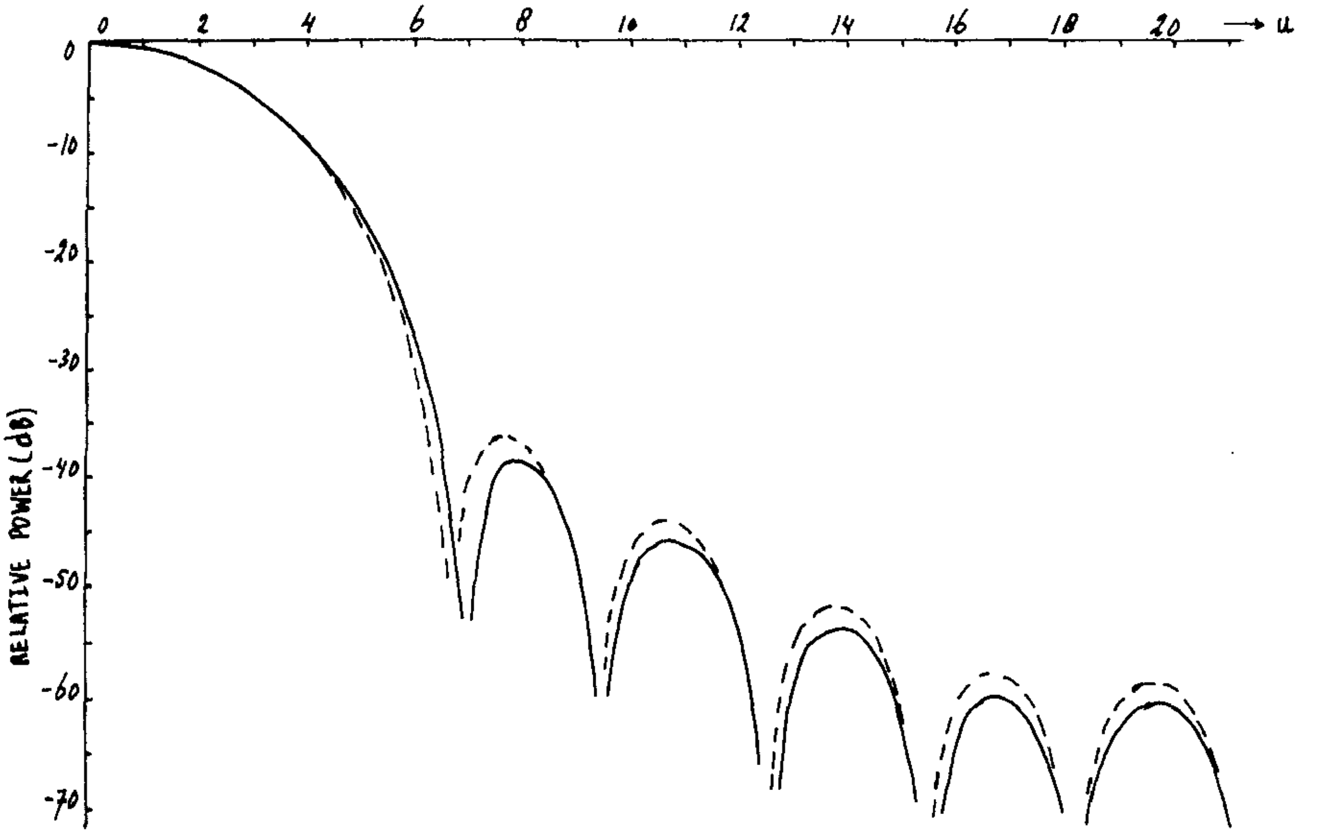

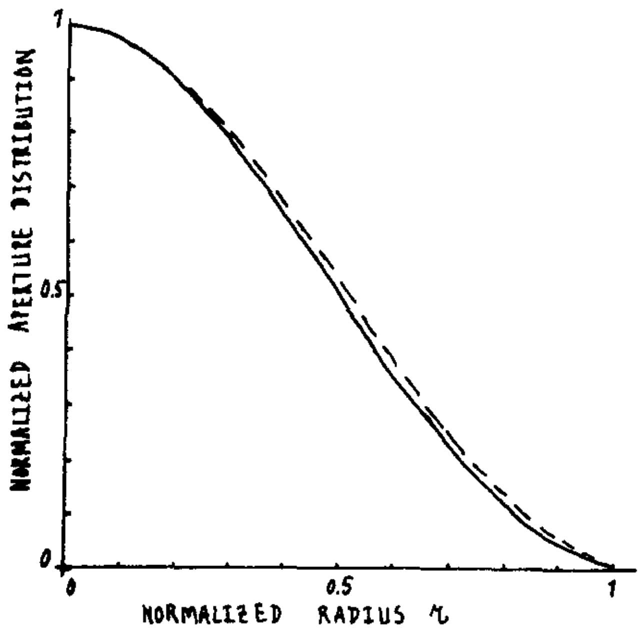

		1° RUN	2° RUN
SIDELOBE LEVELS	PRESCRIBED	COMPUTED	
	-36 dB	-38.7 dB	-36.2 d
	-44	-45.8	-44.1
	-52	-54.0	-51.9
	-60	-60.0	-57.8
	—	-60.6	-58.9
ZEROS	u_1+t_1	6.9149	6.6311
	u_2+t_2	9.4503	9.3083
	u_3+t_3	12.5332	12.404
	u_4+t_4	15.4167	15.3411
	u_5	18.0711	18.0711
EXCITATION COEFFICIENTS			
	a_0	5.13020	5.0524
	a_1	1.59584	1.3208
	a_2	-0,19573	-0.1999
	a_3	0.09705	0.098
	a_4	-0.03639	-0.03
EFFICIENCY		0.5418	0.565
GAIN REDUCTION		2.66 dB	2.48
u_{3dB}		4.66	4.56

FIG. 32 : APERTURE DISTRIBUTION $\sum_{m=0}^{4} a_m J_0(u_m r)$ AND RADIATION PATTERN

——— FIRST APPROXIMATION — — — SECOND APPROXIMATION

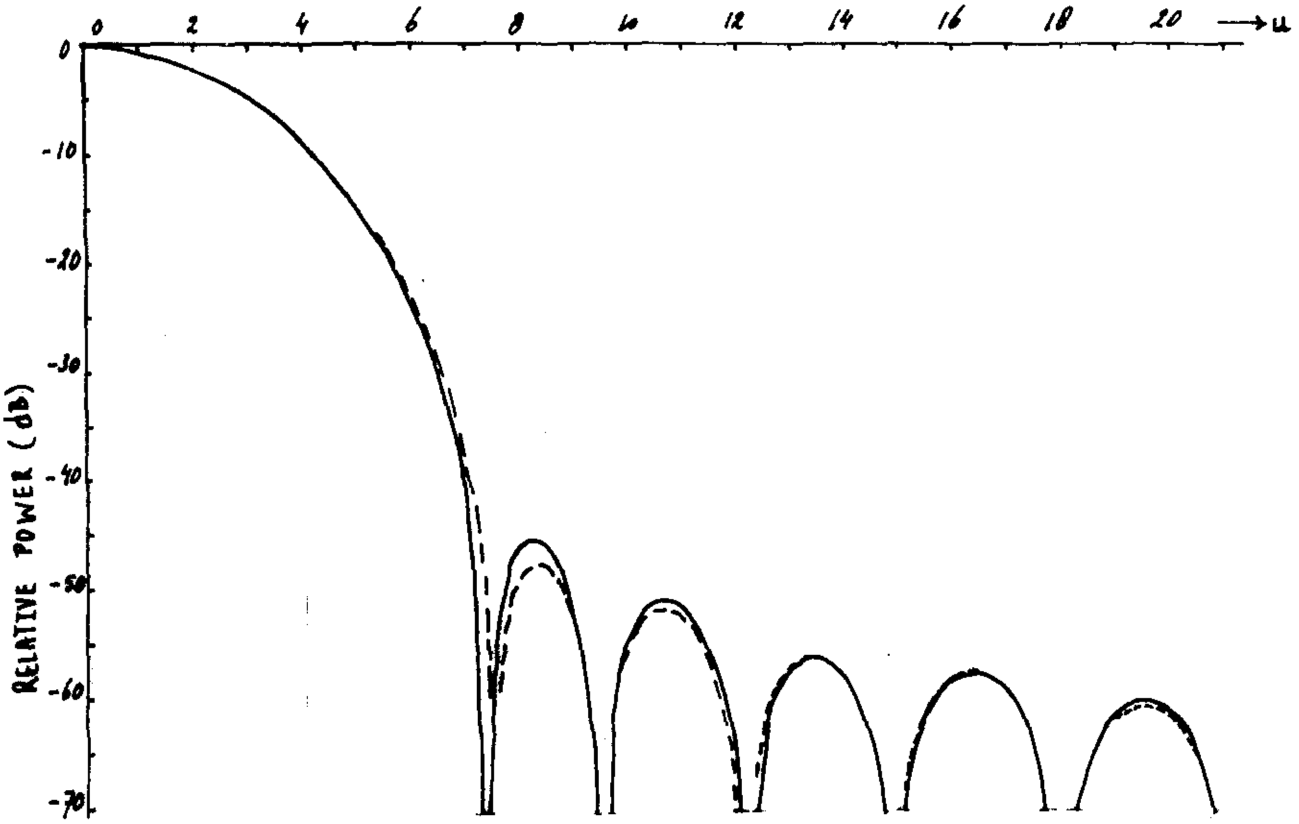

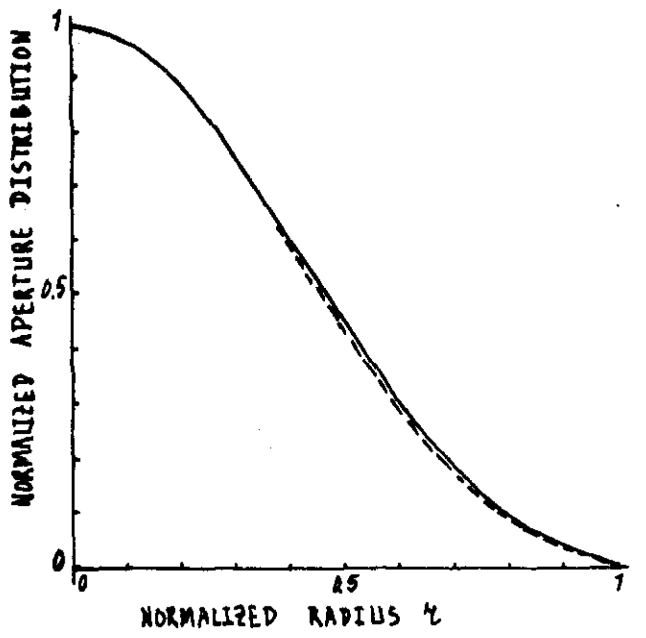

		1°RUN	2°RUN
SIDELOBE LEVELS	PRESCRIBED	COMPUTED	
	-48 dB	-46.6 dB	-47.5 dB
	-52	-51.7	-52.0
	-56	-56.3	-56.2
	–	-57.5	-57.7
	–	-60.4	-60.6
ZEROS	u_1+t_1	7.4891	7.6179
	u_2+t_2	9.5512	9.5527
	u_3+t_3	12.2434	12.1817
	u_4	14.9309	14.9309
EXCITATION COEFFICIENTS			
	a_0	5.22366	5.24177
	a_1	1.98776	2.06196
	a_2	-0.11904	-0.10219
	a_3	0.04052	0.03323
EFFICIENCY		0.5126	0.5071
GAIN REDUCTION		2.90 dB	2.95 dB
u_{3dB}		4.77	4.79

FIG. 33: APERTURE DISTRIBUTION $\sum_{n=0}^{3} a_n J_0(u_n r)$ AND RADIATION PATTERN.

——— FIRST APPROXIMATION — — — SECOND APPROXIMATION.

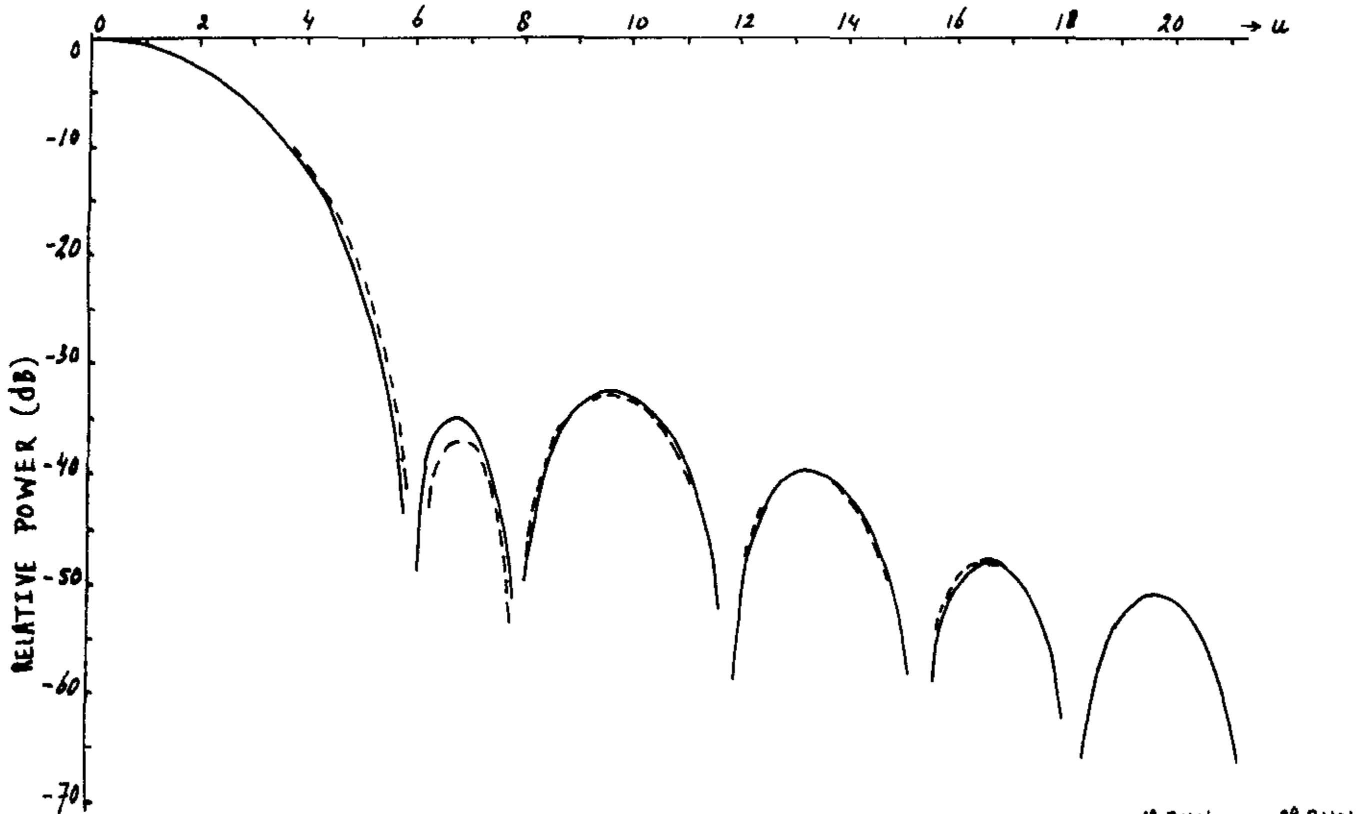

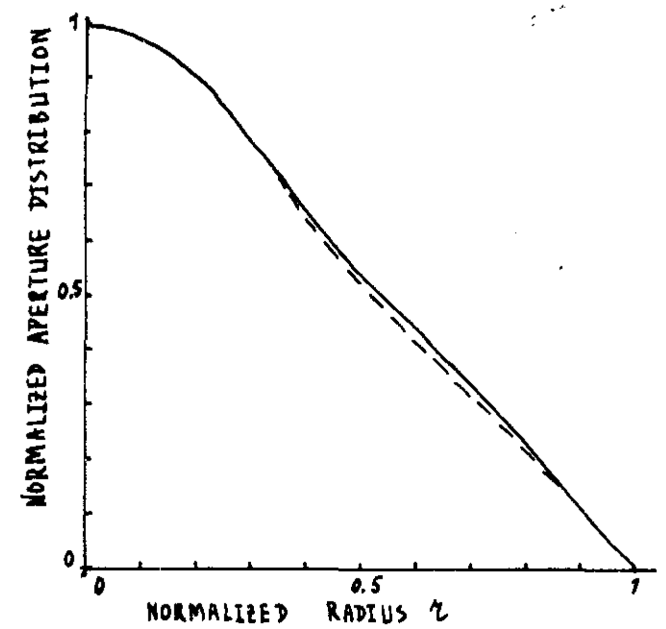

		1° RUN	2° RUN
SIDELOBE LEVELS	PRESCRIBED	COMPUTED	
	−37.5 dB	−34.7 dB	−36.8
	−32.5	−32.2	−32.5
	−40.0	−39.7	−39.7
	−48.0	−48.0	−47.8
	—	−50.9	−50.9
ZEROS	u_1+t_1	5.8683	5.996
	u_2+t_2	7.8631	7.797
	u_3+t_3	11.7249	11.676
	u_4+t_4	15.1971	15.158
	u_5	18.0711	18.071
EXCITATION COEFFICIENTS			
	a_0	4.67754	4.7065
	a_1	0.37616	0.4878
	a_2	0.45560	0.454
	a_3	−0.03249	−0.057
	a_4	−0.07885	−0.06
EFFICIENCY		0.6753	0.665
GAIN REDUCTION		1.71 dB	1.77
u_{3dB}		4.18	4.21

FIG. 34 : APERTURE DISTRIBUTION $\sum_{n=0}^{4} a_n J_0(u_n r)$ AND RADIATION PATTERN

——— FIRST APPROXIMATION   – – – SECOND APPROXIMATION

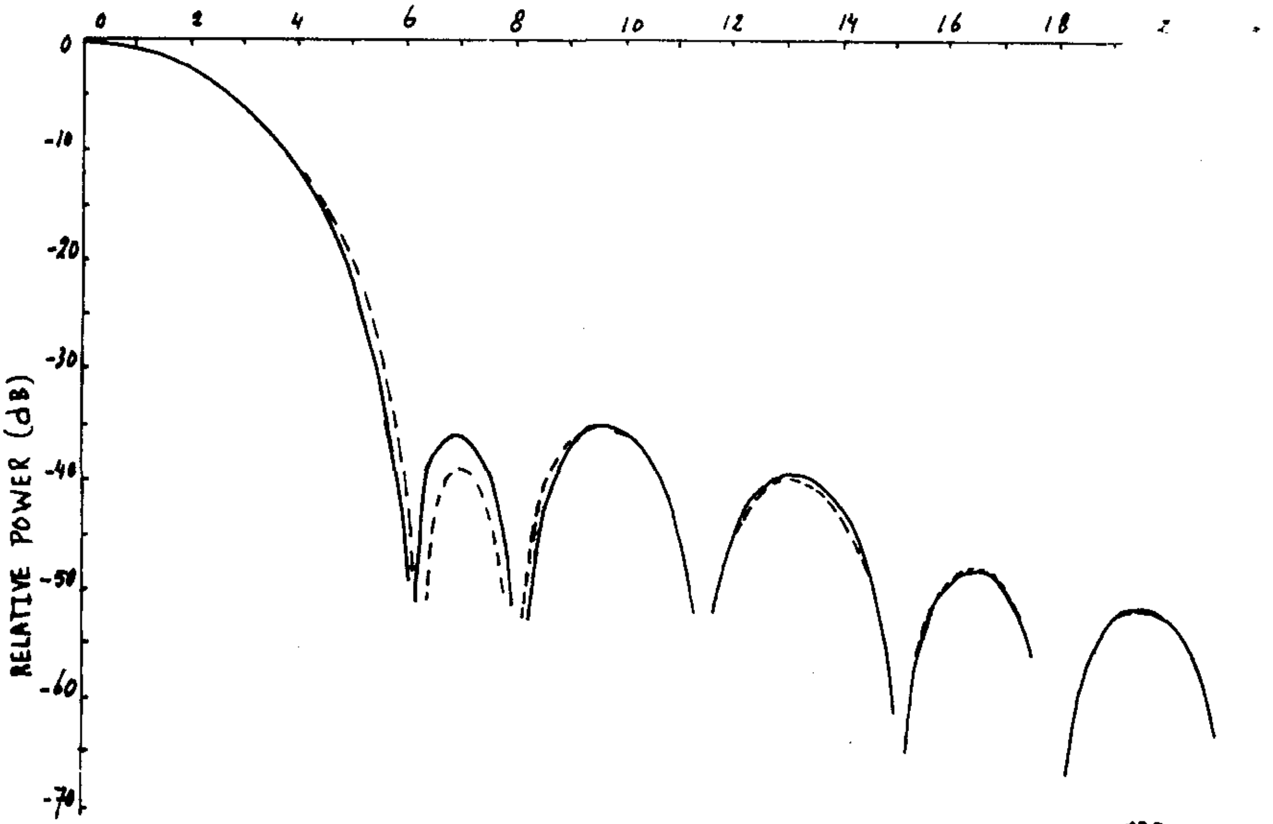

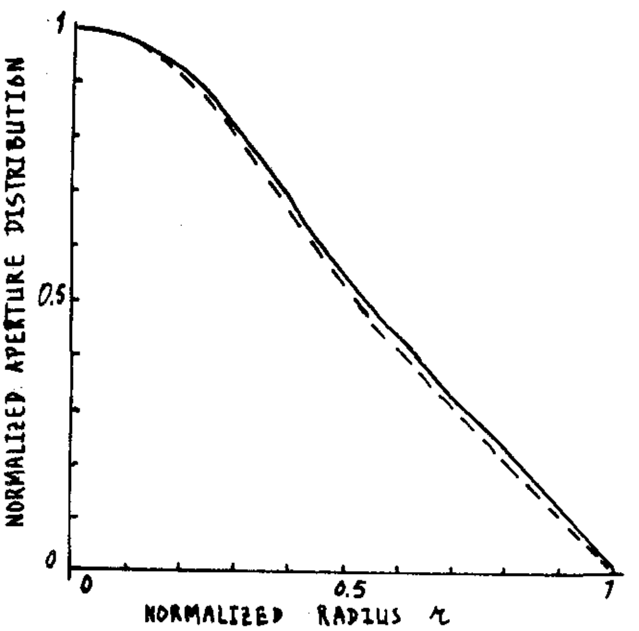

		1° RUN	2° RUN
SIDELOBE LEVELS	PRESCRIBED	COMPUTED	
	-40 dB	-35.7 dB	-39.0 dB
	-35	-35.1	-35.1
	-40	-39.4	-39.7
	-48	-48.0	-47.8
	—	-51.2	-51.3
ZEROS	u_1+t_1	6.0176	6.2035
	u_2+t_2	8.0597	7.9238
	u_3+t_3	11.4797	11.4777
	u_4+t_4	15.1495	15.0926
	u_5	18.0711	18.0711
EXCITATION COEFFICIENTS			
	a_0	4.73751	4.77347
	a_1	0.53422	0.67895
	a_2	0.28333	0.31522
	a_3	-0.13435	-0.13098
	a_4	-0.06371	-0.04631
EFFICIENCY		0.6575	0.6455
GAIN REDUCTION		1.82 dB	1.90 dB
u_{3dB}		4.24	4.27

FIG. 35 : APERTURE DISTRIBUTION $\sum_{n=0}^{4} a_m J_0(u_m r)$ AND RADIATION PATTERN.

——— FIRST APPROXIMATION – – – SECOND APPROXIMATION.

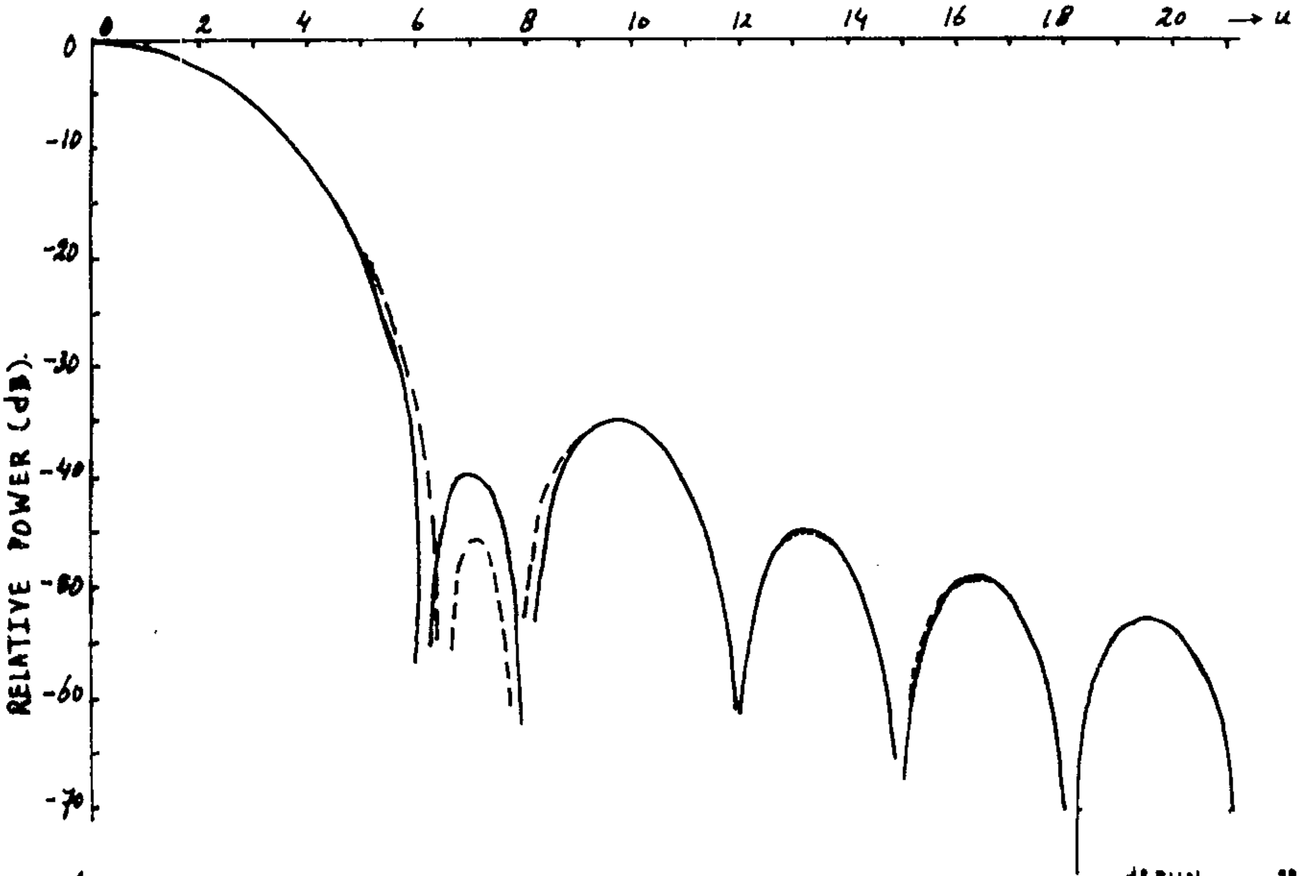

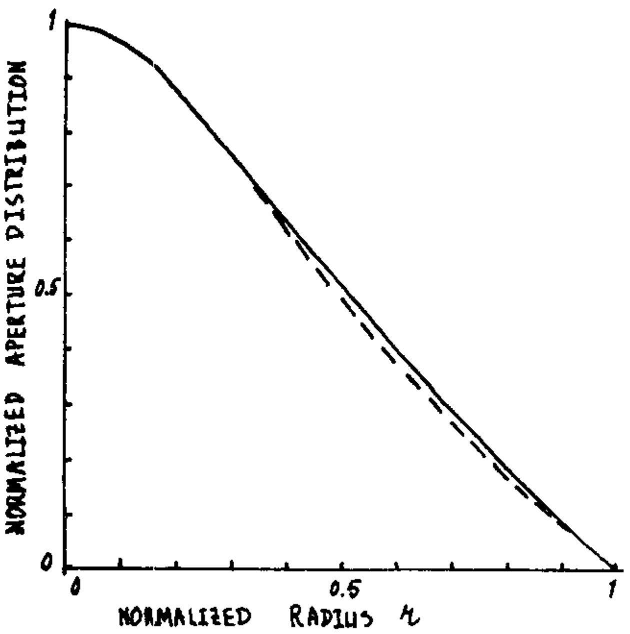

		1° RUN	2° RUN
SIDE LOBE LEVELS	PRESCRIBED	COMPUTED	
	-50 dB	-39.7 dB	-46.0
	-35	-35.1	-35.1
	-45	-45.1	-44.7
	—	-49.0	-49.1
	—	-52.8	-52.8
ZEROS	u_1+t_1	6.3447	6.5973
	u_2+t_2	8.0541	7.8316
	u_3+t_3	11.9915	11.9352
	u_4	14.9309	14.9309
EXCITATION COEFFICIENTS			
	a_0	4.84212	4.87354
	a_1	0.83406	0.97386
	a_2	0.25238	0.29944
	a_3	0.06723	0.0483[illegible]
EFFICIENCY		0.6251	0.6143
GAIN REDUCTION		2.04 dB	2.11 dB
u_{3dB}		4.34	4.37.

FIG. 36 : APERTURE DISTRIBUTION $\sum_{n=0}^{3} a_n J_0(u_n r)$ AND RADIATION PATTERN
—— FIRST APPROXIMATION – – – SECOND APPROXIMATION

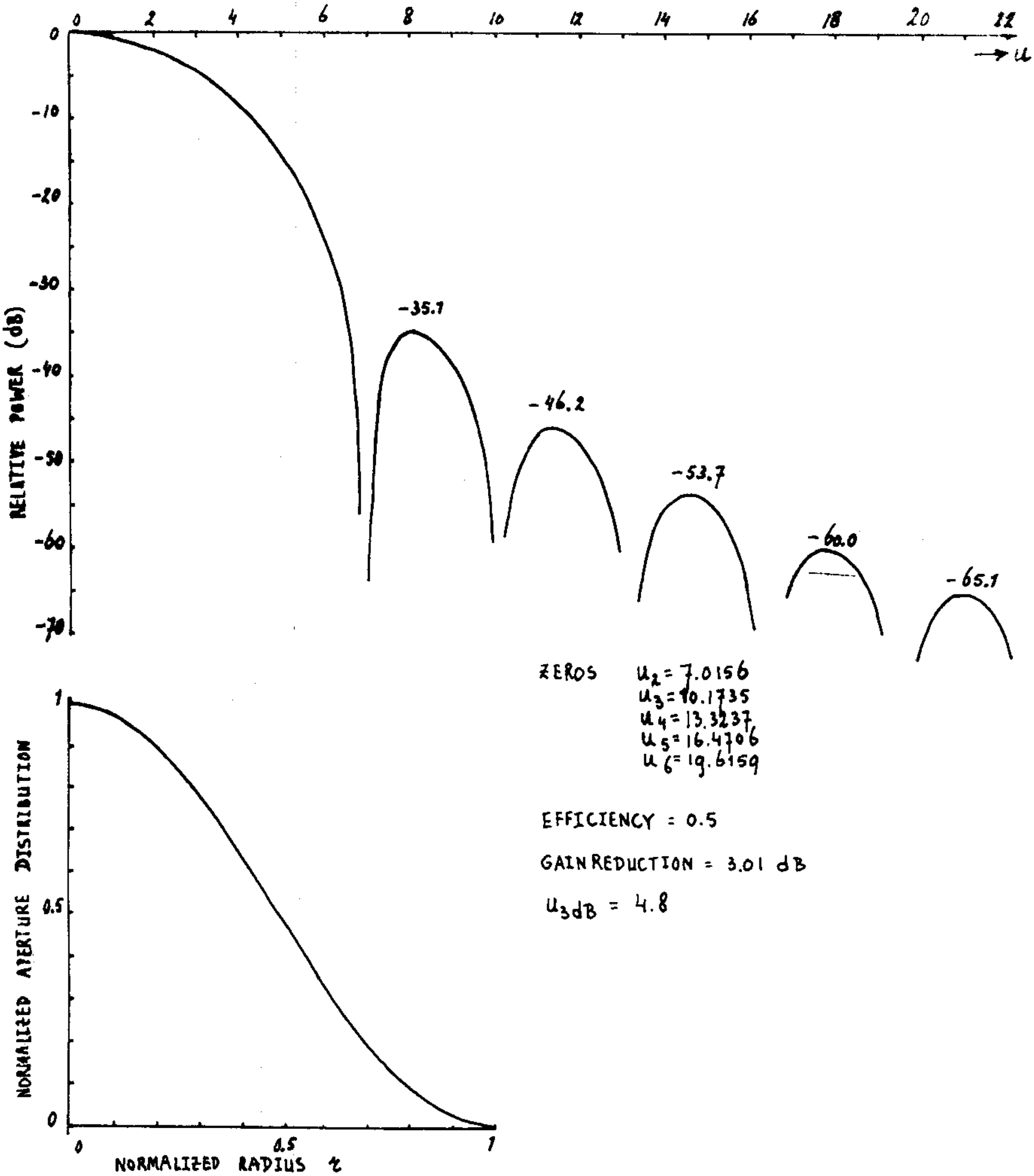

FIG. 37 : APERTURE DISTRIBUTION $J_0(3.8317r) - J_0(3.8317)$ (NORMALIZED) AND RADIATION PATTERN

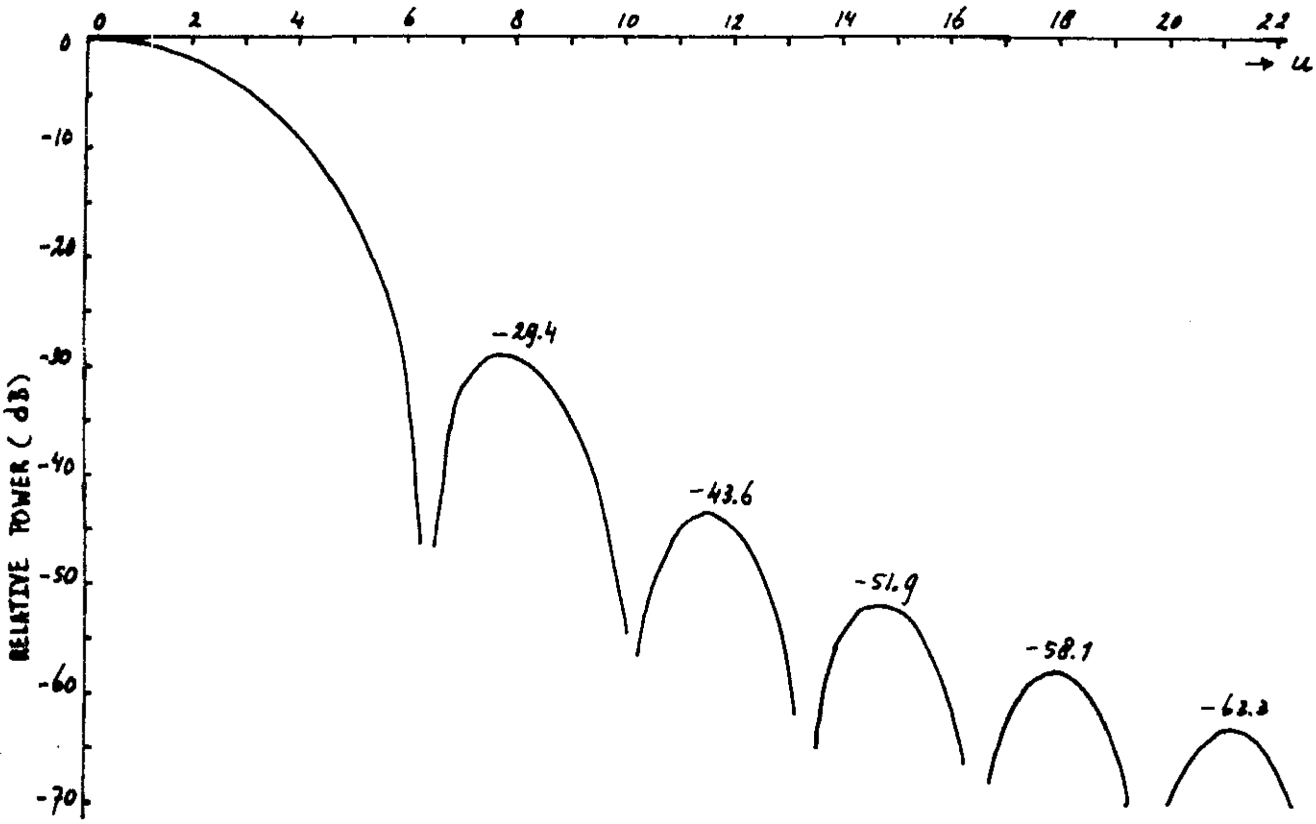

SIDELOBE LEVEL	PRESCRIBED	COMPUTED
	-30 dB	-29.4 dB

ZEROS $u_2 + t_2 = 6.4022$
$u_3 = 10.1735$

EXCITATION COEFFICIENTS
$a_1 = 4.54238$
$a_2 = -0.56756$

EFFICIENCY = 0.5423

GAIN REDUCTION = 2.66 dB

$u_{3\,dB} = 4.67$

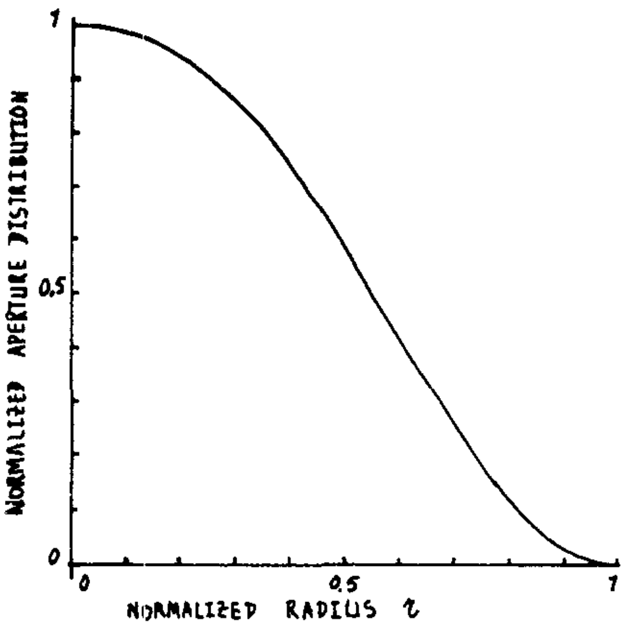

FIG. 38: APERTURE DISTRIBUTION $\sum_{n=1}^{2} a_n \left\{ J_0(u_n r) - J_0(u_n) \right\}$ AND RADIATION PATTERN

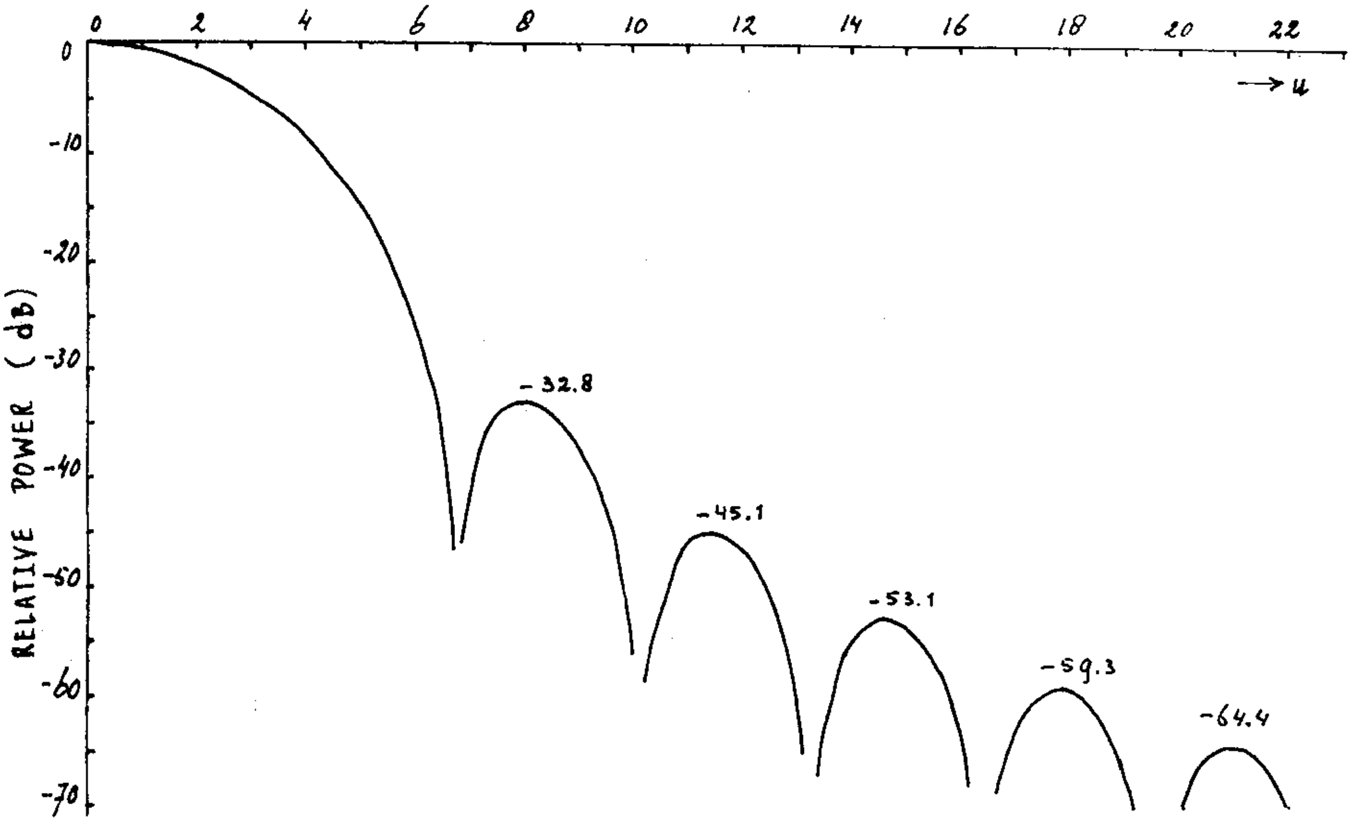

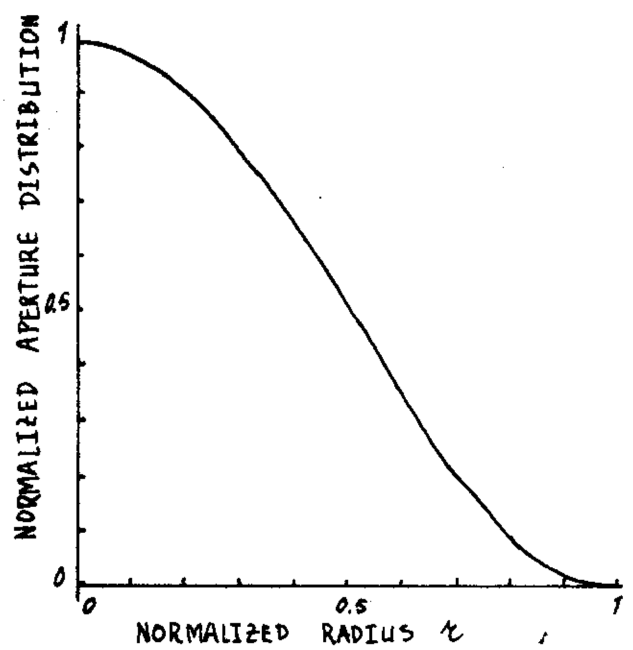

SIDELOBE LEVEL	PRESCRIBED	COMPUTED
	-33 dB	-32.8 dB

ZEROS $u_2 + t_2 = 6.7788$
$u_3 = 10.1735$

EXCITATION COEFFICIENTS
$a_1 = 4.81608$
$a_2 = -0.20040$

EFFICIENCY = 0.5150

GAIN REDUCTION = 2.88 dB

$u_{3\,dB} = 4.79$

FIG. 3g: APERTURE DISTRIBUTION $\sum_{n=1}^{2} a_n \{ J_0(u_n r) - J_0(u_n) \}$ AND RADIATION PATTERN.

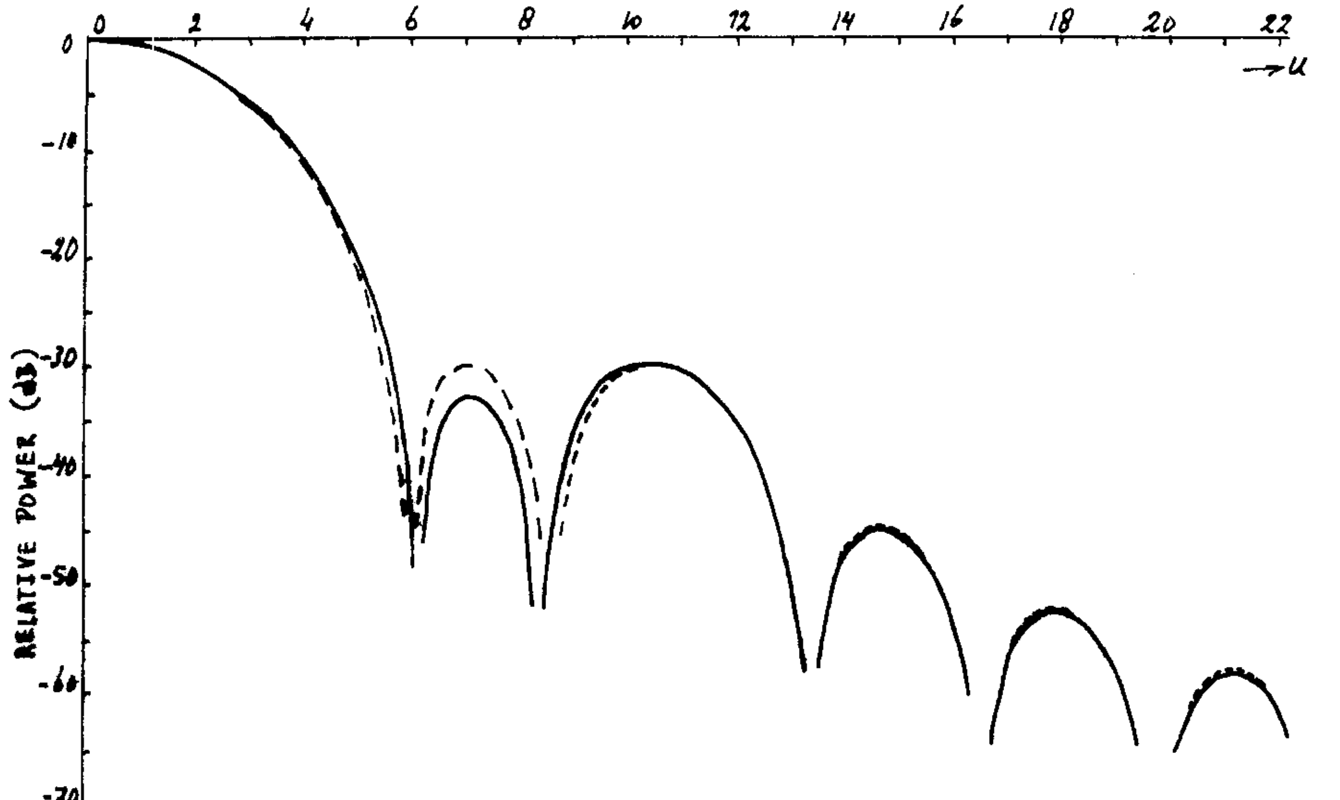

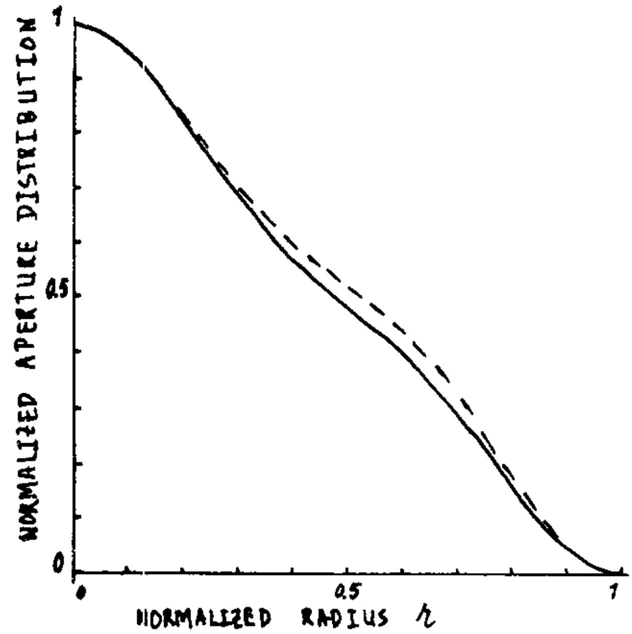

		PRESCRIBED	1° RUN (COMPUTED)	2° RUN (COMPUTED)
SIDELOBE LEVELS		−30 dB	−32.9 dB	−29.7
		−30	−29.8	−30.0
		—	−45.2	−45.1
		—	−52.5	−52.3
		—	−58.1	−57.9
ZEROS	u_2+t_2		6.1159	5.9024
	u_3+t_3		8.3551	8.534
	u_4		13.3237	13.323
EXCITATION COEFFICIENTS	a_1		3.95683	3.8103
	a_2		−0.50209	−0.7216
	a_3		1.02260	0.9948
EFFICIENCY			0.6036	0.618
GAIN REDUCTION			2.19 dB	2.08
u_{3dB}			4.42	4.37

FIG. 40: APERTURE DISTRIBUTION $\sum_{n=1}^{3} a_n \{ J_0(u_n r) - J_0(u_n) \}$ AND RADIATION PATTERN

——— FIRST APPROXIMATION. – – – SECOND APPROXIMATION

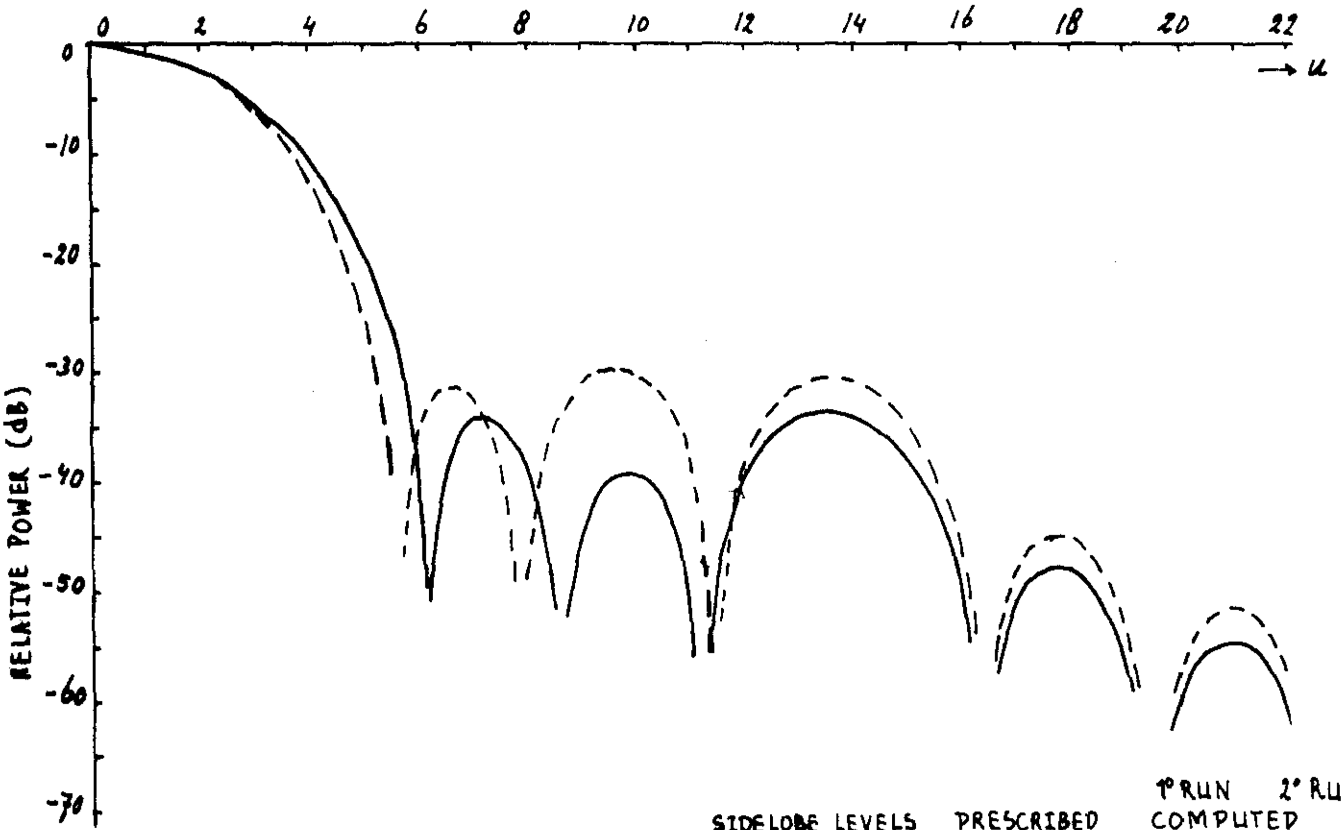

SIDELOBE LEVELS	PRESCRIBED	COMPUTED 1° RUN	2° RUN
	−30 dB	−34.0 dB	−31.3 dB
	−30	−39.0	−29.6
	−30	−33.5	−30.3
	—	−48.0	−44.8
	—	−54.7	−51.6
ZEROS u_2+t_2		6.2085	5.6668
u_3+t_3		8.6539	7.8774
u_4+t_4		11.2505	11.5248
u_5		16.4706	16.4706
EXCITATION COEFFICIENTS a_1		3.95649	3.31466
a_2		−0.43250	−0.51732
a_3		0.33698	0.94230
a_4		−0.88022	−1.25495
EFFICIENCY		0.6056	0.6737
GAIN REDUCTION		2.18 dB	1.72 dB
$u_{3\,dB}$		4.41	4.18

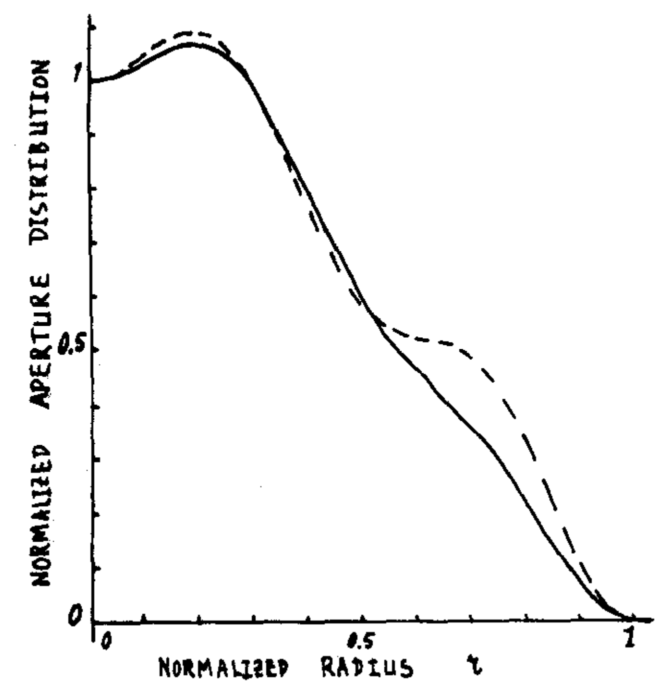

FIG. 41: APERTURE DISTRIBUTION $\sum_{m=1}^{4} a_m \{ J_0(u_m r) - J_0(u_m) \}$ AND RADIATION PATTERN

——— FIRST APPROXIMATION. — — SECOND APPROXIMATION.

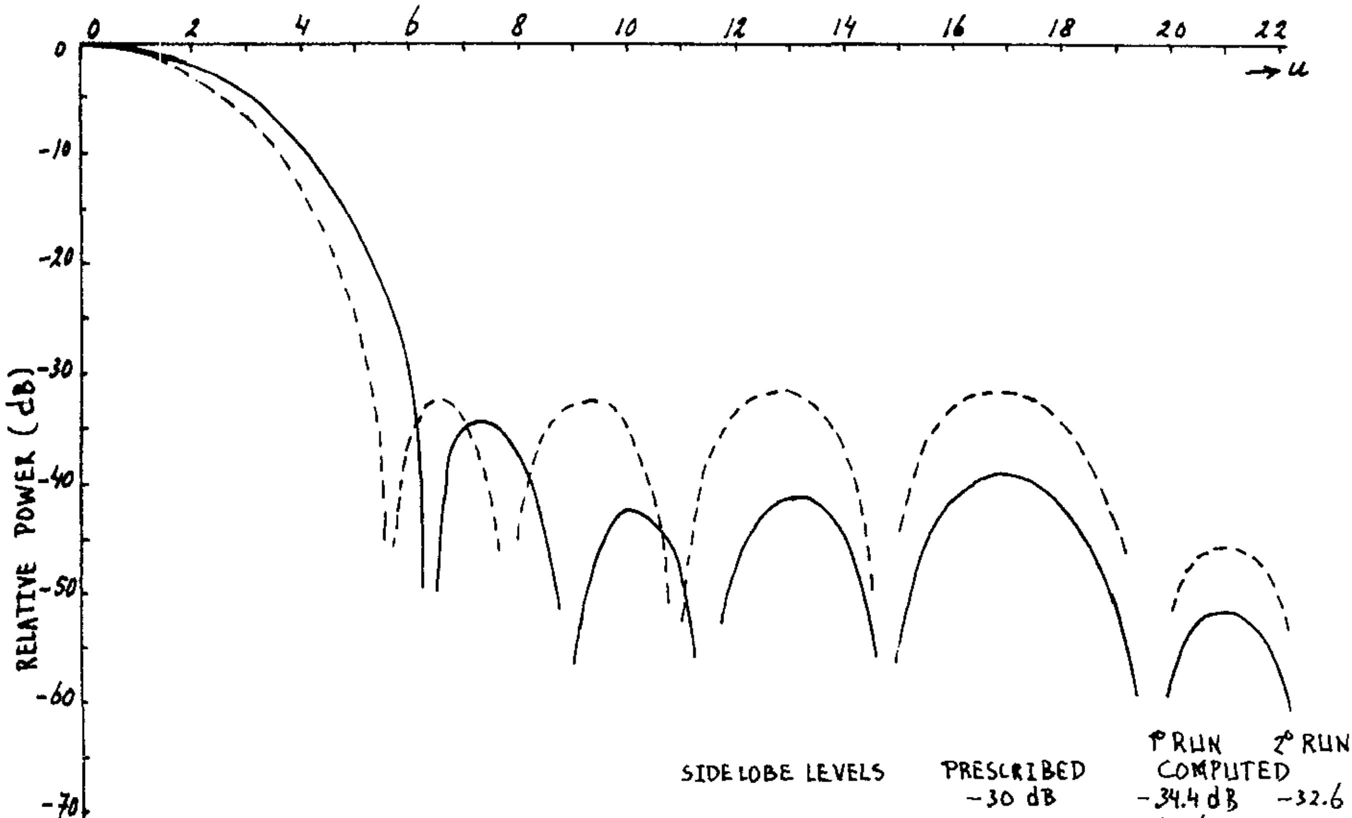

SIDE LOBE LEVELS	PRESCRIBED	1° RUN COMPUTED	2° RUN COMPUTED
	-30 dB	-34.4 dB	-32.6
	-30	-42.6	-32.5
	-30	-41.3	-31.6
	-30	-39.3	-31.8
	—	-52.0	-45.5
ZEROS u_2+t_2		6.3264	5.6608
u_3+t_3		8.9589	7.7894
u_4+t_4		11.4533	10.898
u_5+t_5		14.7756	14.672
u_6		19.6159	19.615
EXCITATION COEFFICIENTS			
a_1		4.07388	3.1891
a_2		-0.39165	-0.4165
a_3		0.23652	0.4880
a_4		-0.35167	-0.9710
a_5		0.53647	1.303
EFFICIENCY		0.5943	0.6907
GAIN REDUCTION		2.26 dB	1.61 d
$u_{3\,dB}$		4.45	4.12

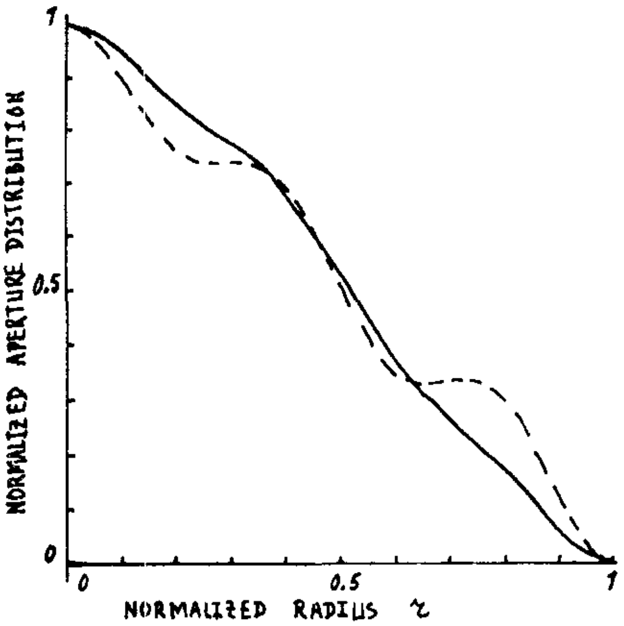

FIG. 42: APERTURE DISTRIBUTION $\sum_{n=1}^{5} a_n \{ J_0(u_n r) - J_0(u_n) \}$ AND

RADIATION PATTERN.

——— FIRST APPROXIMATION. - - - SECOND APPROXIMATION.

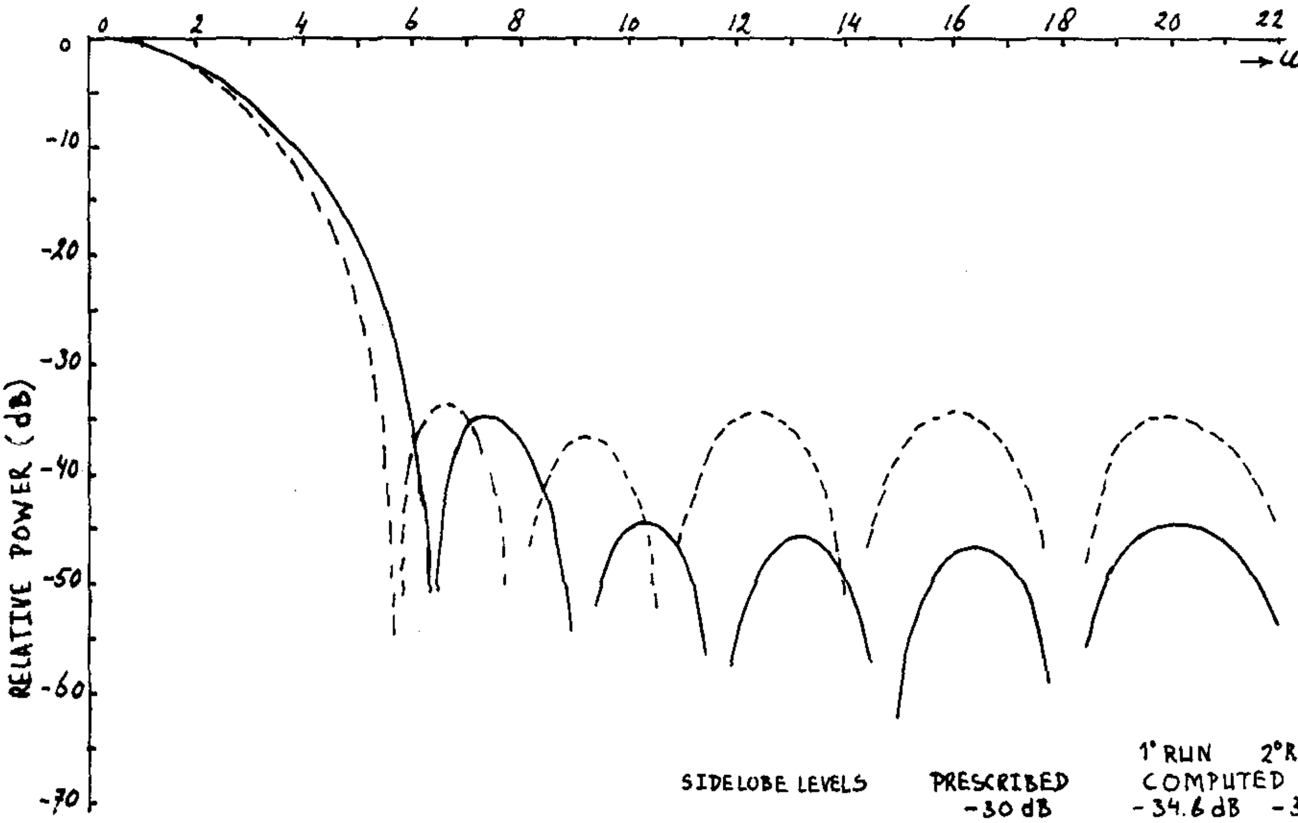

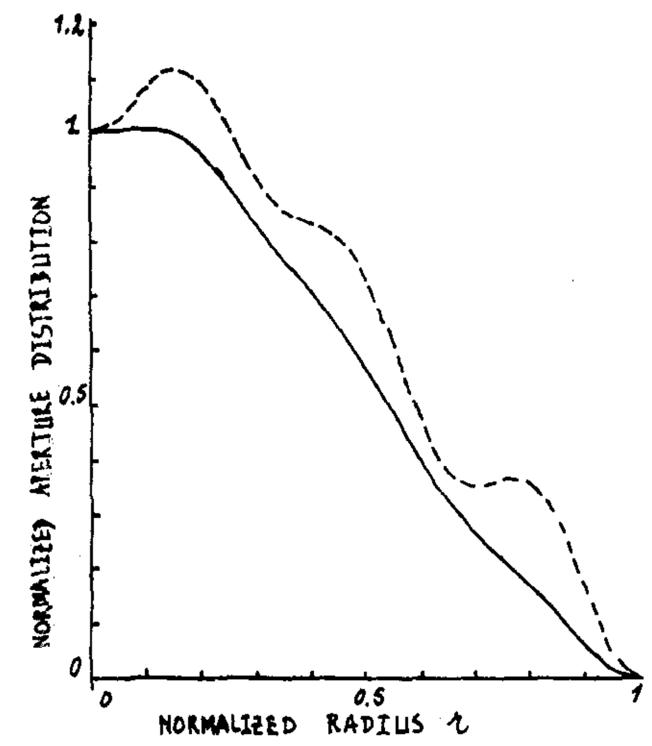

		PRESCRIBED	1° RUN COMPUTED	2° RUN COMPUTED
SIDELOBE LEVELS		-30 dB	-34.6 dB	-33.3 dB
		-30	-44.0	-36.5
		-30	-45.6	-34.3
		-30	-46.5	-34.2
		-30	-44.4	-34.8
ZEROS	u_2+t_2		6.4220	5.7537
	u_3+t_3		9.1755	7.9871
	u_4+t_4		11.7535	10.6564
	u_5+t_5		14.8248	14.1761
	u_6+t_6		18.0883	17.9880
	u_7		22.7601	22.7601
EXCITATION COEFFICIENTS	a_1		4.18603	3.26319
	a_2		-0.35600	-0.42152
	a_3		0.19937	0.24560
	a_4		-0.21808	-0.54793
	a_5		0.24405	0.93786
	a_6		-0.34298	-1.07972
EFFICIENCY			0.5827	0.6859
GAIN REDUCTION			2.35 dB	1.64 dB
u_{3dB}			4.50	4.14

FIG. 43 : APERTURE DISTRIBUTION $\sum_{n=1}^{6} a_n \left\{ J_0(u_n r) - J_0(u_n) \right\}$ AND RADIATION PATTERN.

——— FIRST APPROXIMATION. — — — SECOND APPROXIMATION.

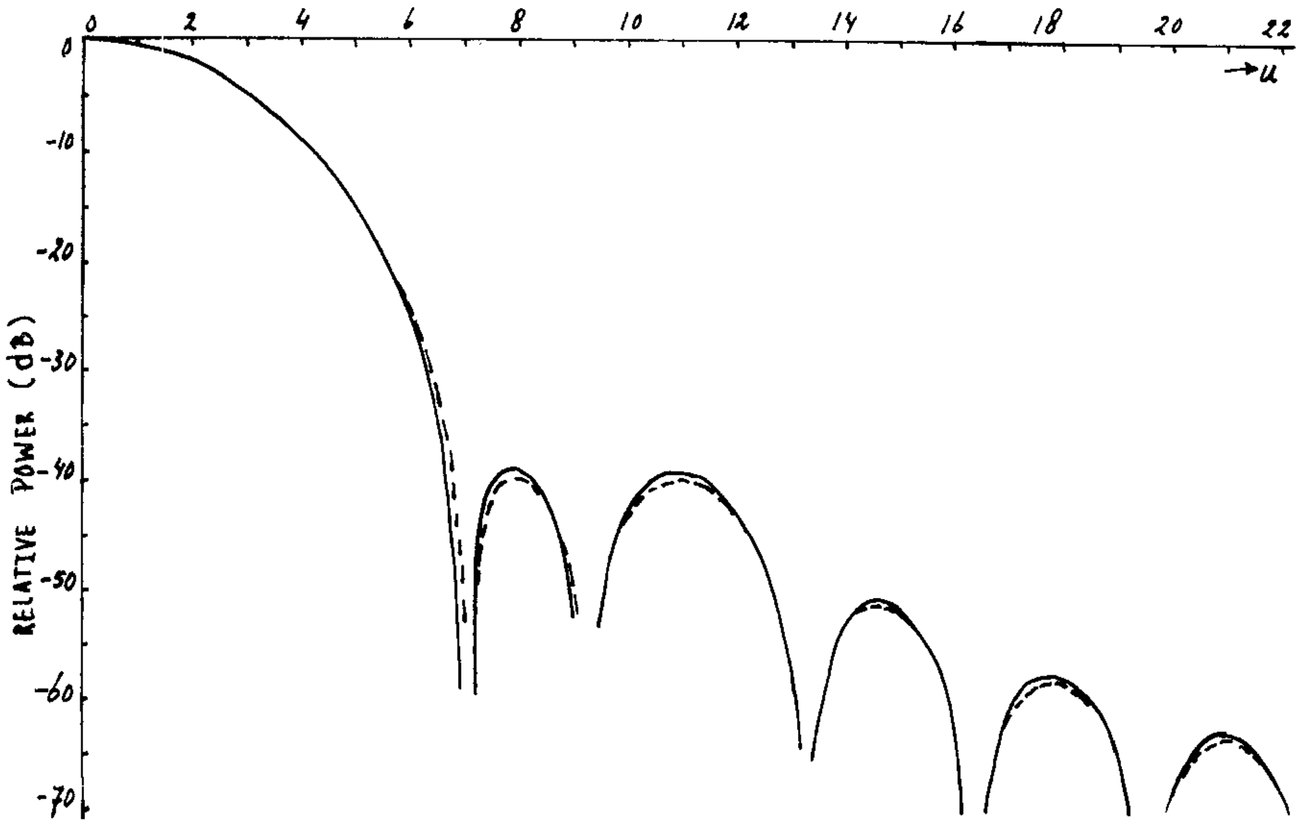

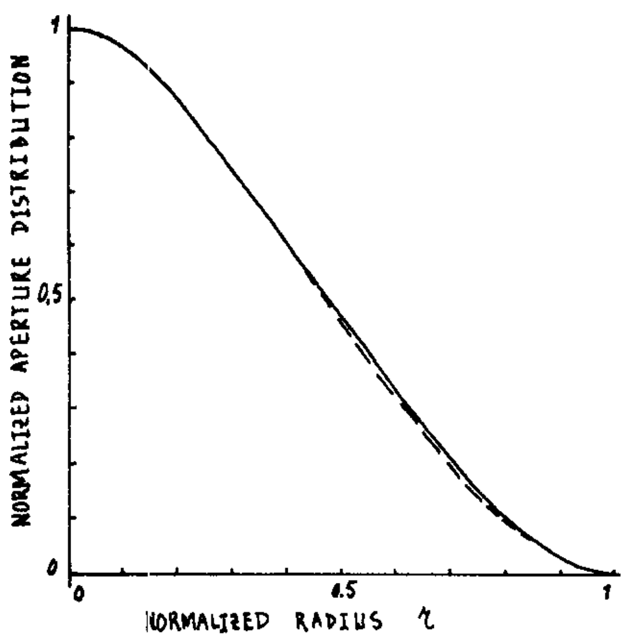

		PRESCRIBED	1° RUN COMPUTED	2° RUN COMPUTED
SIDE LOBE LEVELS		-40 dB	-38.9 dB	-39.6 dB
		-40	-39.3	-40.0
		—	-51.0	-51.4
		—	-57.7	-58.1
		—	-63.0	-63.3
ZEROS	u_2+t_2		7.0360	7.1141
	u_3+t_3		9.2497	9.2957
	u_4		13.3237	13.3237
EXCITATION COEFFICIENTS	a_1		4.80584	4.85997
	a_2		0.01409	0.06470
	a_3		0.27406	0.24761
EFFICIENCY			0.5160	0.5104
GAIN REDUCTION			2.87 dB	2.92 dB
u_{3dB}			4.77	4.80

FIG. 44 : APERTURE DISTRIBUTION $\sum_{n=1}^{3} a_n\{J_0(u_n r) - J_0(u_n)\}$ AND RADIATION PATTERN.

—— FIRST APPROXIMATION. - - - SECOND APPROXIMATION

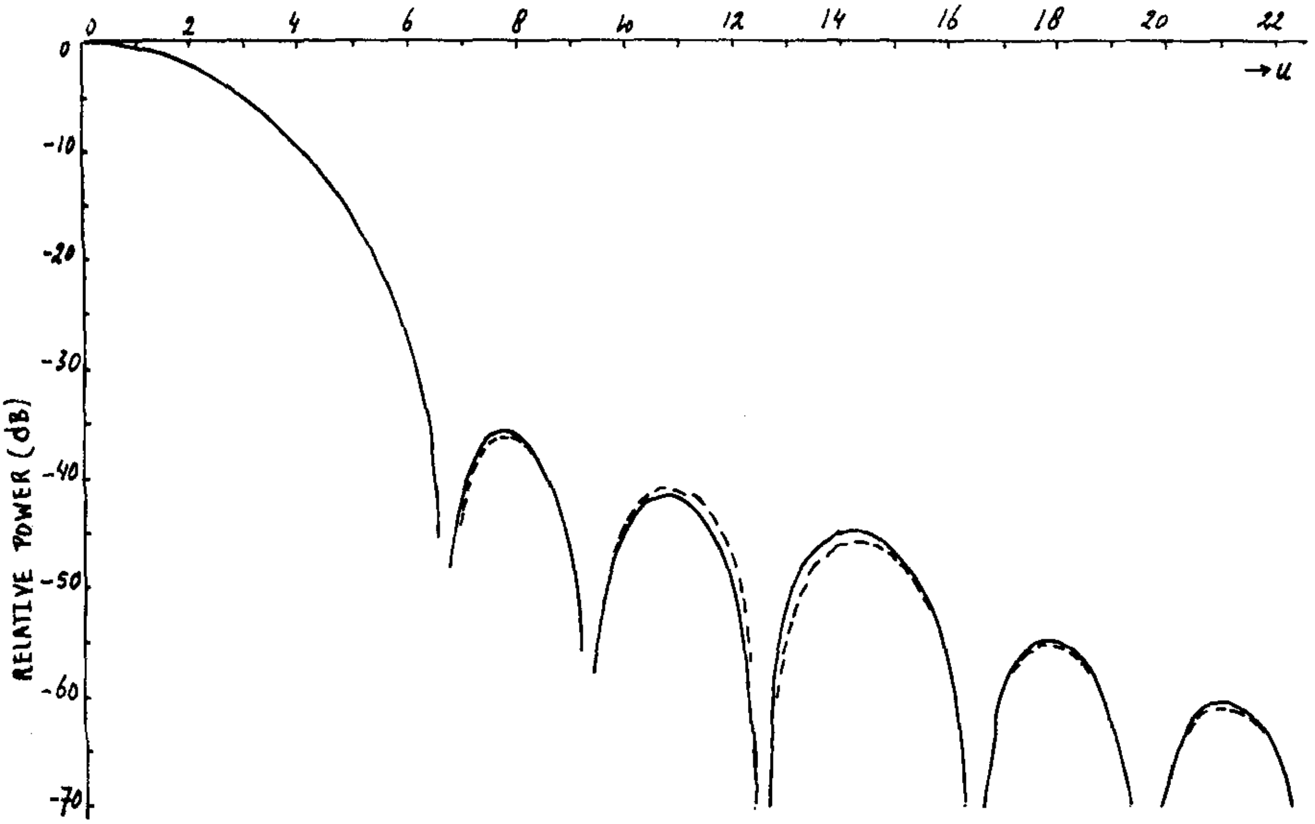

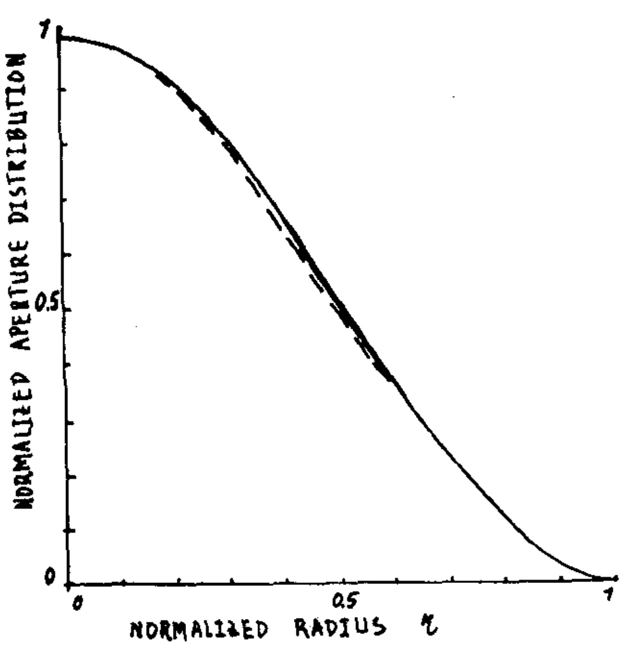

		PRESCRIBED	1° RUN COMPUTED	2° RUN COMPUTED
SIDELOBE LEVELS		-36 dB	-35.7 dB	-36.0 dB
		-41	-41.5	-41.0
		-46	-44.8	-45.8
		—	-54.9	-55.3
		—	-60.8	-61.1
ZEROS	u_2+t_2		6.7378	6.7701
	u_3+t_3		9.3738	9.3529
	u_4+t_4		12.5248	12.6720
	u_5		16.4706	16.4706
EXCITATION COEFFICIENTS	a_1		4.59268	4.62037
	a_2		-0,18891	-0,16647
	a_3		0.22240	0.23526
	a_4		-0.17283	-0.13790
EFFICIENCY			0.5383	0.5354
GAIN REDUCTION			2.69 dB	2.71 dB
u_{3dB}			4.68	4.69

FIG. 45: APERTURE DISTRIBUTION $\sum_{m=1}^{4} a_m \{J_0(u_m r) - J_0(u_m)\}$ AND RADIATION PATTERN.

——— FIRST APPROXIMATION — — — SECOND APPROXIMATION.

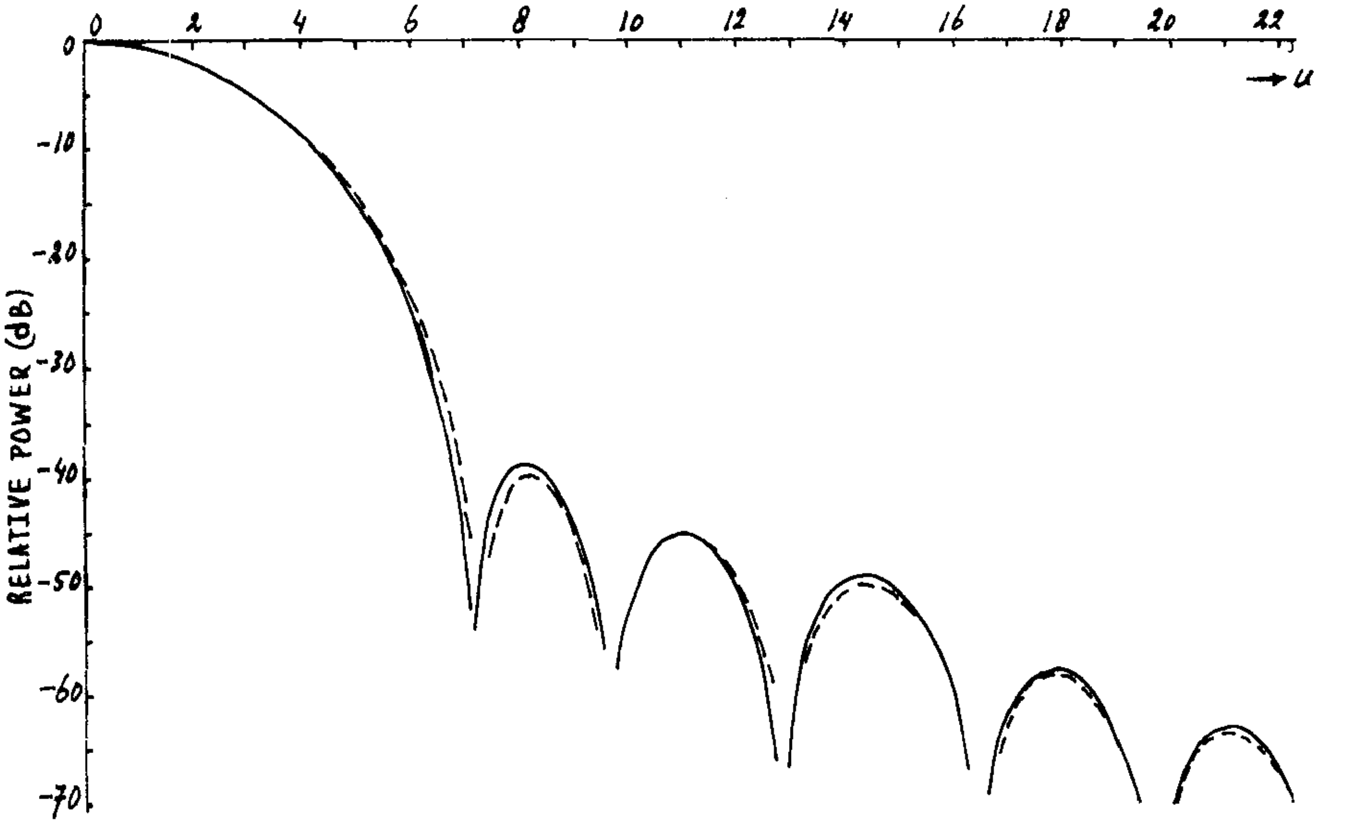

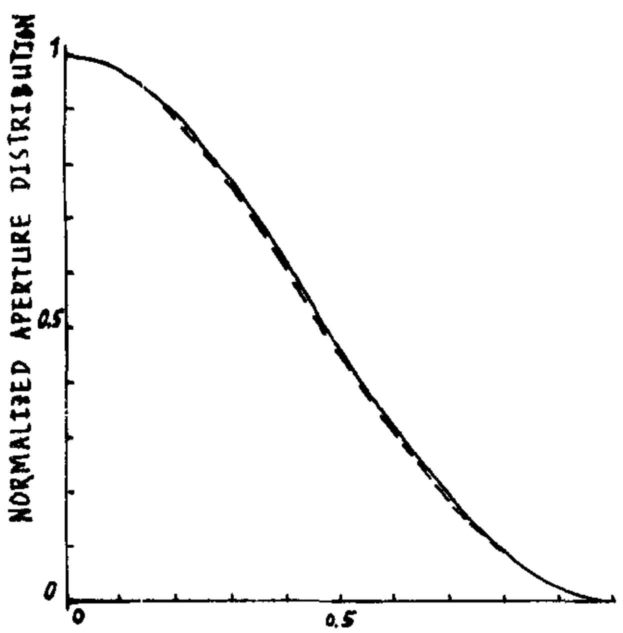

		PRESCRIBED	1° RUN COMPUTED	2° RUN COMPUTED
SIDELOBE LEVELS		-40 dB	-38.7 dB	-39.9 d
		-45	-45.0	-45.0
		-50	-49.0	-49.8
		—	-57.7	-58.2
		—	-63.2	-63.6
ZEROS	u_2+t_2		7.1637	7.2684
	u_3+t_3		9.7135	9.6908
	u_4+t_4		12.7739	12.8619
	u_5		16.4706	16.4706
EXCITATION COEFFICIENTS	a_1		4.93215	4.99166
	a_2		0.10293	0.17149
	a_3		0.10339	0.1051
	a_4		-0.08423	-0.0678
EFFICIENCY			0.5032	0.4972
GAIN REDUCTION			2.98 dB	3.04 d
u_{3dB}			4.83	4.85

FIG. 4b : APERTURE DISTRIBUTION $\sum_{m=1}^{4} a_m \{ J_0(u_m r) - J_0(u_m) \}$ AND RADIATION PATTERN.

——— FIRST APPROXIMATION. - - - SECOND APPROXIMATION

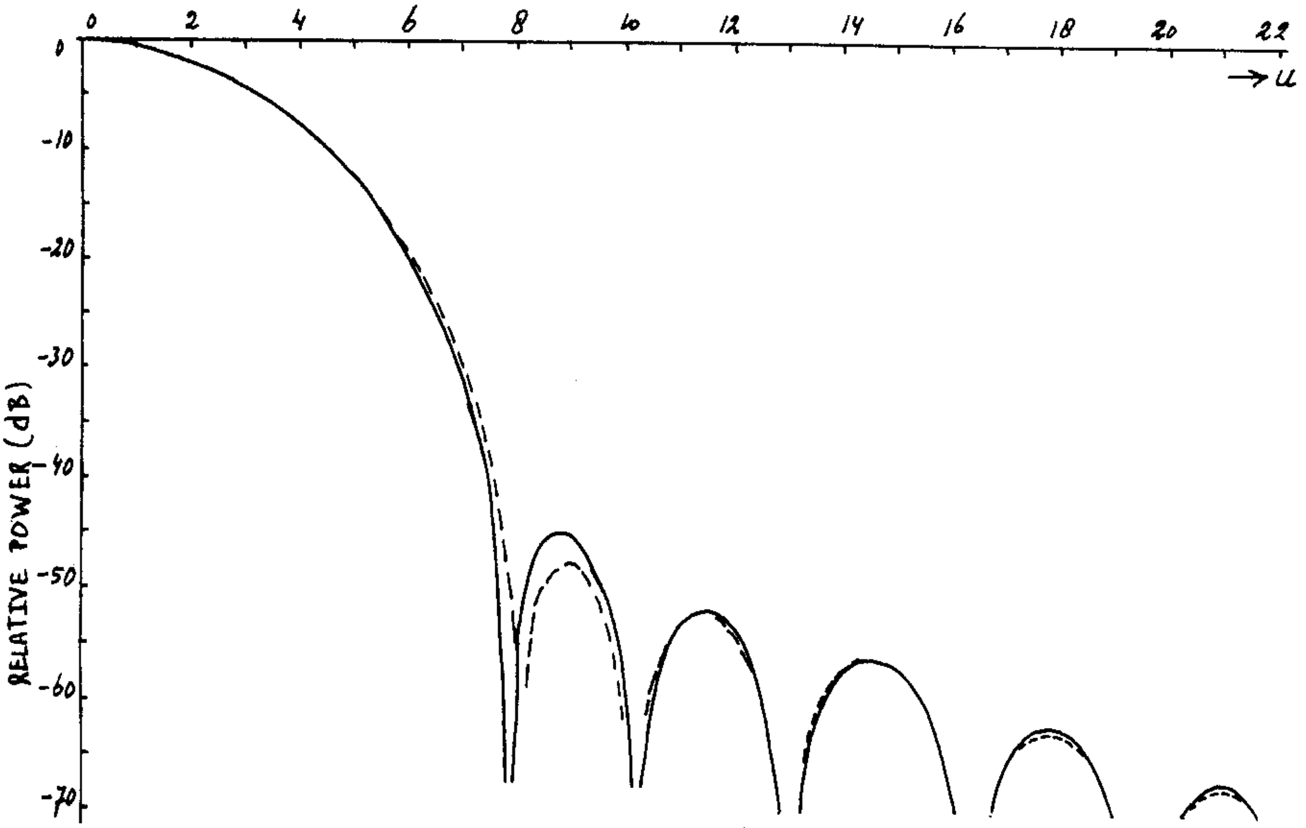

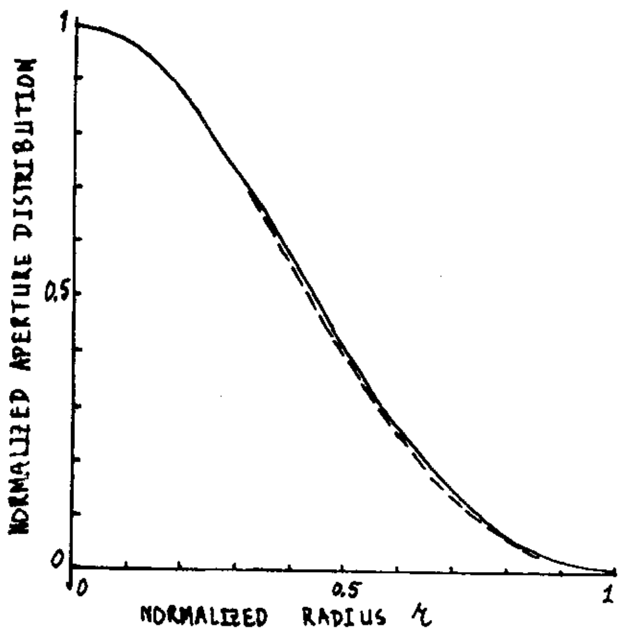

		1° RUN	2° RUN
SIDELOBE LEVELS	PRESCRIBED	COMPUTED	
	-48 dB	-44.8 dB	-47.4 dB
	-52	-51.7	-51.9
	-56	-55.9	-55.8
	—	-62.4	-62.5
	—	-67.7	-67.5
ZEROS	u_2+t_2	7.9528	8.1260
	u_3+t_3	10.2990	10.2130
	u_4+t_4	13.1321	13.0835
	u_5	16.4706	16.4706
EXCITATION COEFFICIENTS			
	a_1	5.44144	5.49201
	a_2	0.63526	0.71632
	a_3	-0.01787	-0.00509
	a_4	-0.01577	-0.01938
EFFICIENCY		0.4524	0.4473
GAIN REDUCTION		3.45 dB	3.49 dB
$u_{3\,dB}$		5.07	5.10

FIG. 47 : APERTURE DISTRIBUTION $\sum_{n=1}^{4} a_n \left\{ J_0(u_n r) - J_0(u_n) \right\}$ AND RADIATION PATTERN.

——— FIRST APPROXIMATION. - - - SECOND APPROXIMATION

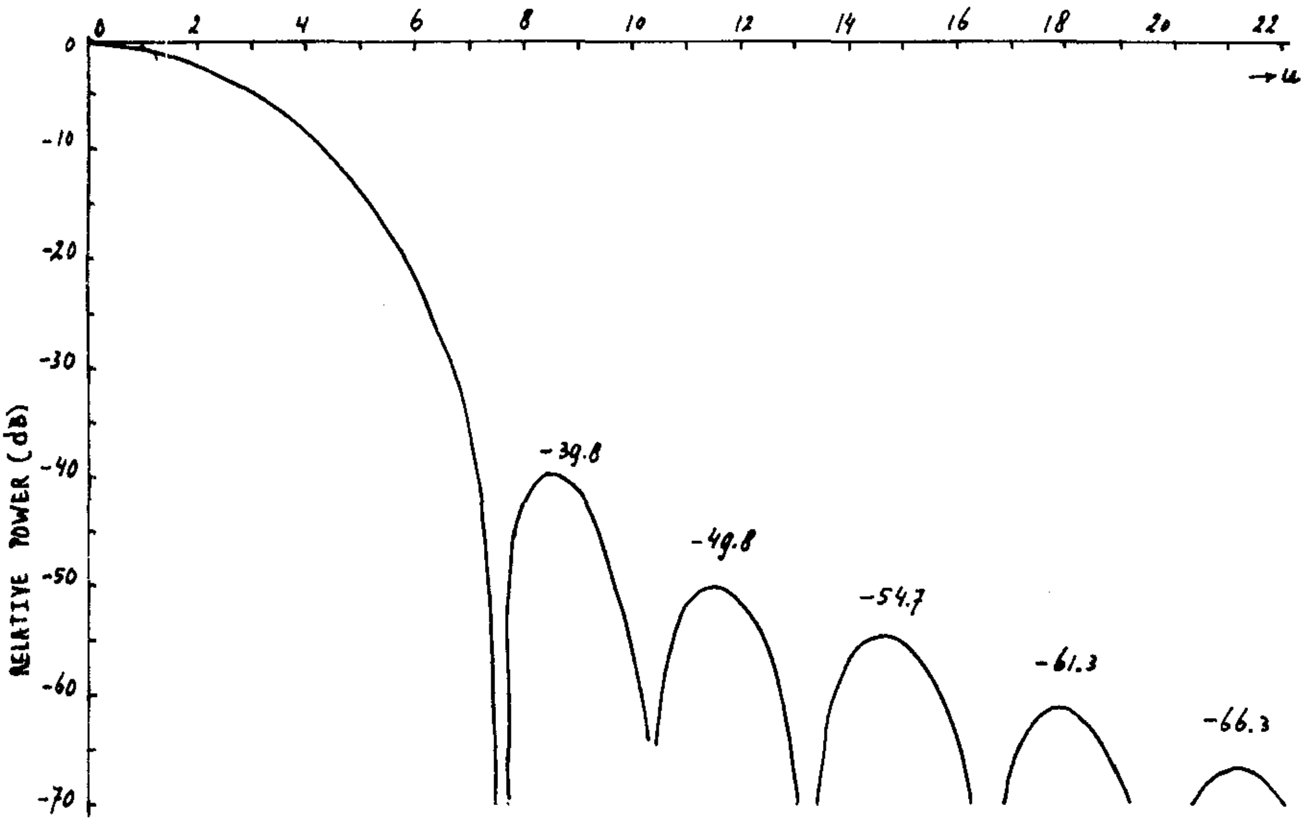

SIDE LOBE LEVELS	PRESCRIBED	COMPUTED
	-40 dB	-39.8 dB
	-50	-49.8
	-55	-54.7

ZEROS
$u_2 + t_2 = 7.5071$
$u_3 + t_3 = 10.3074$
$u_4 + t_4 = 13.1647$
$u_5 = 16.4706$

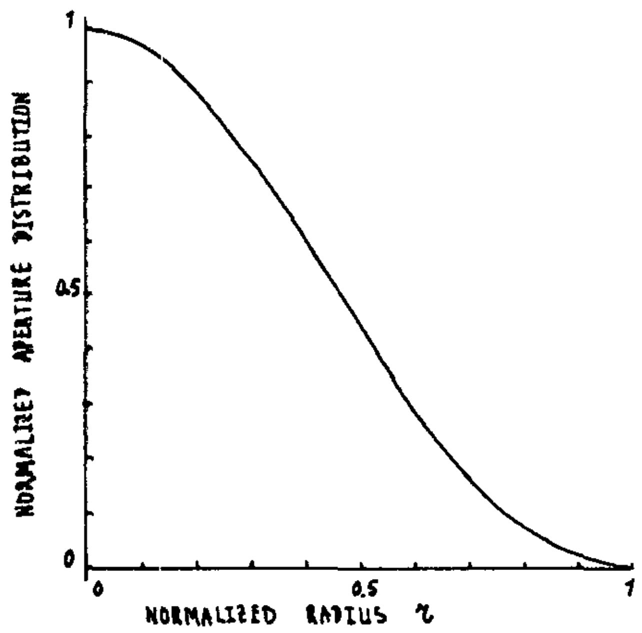

EXCITATION COEFFICIENTS
$a_1 = 5.24415$
$a_2 = 0.36430$
$a_3 = -0.02526$
$a_4 = -0.01543$

EFFICIENCY = 0.4719

GAIN REDUCTION = 3.26 dB

$u_{3dB} = 4.98$

FIG. 48: APERTURE DISTRIBUTION $\sum_{m=1}^{4} a_m \{ J_0(u_m r) - J_0(u_m) \}$ AND RADIATION PATTERN.

EINDHOVEN UNIVERSITY OF TECHNOLOGY
THE NETHERLANDS
DEPARTMENT OF ELECTRICAL ENGINEERING

Reports:

1) **Dijk, J., M. Jeuken and E.J. Maanders**
AN ANTENNA FOR A SATELLITE COMMUNICATION GROUND STATION (PROVISIONAL ELECTRICAL DESIGN).
TH-Report 68-E-01. 1968. ISBN 90-6144-001-7

2) **Veefkind, A., J.H. Blom and L.H.Th. Rietjens**
THEORETICAL AND EXPERIMENTAL INVESTIGATION OF A NON-EQUILIBRIUM PLASMA IN A MHD CHANNEL. Submitted to the Symposium on Magnetohydrodynamic Electrical Power Generation, Warsaw, Poland, 24-30 July, 1968.
TH-Report 68-E-02. 1968. ISBN 90-6144-002-5

3) **Boom, A.J.W. van den and J.H.A.M. Melis**
A COMPARISON OF SOME PROCESS PARAMETER ESTIMATING SCHEMES.
TH-Report 68-E-03. 1968. ISBN 90-6144-003-3

4) **Eykhoff, P., P.J.M. Ophey, J. Severs and J.O.M. Oome**
AN ELECTROLYTIC TANK FOR INSTRUCTIONAL PURPOSES REPRESENTING THE COMPLEX-FREQUENCY PLANE.
TH-Report 68-E-02. 1968. ISBN 90-6144-004-1

5) **Vermij, L. and J.E. Daalder**
ENERGY BALANCE OF FUSING SILVER WIRES SURROUNDED BY AIR.
TH-Report 68-E-05. 1968. ISBN 90-6144-005-X

6) **Houben, J.W.M.A. and P. Massee**
MHD POWER CONVERSION EMPLOYING LIQUID METALS.
TH-Report 69-E-06. 1969. ISBN 90-6144-006-8

7) **Heuvel, W.M.C. van den and W.F.J. Kersten**
VOLTAGE MEASUREMENT IN CURRENT ZERO INVESTIGATIONS.
TH-Report 69-E-07. 1969. ISBN 90-6144-007-6

8) **Vermij, L.**
SELECTED BIBLIOGRAPHY OF FUSES.
TH-Report 69-E-08. 1969. ISBN 90-6144-008-4

9) **Westenberg, J.Z.**
SOME IDENTIFICATION SCHEMES FOR NON-LINEAR NOISY PROCESSES.
TH-Report 69-E-09. 1969. ISBN 90-6144-009-2

10) **Koop, H.E.M., J. Dijk and E.J. Maanders**
ON CONICAL HORN ANTENNAS.
TH-Report 70-E-10. 1970. ISBN 90-6144-010-6

11) **Veefkind, A.**
NON-EQUILIBRIUM PHENOMENA IN A DISC-SHAPED MAGNETOHYDRODYNAMIC GENERATOR.
TH-Report 70-E-11. 1970. ISBN 90-6144-011-4

12) **Jansen, J.K.M., M.E.J. Jeuken and C.W. Lambrechtse**
THE SCALAR FEED.
TH-Report 70-E-12. 1969. ISBN 90-6144-012-2

13) **Teuling, D.J.A.**
ELECTRONIC IMAGE MOTION COMPENSATION IN A PORTABLE TELEVISION CAMERA.
TH-Report 70-E-13. 1970. ISBN 90-6144-013-0

EINDHOVEN UNIVERSITY OF TECHNOLOGY
THE NETHERLANDS
DEPARTMENT OF ELECTRICAL ENGINEERING

Reports:

14) **Lorencin, M.**
AUTOMATIC METEOR REFLECTIONS RECORDING EQUIPMENT.
TH-Report 70-E-14. 1970. ISBN 90-6144-014-9

15) **Smets, A.S.**
THE INSTRUMENTAL VARIABLE METHOD AND RELATED IDENTIFICATION SCHEMES.
TH-Report 70-E-15. 1970. ISBN 90-6144-015-7

16) **White, Jr., R.C.**
A SURVEY OF RANDOM METHODS FOR PARAMETER OPTIMIZATION.
TH-Report 70-E-16. 1971. ISBN 90-6144-016-5

17) **Talmon, J.L.**
APPROXIMATED GAUSS-MARKOV ESTIMATORS AND RELATED SCHEMES.
TH-Report 71-E-17. 1971. ISBN 90-6144-017-3

18) **Kalášek, V.**
MEASUREMENT OF TIME CONSTANTS ON CASCADE D.C. ARC IN NITROGEN.
TH-Report 71-E-18. 1971. ISBN 90-6144-018-1

19) **Hosselet, L.M.L.F.**
OZONBILDUNG MITTELS ELEKTRISCHER ENTLADUNGEN.
TH-Report 71-E-19. 1971. ISBN 90-6144-019-X

20) **Arts, M.G.J.**
ON THE INSTANTANEOUS MEASUREMENT OF BLOODFLOW BY ULTRASONIC MEANS.
TH-Report 71-E-20. 1971. ISBN 90-6144-020-3

21) **Roer, Th.G. van de**
NON-ISO THERMAL ANALYSIS OF CARRIER WAVES IN A SEMICONDUCTOR.
TH-Report 71-E-21. 1971. ISBN 90-6144-021-1

22) **Jeuken, P.J., C. Huber and C.E. Mulders**
SENSING INERTIAL ROTATION WITH TUNING FORKS.
TH-Report 71-E-22. 1971. ISBN 90-6144-022-X

23) **Dijk, J., J.M. Berends and E.J. Maanders**
APERTURE BLOCKAGE IN DUAL REFLECTOR ANTENNA SYSTEMS - A REVIEW.
TH-Report 71-E-23. 1971. ISBN 90-6144-023-8

24) **Kregting, J. and R.C. White, Jr.**
ADAPTIVE RANDOM SEARCH.
TH-Report 71-E-24. 1971. ISBN 90-6144-024-6

25) **Damen, A.A.H. and H.A.L. Piceni**
THE MULTIPLE DIPOLE MODEL OF THE VENTRICULAR DEPOLARISATION.
TH-Report 71-E-25. 1971. ISBN 90-6144-025-4

26) **Bremmer, H.**
A MATHEMATICAL THEORY CONNECTING SCATTERING AND DIFFRACTION PHENOMENA, INCLUDING BRAGG-TYPE INTERFERENCES.
TH-Report 71-E-26. 1971. ISBN 90-6144-026-2

27) **Bokhoven, W.M.G. van**
METHODS AND ASPECTS OF ACTIVE RC-FILTERS SYNTHESIS.
TH-Report 71-E-27. 1970. ISBN 90-6144-027-0

28) **Boeschoten, F.**
TWO FLUIDS MODEL REEXAMINED FOR A COLLISIONLESS PLASMA IN THE STATIONARY STATE.
TH-Report 72-E-28. 1972. ISBN 90-6144-028-9

EINDHOVEN UNIVERSITY OF TECHNOLOGY
THE NETHERLANDS
DEPARTMENT OF ELECTRICAL ENGINEERING

Reports:

29) REPORT ON THE CLOSED CYCLE MHD SPECIALIST MEETING. Working group of the joint ENEA/IAEA International MHD Liaison Group.
Eindhoven, The Netherlands, September 20-22, 1971. Edited by **L.H.Th. Rietjens.**
TH-Report 72-E-29. 1972. ISBN 90-6144-029-7

30) **Kessel, C.G.M. van and J.W.M.A. Houben**
LOSS MECHANISMS IN AN MHD GENERATOR.
TH-Report 72-E-30. 1972. ISBN 90-6144-030-0

31) **Veefkind, A.**
CONDUCTION GRIDS TO STABILIZE MHD GENERATOR PLASMAS AGAINST IONIZATION INSTABILITIES.
TH Report 72-E-31. 1972. ISBN 90-6144-031-9

32) **Daalder, J.E., and C.W.M. Vos**
DISTRIBUTION FUNCTIONS OF THE SPOT DIAMETER FOR SINGLE- AND MULTI-CATHODE DISCHARGES IN VACUUM.
TH-Report 73-E-32. 1973. ISBN 90-6144-032-7

33) **Daalder, J.E.**
JOULE HEATING AND DIAMETER OF THE CATHODE SPOT IN A VACUUM ARC.
TH-Report 73-E-33. 1973. ISBN 90-6144-033-5

34) **Huber, C.**
BEHAVIOUR OF THE SPINNING GYRO ROTOR.
TH-Report 73-E-34. 1973. ISBN 90-6144-034-3

35) **Bastian, C. et al.**
THE VACUUM ARC AS A FACILITY FOR RELEVANT EXPERIMENTS IN FUSION RESEARCH. Annual Report 1972. EURATOM-T.H.E. Group 'Rotating Plasma'.
TH-Report 73-E-35. 1973. ISBN 90-6144-035-1

36) **Blom, J.A.**
ANALYSIS OF PHYSIOLOGICAL SYSTEMS BY PARAMETER ESTIMATION TECHNIQUES.
TH-Report 73-E-36. 1973. ISBN 90-6144-036-X

37) **Cancelled**

38) **Andriessen, F.J., W. Boerman and I.F.E.M. Holtz**
CALCULATION OF RADIATION LOSSES IN CYLINDER SYMMETRIC HIGH PRESSURE DISCHARGES BY MEANS OF A DIGITAL COMPUTER.
TH-Report 73-E-38. 1973. ISBN 90-6144-038-6

39) **Dijk, J., C.T.W. van Diepenbeek, E.J. Maanders and L.F.G. Thurlings**
THE POLARIZATION LOSSES OF OFFSET ANTENNAS.
TH-Report 73-E-39. 1973. ISBN 90-6144-039-4

40) **Goes, W.P.**
SEPARATION OF SIGNALS DUE TO ARTERIAL AND VENOUS BLOOD FLOW IN THE DOPPLER SYSTEM THAT USES CONTINUOUS ULTRASOUND.
TH-Report 73-E-40. 1973. ISBN 90-6144-040-8

41) **Damen, A.A.H.**
A COMPARATIVE ANALYSIS OF SEVERAL MODELS OF THE VENTRICULAR DEPOLARIZATION; INTRODUCTION OF A STRING-MODEL.
TH-Report 73-E-41. 1973. ISBN 90-6144-041-6

EINDHOVEN UNIVERSITY OF TECHNOLOGY
THE NETHERLANDS
DEPARTMENT OF ELECTRICAL ENGINEERING

Reports:

42) **Dijk, G.H.M. van**
THEORY OF GYRO WITH ROTATING GIMBAL AND FLEXURAL PIVOTS.
TH-Report 73-E-42. 1973. ISBN 90-6144-042-4

43) **Breimer, A.J.**
ON THE IDENTIFICATION OF CONTINOUS LINEAR PROCESSES.
TH-Report 74-E-43. 1974. ISBN 90-6144-043-2

44) **Lier, M.C. van and R.H.J.M. Otten**
CAD OF MASKS AND WIRING.
TH-Report 74-E-44. 1974. ISBN 90-6144-044-0

45) **Bastian, C. et al.**
EXPERIMENTS WITH A LARGE SIZED HOLLOW CATHODE DISCHARDE FED WITH ARGON. Annual Report 1973. EURATOM-T.H.E. Group 'Rotating Plasma'.
TH-Report 74-E-45. 1974. ISBN 90-6144-045-9

46) **Roer, Th.G. van de**
ANALYTICAL SMALL-SIGNAL THEORY OF BARITT DIODES.
TH-Report 74-E-46. 1974. ISBN 90-6144-046-7

47) **Leliveld, W.H.**
THE DESIGN OF A MOCK CIRCULATION SYSTEM.
TH-Report 74-E-47. 1974. ISBN 90-6144-047-5

48) **Damen, A.A.H.**
SOME NOTES ON THE INVERSE PROBLEM IN ELECTRO CARDIOGRAPHY.
TH-Report 74-E-48. 1974. ISBN 90-6144-048-3

49) **Meeberg, L. van de**
A VITERBI DECODER.
TH-Report 74-E-49. 1974. ISBN 90-6144-049-1

50) **Poel, A.P.M. van der**
A COMPUTER SEARCH FOR GOOD CONVOLUTIONAL CODES.
TH-Report 74-E-50. 1974. ISBN 90-6144-050-5

51) **Sampic, G.**
THE BIT ERROR PROBABILITY AS A FUNCTION PATH REGISTER LENGTH IN THE VITERBI DECODER.
TH-Report 74-E-51. 1974. ISBN 90-6144-051-3

52) **Schalkwijk, J.P.M.**
CODING FOR A COMPUTER NETWORK.
TH-Report 74-E-52. 1974. ISBN 90-6144-052-1

53) **Stapper, M.**
MEASUREMENT OF THE INTENSITY OF PROGRESSIVE ULTRASONIC WAVES BY MEANS OF RAMAN-NATH DIFRACTION.
TH-Report 74-E-53. 1974. ISBN 90-6144-053-X

54) **Schalkwijk, J.P.M. and A.J. Vinck**
SYNDROME DECODING OF CONVOLUTIONAL CODES.
TH-Report 74-E-54. 1974. ISBN 90-6144-054-8

55) **Yakimov, A.**
FLUCTUATIONS IN IMPATT-DIODE OSCILLATORS WITH LOW Q-FACTORS.
TH-Report 74-E-55. 1974. ISBN 90-6144-055-6

EINDHOVEN UNIVERSITY OF TECHNOLOGY
THE NETHERLANDS
DEPARTMENT OF ELECTRICAL ENGINEERING

Reports:

56) **Plaats, J. van der**
ANALYSIS OF THREE CONDUCTOR COAXIAL SYSTEMS. Computer-aided determination of the frequency characteristics and the impulse and step response of a two-port consisting of a system of three coaxial conductors terminating in lumped impedances.
TH-Report 75-E-56. 1975. ISBN 90-6144-056-4

57) **Kalken, P.J.H. and C. Kooy**
RAY-OPTICAL ANALYSIS OF A TWO DIMENSIONAL APERTURE RADIATION PROBLEM.
TH-Report 75-E-57. 1975. ISBN 90-6144-057-2

58) **Schalkwijk, J.P.M., A.J. Vinck and L.J.A.E. Rust**
ANALYSIS AND SIMULATION OF A SYNDROME DECODER FOR A CONSTRAINT LENGTH $k = 5$, RATE $R = ½$ BINARY CONVOLUTIONAL CODE.
TH-Report 75-E-58. 1975. ISBN 90-6144-058-0.

59) **Boeschoten, F. et al.**
EXPERIMENTS WITH A LARGE SIZED HOLLOW CATHODE DISCHARGE FED WITH ARGON, II. Annual Report 1974. EURATOM-T.H.E. Group 'Rotating Plasma'.
TH-Report 75-E-59. 1975. ISBN 90-6144-059-9

60) **Maanders, E.J.**
SOME ASPECTS OF GROUND STATION ANTENNAS FOR SATELLITE COMMUNICATION.
TH-Report 75-E-60. 1975. ISBN 90-6144-060-2

61) **Mawira, A. and J. Dijk**
DEPOLARIZATION BY RAIN: Some Related Thermal Emission Considerations.
TH-Report 75-E-61. 1975. ISBN 90-6144-061-0

62) **Safak, M.**
CALCULATION OF RADIATION PATTERNS OF REFLECTOR ANTENNAS BY HIGH-FREQUENCY ASYMPTOTIC TECHNIQUES.
TH-Report 76-E-62. 1976. ISBN 90-6144-062-9

63) **Schalkwijk, J.P.M. and A.J. Vinck**
SOFT DECISION SYNDROME DECODING.
TH-Report 76-E-63. 1976. ISBN 90-6144-063-7

64) **Damen, A.A.H.**
EPICARDIAL POTENTIALS DERIVED FROM SKIN POTENTIAL MEASUREMENTS.
TH-Report 76-E-64. 1976. ISBN 90-6144-064-5

65) **Bakhuizen, A.J.C. and R. de Boer**
ON THE CALCULATION OF PERMEANCES AND FORCES BETWEEN DOUBLY SLOTTED STRUCTURES.
TH-Report 76-E-65. 1976. ISBN 90-6144-065-3

66) **Geutjes, A.J.**
A NUMERICAL MODEL TO EVALUATE THE BEHAVIOUR OF A REGENERATIVE HEAT EXCHANGER AT HIGH TEMPERATURE.
TH-Report 76-E-66. 1976. ISBN 90-6144-066-1

67) **Boeschoten, F. et al.**
EXPERIMENTS WITH A LARGE SIZED HOLLOW CATHODE DISCHARGE, III; concluding work Jan. 1975 to June 1976 of the EURATOM-THE Group 'Rotating Plasma'.
TH-Report 76-E-67. 1976. ISBN 90-6144-067-X

68) **Cancelled.**

EINDHOVEN UNIVERSITY OF TECHNOLOGY
THE NETHERLANDS
DEPARTMENT OF ELECTRICAL ENGINEERING

Reports:

69) **Merck, W.F.H. and A.F.C. Sens**
THOMSON SCATTERING MEASUREMENTS ON A HOLLOW CATHODE DISCHARGE.
TH-Report 76-E-69. 1976. ISBN 90-6144-069-6

70) **Jongbloed, A.A.**
STATISTICAL REGRESSION AND DISPERSION RATIOS IN NONLINEAR SYSTEM IDENTIFICATION.
TH-Report 77-E-70. 1977. ISBN 90-6144-070-X

71) **Barrett, J.F.**
BIBLIOGRAPHY ON VOLTERRA SERIES HERMITE FUNCTIONAL EXPANSIONS AND RELATED SUBJECTS.
TH-Report 77-E-71. 1977. ISBN 90-6144-071-8

72) **Boeschoten, F. and R. Komen**
ON THE POSSIBILITY TO SEPARATE ISOTOPES BY MEANS OF A ROTATING PLASMA COLUMN: Isotope separation with a hollow cathode discharge.
TH-Report 77-E-72. 1977. ISBN 90-6144-072-6

73) **Schalkwijk, J.P.M., A.J. Vinck and K.A. Post**
SYNDROME DECODING OF BINARY RATE-k/n CONVOLUTIONAL CODES.
TH-Report 77-E-73. 1977. ISBN 90-6144-073-4

74) **Dijk, J., E.J. Maanders and J.M.J. Oostvogels**
AN ANTENNA MOUNT FOR TRACKING GEOSTATIONARY SATELLITES.
TH-Report 77-E-74. 1977. ISBN 90-6144-074-2

75) **Vinck, A.J., J.G. van Wijk and A.J.P. de Paepe**
A NOTE ON THE FREE DISTANCE FOR CONVOLUTIONAL CODES.
TH-Report 77-E-75. 1977. ISBN 90-6144-075-0

76) **Daalder, J.E.**
RADIAL HEAT FLOW IN TWO COAXIAL CYLINDRICAL DISKS.
TH-Report 77-E-76. 1977. ISBN 90-6144-076-9

77) **Barrett, J.F.**
ON SYSTEMS DEFINED BY IMPLICIT ANALYTIC NONLINEAR FUNCTIONAL EQUATIONS.
TH-Report 77-E-77. 1977. ISBN 90-6144-077-7

78) **Jansen, J. and J.F. Barrett**
ON THE THEORY OF MAXIMUM LIKELIHOOD ESTIMATION OF STRUCTURAL RELATIONS. Part 1: One dimensional case.
TH-Report 78-E-78. 1977. ISBN 90-6144-078-5

79) **Borghi, C.A., A.F.C. Sens, A. Veefkind and L.H.Th. Rietjens**
EXPERIMENTAL INVESTIGATION ON THE DISCHARGE STRUCTURE IN A NOBLE GAS MHD GENERATOR.
TH-Report 78-E-79. 1978. ISBN 90-6144-079-3

80) **Bergmans, T.**
EQUALIZATION OF A COAXIAL CABLE FOR DIGITAL TRANSMISSION: Computer-optimized location of poles and zeros of a constant-resistance network to equalize a coaxial cable 1.2/4.4 for high-speed digital transmission (140 Mb/s).
TH-Report 78-E-80. 1978. ISBN 90-6144-080-7

EINDHOVEN UNIVERSITY OF TECHNOLOGY
THE NETHERLANDS
DEPARTMENT OF ELECTRICAL ENGINEERING

Reports:

81) **Kam, J.J. van der and A.A.H. Damen**
OBSERVABILITY OF ELECTRICAL HEART ACTIVITY STUDIES WITH THE SINGULAR VALUE DECOMPOSITION
TH-Report 78-E-81. 1978. ISBN 90-6144-081-5

82) **Jansen, J. and J.F. Barrett**
ON THE THEORY OF MAXIMUM LIKELIHOOD ESTIMATION OF STRUCTURAL RELATIONS. Part 2: Multi-dimensional case.
TH-Report 78-E-82. 1978. ISBN 90-6144-082-3

83) **Etten, W. van and E. de Jong**
OPTIMUM TAPPED DELAY LINES FOR THE EQUALIZATION OF MULTIPLE CHANNEL SYSTEMS.
TH-Report 78-E-83. 1978. ISBN 90-6144-083-1

83) **Vinck, A.J.**
MAXIMUM LIKELIHOOD SYNDROME DECODING OF LINEAR BLOCK CODES.
TH-Report 78-E-84. 1978. ISBN 90-6144-084-X

85) **Spruit, W.P.**
A DIGITAL LOW FREQUENCY SPECTRUM ANALYZER, USING A PROGRAMMABLE POCKET CALCULATOR.
TH-Report 78-E-85. 1978. ISBN 90-6144-085-8

86) **Beneken, J.E.W. et al**
TREND PREDICTION AS A BASIS FOR OPTIMAL THERAPY.
TH-Report 78-E-86. 1978. ISBN 90-6144-086-6

87) **Geus, C.A.M. and J. Dijk**
CALCULATION OF APERTURE AND FAR-FIELD DISTRIBUTION FROM MEASUREMENTS IN THE FRESNEL ZONE OF LARGE REFLECTOR ANTENNAS.
TH-Report 78-E-87. 1978. ISBN 90-6144-087-4

88) **Hajdasinski, A.K.**
THE GAUSS-MARKOV APPROXIMATED SCHEME FOR IDENTIFICATION OF MULTIVARIABELE DYNAMICAL SYSTEMS VIA THE REALIZATION THEORY.
An Explicit Approach.
TH-Report 78-E-88. 1978. ISBN 90-6144-088-2

89) **Niederlinski, A.**
THE GLOBAL ERROR APPROACH TO THE CONVERGENDE OF CLOSED-LOOP IDENTIFICATION, SELF-TUNING REGULATORS AND SELF-TUNING PREDICTORS.
TH-Report 78-E-89. 1978. ISBN 90-6144-089-0

90) **Vinck, A.J. and A.J.P. de Paepe**
REDUCING THE NUMBER OF COMPUTATIONS IN STACK DECODING OF CONVOLUTIONAL CODES BY EXPLOITING SYMMETRIES OF THE ENCODER.
TH-Report 78-E-90. 1978. ISBN 90-6144-090-4

91) **Geutjes, A.J. and D.J. Kleyn**
A PARAMETRIC STUDY OF 1000 MWe COMBINED CLOSED CYCLE MHD/STEAM ELECTRICAL POWER GENERATING PLANTS.
TH-Report 78-E-91. 1978. ISBN 90-6144-091-2

92) **Massee, P.**
THE DISPERSION RELATION OF ELECTROTHERMAL WAVES IN A NONEQUILIBRIUM MHD PLASMA.
TH-Report 78-E-92. 1978. ISBN 90-6144-092-0

EINDHOVEN UNIVERSITY OF TECHNOLOGY
THE NETHERLANDS
DEPARTMENT OF ELECTRICAL ENGINEERING

Reports:

93) Duin, C.A. van
DIPOLE SCATTERING OF ELECTROMAGNETIC WAVES PROPAGATION THROUGH A RAIN MEDIUM. TH-Report 79-E-93. 1979. ISBN 90-6144-093-9

94) Kuijper, A.H. de and L.K.J. Vandamme
CHARTS OF SPATIAL NOISE DISTRIBUTION IN PLANAR RESISTORS WITH FINITE CONTACTS. TH-Report 79-E-94. 1979. ISBN 90-6144-094-7

95) Hajdasinski, A.K. and A.A.H. Damen
REALIZATION OF THE MARKOV PARAMETER SEQUENCES USING THE SINGULAR VALUE DECOMPOSITION OF THE HANKEL MATRIX. TH-Report 79-E-95. 1979.
ISBN 90-6144-095-5

96) Stepanov, B.
ELECTRON MOMENTUM TRANSFER CROSS-SECTION IN CESIUM AND RELATED CALCULATIONS OF THE LOCAL PARAMETERS OF Cs + Ar MHD PLASMAS. TH-Report 79-E-96. 1979.
ISBN 90-6144-096-3

97) Worm, S.C.J.
RADIATION PATTERNS OF CIRCULAR APERTURES WITH PRESCRIBED SIDELOBE LEVELS.
TH-Report 79-E-97. 1979. ISBN 90-6144-097-1